SYNERGISTIC EFFECTS OF BONE SURFACE MIMIC TOPOGRAPHY AND CHEMISTRY ON OSTEOGENIC STEM CELL DIFFERENTIATION AND OSTEOIMMUNOMODULATION

by

Birgün Özçolak

B.S., in Molecular Biology and Genetics, Boğaziçi University, 2014

M.S., in Biomedical Engineering, Boğaziçi University, 2016

Submitted to the Institute of Biomedical Engineering

in partial fulfillment of the requirements

for the degree of

Doctor

of

Philosophy

Boğaziçi University

2024

SYNERGISTIC EFFECTS OF BONE SURFACE MIMIC TOPOGRAPHY AND CHEMISTRY ON OSTEOGENIC STEM CELL DIFFERENTIATION AND OSTEOIMMUNOMODULATION

APPROVED BY:

Prof. Dr. Bora Garipcan .....
(Thesis Advisor)

Assist. Prof. Dr. Mustafa Kemal Ruhi .....

Assoc. Prof. Dr. Duygu Ege .....

Assoc. Prof. Dr. Sedat Odabaş .....

Prof. Dr. Lokman Uzun .....

DATE OF APPROVAL: 05.06.2024

Hope is like the sun. If you only believe in it when you see it,

you'll never make it through the night...

Princess Leia

ACKNOWLEDGMENTS

I'd like to express my heartfelt appreciation to many people who supported me to complete my thesis successfully. First and foremost, I want to thank my advisor, Prof. Dr. Bora Garipcan. Throughout my research journey, his continuous support, encouragement, and mentorship have significantly shaped my academic and professional development. He taught me that before becoming a good professor, I needed to be a decent person, and I am grateful to have had an advisor who demonstrated both attributes. He instilled in me the discipline of hard work, the importance of having a backup plan, the value of empathizing with colleagues to create high-quality work, and the significance of learning from our mistakes. I'm grateful to him for guiding me through the thorny trails of academics and for being one of my greatest blessings. I would also like to thank my outstanding committee members, Assoc. Prof. Dr. Sedat Odabaş, Assoc. Prof. Dr. Özgür Kocatürk, and Asst. Prof. Dr. Mustafa Kemal Ruhi for their helpful criticism and insightful contributions to my thesis.

I would like to extend my heartfelt gratitude to Prof. Dr. Fikrettin Şahin for his invaluable contributions and unwavering support throughout the completion of my thesis. I am also deeply thankful for the steadfast support of my laboratory colleagues Sabra Rostami, Dilara Perver, Berkay Erenay, Sezin Eren Demirbüken, and Bengü Aktaş.

I owe a special debt of gratitude to two incredibly important people in my life, my mother and my son, Mehmet Ertuğrul. Family is everything, especially when navigating the challenging paths of academia. My mother not only endured sleepless nights raising me but also cared for my son while I wrote my thesis. Each time I stumbled; she lifted me up stronger than before. My son, the most special, soft-hearted, sweetest child, never got upset with me for not being able to spend time with him. His smile, which warmed my heart, gave me the strength to keep going. If this thesis exists today, it is largely due to his smile.

I am thankful for the financial support provided by TUBITAK (The Scientific and Technological Research Council of Turkey) under grant numbers 113S730 and 121M969, as well as the partial funding from the Boğaziçi University Research Fund (BAP) under grant number 6701. I also appreciate the assistance from the İlim Yayma Vakfı Ph.D. Fellowship program.

ACADEMIC ETHICS AND INTEGRITY STATEMENT

I, Birgün Özçolak, hereby certify that I am aware of the Academic Ethics and Integrity Policy issued by the Council of Higher Education (YÖK) and I fully acknowledge all the consequences due to its violation by plagiarism or any other way.

Name :

Signature:

Date:

ABSTRACT

SYNERGISTIC EFFECTS OF BONE SURFACE MIMIC TOPOGRAPHY AND CHEMISTRY ON OSTEOGENIC STEM CELL DIFFERENTIATION AND OSTEOIMMUNOMODULATION

The term "osteoimmunomodulation" refers to regulating immune responses to enhance bone healing. Osteoimmunology highlights the significant role of immune cells in bone repair. Conventional bone repair approaches often neglect the immune response, causing discrepancies between *in vitro* and *in vivo* environments. A suitable osteo-immune environment is crucial for successful bone regeneration. Surface and bulk properties like surface charge, porosity, pore size, wettability, bioactive ion release, and surface topography significantly affect cell behavior on biomaterials. These features influence cell adhesion, proliferation, stem cell differentiation, and immune cell behavior, including macrophage polarization. This thesis explored how the topographical and chemical characteristics of bone surfaces affect cellular behavior, specifically promoting osteogenic differentiation and enhancing osteoimmunomodulation. Model Poly-L-Lactic Acid (PLA) membranes were produced to mimic natural bone surface properties through soft lithography technique. To enhance biomimicry, BSM PLA membranes were modified with collagen type I (Col-I) and hydroxyapatite (HA). The effect of these membranes on the osteogenic differentiation of adipose-derived mesenchymal stem cells (ADMSC) and on osteoimmunomodulation using RAW 264.7 macrophage cells was examined. HA-deposited BSM PLA membranes promoted osteogenic differentiation in ADMSC and stimulated sequential M1 and M2 macrophage polarizations in RAW 264.7 macrophage cells. These results lay the groundwork for future biomaterials research by demonstrating the capability of HA-deposited BSM PLA membranes topromote osteogenic differentiation and stimulate the osteoimmune response.

Keywords: Biomimetic, Osteoimmunomodulation, Macrophages, Macrophage polarization, Osteogenic Differentiation, Stem Cells.

ÖZET

KEMİK YÜZEY TOPOGRAFYASI VE KİMYASI TAKLİDİNİN OSTEOJENİK FARKLILAŞMA VE OSTEOİMMÜNOMODULASYON ÜZERİNDEKİ SİNERJİK ETKİLERİ

"Osteoimmünomodülasyon" terimi, kemik iyileşmesini artırmak için bağışıklık yanıtını düzenlenmesini ifade eder. Osteoimmünoloji, kemik onarımında bağışıklık hücrelerinin önemini vurgular. Geleneksel kemik onarım yaklaşımları, bağışıklık yanıtını göz ardı ederek *in vitro* ve *in vivo* ortamlar arasında tutarsızlıklara neden olur. Başarılı kemik rejenerasyonu için uygun osteo-immün ortam gereklidir. Yüzey yükü, gözeneklilik, gözenek boyutu, ıslanabilirlik, biyoaktif iyon salınımı ve yüzey topografyası gibi yüzey ve kütle özellikleri, biyomalzemeler üzerindeki hücre davranışını önemli ölçüde etkiler. Bu özellikler, hücre yapışması, çoğalması, kök hücre farklılaşması ve makrofaj polarizasyonu gibi bağışıklık hücresi davranışlarını etkiler. Bu tez, kemik yüzeyi topografik ve kimyasal özelliklerinin hücre davranışını nasıl etkilediğini, özellikle osteojenik farklılaşma ve osteoimmünomodülasyona etkisini araştırmıştır. Kemiğin doğal yüzey özelliklerini taklit etmek için model Poli-L-Laktik Asit (PLA) membranlar, yumuşak litografi tekniğiyle üretilmiştir. Biyomimikriyi artırmak için BSM PLA membranlar, tip-I kollajen (Col-I) ve hidroksiapatit (HA) ile modifiye edilmiştir. Bu membranların osteojenik farklılaşma üzerindeki etkisi yağ doku kaynaklı mezenkimal kök hücreler (ADMSC) ve osteoimmünomodülasyon üzerindeki etkisi RAW 264.7 makrofaj hücreleri kullanılarak incelenmiştir. HA kaplı BSM PLA membranlar, ADMSC'lerde osteojenik farklılaşmayı teşvik etmiş ve RAW 264.7 makrofaj hücrelerinde sıralı M1 ve M2 makrofaj polarizasyonunu desteklemiştir. Bu bulgular, HA kaplı BSM PLA membranların kök hücrelerde osteojenik farklılaşmayı teşvik ve osteoimmün yanıtı tetikleme kabiliyeti göstererek, gelecekteki biyomalzeme araştırmaları için zemin hazırlamaktadır.

Anahtar Sözcükler: Biyomimetik, Osteoimmunomodülasyon, Makrofajlar, Makrofaj polarizasyonu, Osteojenik Farklılaşma, Kök Hücreler.

TABLE OF CONTENTS

ACKNOWLEDGMENTS iv
ACADEMIC ETHICS AND INTEGRITY STATEMENT vi
ABSTRACT vii
ÖZET viii
LIST OF FIGURES xii
LIST OF SYMBOLS xv
LIST OF ABBREVIATIONS xvii
1. INTRODUCTION 1
1.1 Motivation 1
1.2 Objectives and Outline of the Thesis 5
2. BACKGROUND 7
2.1 Cell Microenvironment 7
2.2 Cell Biomaterial Interaction 10
2.2.1 Surface Topography 13
2.2.2 Surface Chemistry 15
2.3 Stem Cells 16
2.3.1 Stem Cells and Osteogenic Differentiation 18
2.4 Immunomodulation 21
2.4.1 Macrophages 23
2.4.2 Osteoimmunomodulation 25
3. PRODUCTION AND CHARACTERIZATION OF BSM PLA MEMBRANES 29
3.1 Experimental Procedures 30
3.1.1 Instrumentations and Reagents 30
3.1.2 BSM Membrane Production 30
3.1.2.1 Bone Surface Cleaning 30
3.1.2.2 Preparation of PDMS Molds 31
3.1.2.3 Bone Surface Mimicked PLA Production 32
3.1.3 Col-I and HA Immobilization of the BSM PLA Membranes . . . 32
3.1.3.1 Optimization of Col-I Immobilization 32

3.1.4 Physicochemical Characterization of the Col-I and HA Modifications . . . 33
3.1.4.1 Wettability Analysis . . . 33
3.1.4.2 Fourier Transform Infrared Spectroscopy (FTIR) . . . 33
3.1.4.3 X-ray photoelectron spectroscopy (XPS) . . . 34
3.1.4.4 X-ray Diffraction (XRD) . . . 34
3.1.5 Characterization of the Surface Topography of the BSM Membranes 34
3.1.5.1 Atomic Force Microscopy (AFM) . . . 34
3.1.5.2 Scanning Electron Microscopy (SEM) . . . 34
3.1.6 Statistical Analysis . . . 35
3.2 Results . . . 35
3.2.1 Optimization of Collagen Immobilization . . . 35
3.2.2 Physicochemical Characterization of the Col-I and HA Modifications . . . 36
3.2.2.1 Wettability Analysis . . . 36
3.2.2.2 Fourier Transform Infrared Spectroscopy (FTIR) . . . 38
3.2.2.3 X-ray photoelectron spectroscopy (XPS) . . . 39
3.2.2.4 X-ray Diffraction (XRD) . . . 40
3.2.3 Characterization of the Surface Topography of the Unmodified and Modified BSM Membranes . . . 41
3.2.3.1 Scanning Electron Microscopy (SEM) . . . 41
3.2.3.2 Atomic Force Microscopy (AFM) . . . 42
3.3 Discussion . . . 44
4. EFFECTS OF BONE SURFACE TOPOGRAPHY AND CHEMISTRY ON OSTEOGENIC DIFFERENTIATION . . . 47
4.1 Experimental Procedures . . . 48
4.1.1 Instrumentation and Reagents . . . 48
4.1.2 Cell Culture Studies . . . 48
4.1.2.1 Cell Proliferation . . . 49
4.1.2.2 Cell Morphology and Attachment Analysis . . . 50
4.1.2.3 Osteogenic Differentiation Analysis . . . 50
4.1.3 Statistical Analysis . . . 51

4.2 Results . . . 51
4.2.1 Cell Proliferation . . . 51
4.2.2 Cell Morphology and Attachment Analysis . . . 53
4.2.3 Osteogenic Differentiation Analysis . . . 56
4.2.3.1 Alkaline Phosphatase Activity Analysis . . . 56
4.2.3.2 Alizarin Red S Analysis . . . 57
4.3 Discussion . . . 60
5. EFFECTS OF BONE SURFACE TOPOGRAPHY AND CHEMISTRY ON MACROPHAGE POLARIZATION . . . 64
5.1 Experimental Procedures . . . 65
5.1.1 Instrumentation and Reagents . . . 65
5.1.2 Cell Culture Studies . . . 65
5.1.2.1 Cell Viability . . . 66
5.1.2.2 Cell Morphology Analysis . . . 66
5.1.2.3 Cytokine Content Analysis in the Supernatant . . . 66
5.1.2.4 Statistical Analysis . . . 67
5.2 Results . . . 67
5.2.1 Cell Viability . . . 67
5.2.2 Cell Morphology Analysis . . . 69
5.2.3 Cytokine Content Analysis in the Supernatant . . . 72
5.3 Discussion . . . 75
6. CONCLUSION . . . 79
APPENDIX A. CALIBRATION CURVES . . . 82
REFERENCES . . . 83

LIST OF FIGURES

Figure 2.1 Illustration of the key elements of the cellular microenvironment [56]. 8

Figure 2.2 Engineered Microenvironment to Regulate Stem Cell Behavior. The engineered scaffolds create a favorable niche by biochemical and biophysical modifications, enhancing cell differentiation, retention, engraftment, and self-renewal through cell-matrix and cell-to-cell interactions. The optimized microenvironment promotes effective tissue repair and regeneration [104]. 12

Figure 2.3 Diagram showing macrophage polarization into different phenotypes. Macrophages differentiate into M1 (pro-inflammation and phagocytosis), M2a (anti-inflammation and phagocytosis), M2b (antigen presentation and immune regulation), M2c (tissue remodeling and matrix deposition), and M2d (tumor-associated macrophages and angiogenesis promotion) based on various activating stimuli and cytokine production [188]. 24

Figure 3.1 Schematic of BSM-PLA membrane production. a. BSM-PLA Membrane Preparation Process, b. Col-I Modification of BSM-PLA Membrane Preparation Process, c. HA Modification of BSM-PLA Membrane Preparation Process. 31

Figure 3.2 a. Immunohistostaining analysis of unmodified and Col-I modified plain and BSM PLA membranes by using ImageJ, b. Immunohistostaining of unmodified and Col-I modified plain and BSM PLA membranes, c. Quantification of Col-I content by Sirius Red assay (* $p < 0.05$, ** $p < 0.01$, *** $p < 0.001$, **** $p < 0.0001$). 37

Figure 3.3 Characterization of surface wettability of unmodified and modified plain and BSM membranes by WCA analysis. 38

Figure 3.4 Characterization of surface chemical composition by FTIR analysis; I. Unmodified PLA, II. Col-I modified PLA, III. HA modified PLA. 39

Figure 3.5 Characterization of surface chemical composition by XPS analysis; I. Unmodified PLA, II. Col-I modified PLA. 40

Figure 3.6 Characterization of surface crystallinity by XRD Analysis; I. Unmodified PLA, II. HA modified PLA, III. Pure HA. 41

Figure 3.7 SEM and AFM images of the surface 3-D structure of the bone, BSM PDMS mold, unmodified, Col-I and HA modified BSM PLA membranes. 43

Figure 4.1 Schematic of the experimental procedure for osteogenic differentiation of mesenchymal stem cells. ADMSCs are cultured on modified and unmodified BSM PLA membranes, followed by osteogenic differentiation analysis, leading to the formation of osteoblasts. 49

Figure 4.2 The proliferation of the ADMSCs onto unmodified and modified Plain and BSM membranes using the MTT test at day 1, 4, and 7 (* $p < 0.05$, ** $p < 0.01$, *** $p < 0.001$, **** $p < 0.0001$). 53

Figure 4.3 The attachment of ADMSCs onto unmodified and modified Plain and BSM membranes observed using SEM (Scale bars: 100 μm, 500x magnification; 50 μm, 1500x magnification (inlet)). 55

Figure 4.4 The osteogenic differentiation analysis of the ADMSCs onto unmodified and modified Plain and BSM membranes via ALP Analysis at day 7, 14, and 21 (* $p < 0.05$, ** $p < 0.01$, *** $p < 0.001$, **** $p < 0.0001$). 57

Figure 4.5 The osteogenic differentiation analysis of the ADMSCs onto unmodified and modified Plain and BSM membranes via Alizarin Red Analysis (Scale bars: 2000 μm). 60

Figure 5.1 Schematic of the experimental procedure for macrophage polarization. RAW 264.7 cells are cultured on modified and unmodified BSM PLA membranes. The polarization analysis determines whether the macrophages adopt an M1 (pro-inflammatory) or M2 (anti-inflammatory) phenotype. 66

Figure 5.2 Viability of RAW 264.7 cells adherent on unmodified, Col-I modified, and HA modified plain PLA and BSM PLA surfaces measured at day 1, day 3, and day 6 (* $p < 0.05$, ** $p < 0.01$, *** $p < 0.001$, **** $p < 0.0001$). 69

Figure 5.3 SEM images of unmodified, and Col-I and HA modified, plain and BSM membranes on day 1, day 3, and day 6 (Scale bars: 2 μm). 71

Figure 5.4 Pro-Inflammatory and Anti-Inflammatory factor content and amount analysis on unmodified and Col-I and HA modified, plain PLA and BSM PLA membranes by days. (a) IL-6 Concentration, (b) IL-10 Concentration, (c) IL-1β Concentration, (d) IL-1ra Concentration (* $p < 0.05$, ** $p < 0.01$, *** $p < 0.001$, **** $p < 0.0001$). 74

Figure A.1 Calibration Curves. I. IL-6 Calibration Curve, II. IL-1β Calibration Curve, III. IL-10 Calibration Curve, IV. IL-1ra Calibration Curve. 82

LIST OF SYMBOLS

A	absorbance of test wells
A'	absorbance of negative control wells
O=C-N	amide group
N-H	amino group
Å	angstrom
Al-K α	K-Alpha X-rays of aluminum
Ra	average surface roughness
COOH	carboxyl group
C=O	carbonyl group
C-C	carbon-carbon bond
C-H	carbon-hydrogen bond
C-O	carbon-oxygen bond
$(CO_3)^{2-}$	carbonate group
C(RED)	concentration of reduced AlamarBlue
C(OX)	concentration of oxidized AlamarBlue
°C	degree Celsius
dL	deciliter
eV	electronvolt
λ_1	570 nm wavelength
λ_2	595 nm wavelength
-CO-O	ester group
g	gram
kV	kilovolt
μm	micrometer
mA	milliampere
mg	milligram
mL	milliliter
mM	millimolar

μM	micromolar
μL	microliter
ϵ_{OX}	molar extinction coefficient of oxidized AlamarBlue
ϵ_{RED}	molar extinction coefficient of reduced AlamarBlue
$(PO_4)^{3-}$	phosphate group
Θ	theta
OD	optical density
V	volt

LIST OF ABBREVIATIONS

ADMSC	Adipose-derived mesenchymal stem cells
AFM	(Atomic Force Microscopy)
ALP	Alkaline phosphatase
ADSC	Adipose-derived stem cells
BSM	Bone Surface Mimicked
CAM	Contact Angle Measurement
Col-I	Collagen Type I
DAB	3,3'-Diaminobenzidine
DMEM	Dulbecco's Modified Eagle's Medium
ESCs	Embryonic Stem Cells
EDAC	1-Ethyl-3-(3-dimethylaminopropyl)carbodiimide
ECM	Extracellular matrix
ELISA	Enzyme-Linked Immunosorbent Assay
FBS	Fetal Bovine Serum
FTIR	Fourier Transform Infrared Spectroscopy
HA	Hydroxyapatite
HMDS	Hexamethyldisilazane
HRP	Horseradish Peroxidase
iPSCs	Induced Pluripotent Stem Cells
IL	Interleukin
MSC	Mesenchymal Stem Cells
NGF	Nerve growth factor
PDMS	Polydimethylsiloxane
PLA	Poly(Lactic Acid)
PLGA	Poly(lactic-co-glycolic acid)
RT-PCR	Reverse Transcription Polymerase Chain Reaction
SEM	Scanning Electron Microscopy
WCA	Water Contact Angle

WST-1	Water Soluble Tetrazolium-1
XPS	X-ray Photoelectron Spectroscopy
XRD	X-ray Diffraction

1. INTRODUCTION

1.1 Motivation

The cell microenvironment is a complex and dynamic system that controls cellular activity and keeps tissues stable. The cell microenvironment is made up of four key components: the physicochemical environment, soluble signaling molecules, cell to cell interactions, and extracellular matrix (ECM). For developing effective bone regeneration materials, it is essential to understand the cumulative impacts of these elements on cellular processes like adhesion, proliferation, migration and differentiation [1, 2]. ECM contains proteins like collagen, fibronectin, and laminin, provides structural support as well as biochemical signals, which control cell survival, adherence and differentiation [3]. For example, Col-I encourages mesenchymal stem cells (MSCs) to develop into osteogenic tissues via integrin-mediated signaling pathways [4]. Furthermore, fibronectin promotes motility and adhesion of cells, providing integrin correlation between cells as well as their ECM to control chondrogenic differentiation of MSC [5]. Similarly, laminins interact with cell membrane receptors to establish the molecular basis for cell signaling and cell and ECM interactions, which are important for stem cell osteogenesis [6].

Furthermore, soluble signaling factors, including growth factors cytokines, morphogens and peptides act as chemical messages in the cell microenvironment. They direct cellular behavior. They determine cell fate. These factors operate through autocrine and paracrine signaling pathways [7, 8]. They are important for directing stem cell self-renewal or differentiation. They also regulate immune responses. This includes inflammation and tissue repair [9, 10]. For example, nerve growth factor (NGF) as well as insulin-like growth factor-1 (IGF-1) reduce spasticity. They improve functional recovery following spinal cord injury [11]. Similarly, fibroblast growth factor (FGF) controls osteogenesis and chondrogenesis [12].

The physicochemical environment, which includes mechanical characteristics, topographical cues, pH levels and oxygen tension has also considerable impact on cell behavior and fate [13]. Stem cells respond in lineages based on mechanical stimuli from their surroundings. Cell migration is affected by topographical cues. Spatial organization and differentiation processes are also affected by these cues, which can be found in ECM or produced artificially [14]. For example, Sun *et al.* suggested that stiffness of polyacrylamide hydrogels affects osteogenic differentiation of MSCs [15]. El-Rashidy *et al.* indicated that stiffer matrices promote osteogenic lineage commitment [16]. Diverse microtopographies, such as microgrooves micropillars and micro pits have enhanced osteogenic differentiation of MSCs. This emphasizes the relevance of the physicochemical environment in producing bone regeneration materials [17].

Biomaterials have various surface properties, like topography, chemistry, surface charge, mechanical characteristics, wettability, and roughness. These properties significantly affect HA cells respond, including HA they adhere, migrate, proliferate, differentiate, and polarize, mimicking their natural environment. Thereby, the interface among biomaterials and cells is crucial also for the success of bone regeneration [18, 19].

One of the important factors of biomaterial design is mimicking the topography and chemistry of bone surfaces because it helps create an environment that promotes cell adhesion, growth, and differentiation, like natural bone [20]. By designing biomaterials that closely resemble the natural bone surface, researchers can enhance the integration and functionality of implants and scaffolds used in bone regeneration [21].

Stem cell differentiation into certain cell types is vital for bone regeneration. Osteogenic differentiation, where stem cells transform into osteoblasts, which is responsible for bone formation), is crucial in regenerative medicine, particularly in repairing bone defects and injuries [22, 23]. Various stem cell types, including, MSC, induced pluripotent stem cells (iPSCs) and embryonic stem cells (ESCs), can undergo osteogenic differentiation. MSCs are particularly favored due to their ease of isolation, low immunogenicity, and natural capacity to differentiate into bone-forming cells [24].

The properties of biomaterials, like surface topography, chemical composition, stiffness, and porosity, used as scaffolds have a significant role in the differentiation processesâ success [25]. Similarly, Ventura *et al.* suggested that the surface chemistry of biomaterials, such as the presence of functional groups, can direct differentiation of stem cells to specific lineages, emphasizing their importance of biomaterial properties to control stem cell fate [26]. Zhu et al suggested specific topographic features could improve osteogenic differentiation and cell alignment. For example, microgrooves encourage contact guidance, control cell arrangement, cell extending, and osteogenic differentiation, in order to quicken bone regeneration [27]. Similarly, Palin *et al.* demonstrated that surface roughness significantly impacts cell adhesion and proliferation, emphasizing the importance of mimicking natural bone properties in biomaterials [28]. Webster and his team also reported that nanophase ceramics with surface properties similar to natural bone enhance osteoblast functions [29]. Additionally, Dimitrievska *et al.* found that nanostructured HA coatings more effectively support MSC proliferation and differentiation compared to traditional coatings [30]. Qin *et al.* suggested that collagen-based scaffolds modified with HA could successfully mimic bone surface topography and enhance MSCs' osteogenic potential [31].

Additionally, cell to cell interactions within microenvironment are vital for tissue development, regeneration and immune regulation. In stem cell niches, neighboring cells provide signals. These signals guide stem cell self-renewal. They guide differentiation and lineage commitment [32]. For example, the interaction between MSCs and endothelial cells via paracrine signaling enhances the therapeutic potential of MSCs in tissue regeneration [33]. Neighboring cells in the bone marrow niche regulate hematopoietic stem cell (HSC) behavior by promoting self-renewal [34]. Osteoimmunomodulation, the interaction between the immune system and bone tissue, focuses on HA immune responses affect bone healing and regeneration [35]. In the context of osteoimmunomodulation, immune cells such as macrophages interact with MSCs. This interaction affects their differentiation and promotes bone regeneration [36]. Additionally, macrophage behavior and polarization are critical for immune response and tissue repair. Biomaterial surface properties can also affect macrophage polarization as like cell to cell interaction by promoting either a pro-inflammatory (M1)

or anti-inflammatory (M2) phenotype [37, 38]. Surface topographical features effect macrophage polarization. Wang *et al.* found that 1D wrinkles that generate grooves and ridges have been shown to promote M2 polarization; whereas, 2D wrinkles that create pits and bumps, can stimulate M1 polarization [39]. Chen *et al.* suggested that surface topography can have an impact on macrophage behavior regardless of surface chemistry. Specifically, the increase in topography feature size from 500 nm to 2 μm can restrict macrophage activation and inflammation-related activities [40]. Barth *et al.* also found that macrophages seeded onto rougher surfaces tend to exhibit an M2-like phenotype, which suppresses immune and anti-inflammatory processes, plus promotes angiogenesis, ECM formation, and tissue repair [41]. Similarly, Damanik *et al.* report that microporous structures trigger macrophages to exhibit an M2-like phenotype [42] . Surface chemical composition also affect macrophage polarization. Laquerriere *et al.* suggested that small-diameter HA particles can activate immune cells to release pivotal cytokines, which favor inflammation [43]. Fernandes *et al.* reported that HA granules activate M2 polarization of THP-1 cells more than M1 [44]. According to Sadowska *et al.*, HA-coated materials have a significant effect on triggering the creation of pro-inflammatory cytokines and controlling osteogenic processes [45]. Li Jiashen *et al.* reported that Col-I modified membranes do not have cytotoxic effects on adipose-derived stem cells (ADSC) and can initiate osteogenic differentiation of these cells [46]. Moreover, Col-I can affect the expression of osteogenic factors such as WNT10b, BMP2, BMP6, and OSM, as it generates a rough surface on the material [19, 47, 48]. Correia *et al.* found that unmodified PLA activates M1 macrophage polarization, while Col-I modified PLA macrophages with the same surface properties generally prompt M2 macrophage polarization [49]. During wound healing, macrophages initially adopt the M1 phenotype to control early inflammation, then transition to the M2 phenotype to reduce inflammation and stimulate new tissue formation [50, 51]. Studies have shown that sequential activation of M1 followed by M2 macrophages enhances the healing process, significantly improving bone regeneration outcomes [50, 52].

In summary, bone-like rough and microporous surfaces have been suggested to encourage tissue repair as well as osteogenic differentiation of stem cells while suppressing immune and anti-inflammatory responses. However, none of the different surface

topographies used in the literature directly mimic the natural surface topography of bone. To address this critical gap, the motivation of this thesis is to fabricate a bone-like anisotropic microenvironment by mimicking bone surface topography and chemistry, aiming to achieve the desired osteogenesis and osteoimmunomodulatory response. By mimicking the natural properties of bone and interacting effectively with both immune and stem cells, these materials have the potential to greatly improve bone repair and regeneration outcomes, leading to innovative treatments in regenerative medicine.

1.2 Objectives and Outline of the Thesis

The purpose of this thesis is to observe the effect of bone surface topography and chemistry on cell behavior. Specifically, to examine whether it promotes osteoimmunomodulative responses as well as osteogenic differentiation of stem cells through PLA membranes that mimic natural bone properties using soft lithography. In the first part of the thesis, bone surface topography was simulated on a model surface obtained from bovine femur using soft lithography. To mimic the bone surface microenvironment, BSM membranes were further modified with Col-I and HA. In the second part of the thesis, the effect of membranes on the osteogenic differentiation of ADMSC was examined. These analyzes included Alizarin Red staining, alkaline phosphatase (ALP) activity, and scanning electron microscopy (SEM). In the third and final part, the effect of BSM membranes on osteoimmunomodulation was investigated using RAW 264.7 macrophage cells. In this section, the sequential and synergistic effects of M1 and M2 polarization of macrophages are examined. The findings demonstrated that HA-coated BSM PLA membranes promoted osteogenic differentiation in ADMSCs without using osteogenic differentiation stimulating medium and supported synergistic and sequential M1 and M2 macrophage polarizations in RAW 264.7 macrophage cell lines. These results suggested that HA-coated BSM PLA membranes are prospective approaches to shape the osteoimmune response and promote osteogenic stem cell differentiation, paving the way for future biomaterials research. These results also offer ethical benefits in minimizing animal research and represent a substantial advancement in the improvement of biomaterials, which closely mimic the natural bone microenvironment.

Specific objectives of thesis include:

1. To mimic bone surface topography via soft lithography technique.

2. To mimic bone surface chemistry by modifying bone surface topography mimicked membranes with Col-I and HA.

3. To analyze the effect of bone surface topography mimic on osteogenic differentiation of stem cells by ADMSC differentiation.

4. To observe the effect of bone surface chemistry mimic on osteogenic differentiation of stem cells by studying ADMSC differentiation.

5. To analyze the synergistic effect of bone surface topography and Col-I and HA immobilization on osteogenic differentiation of stem cells by analyzing ADMSC differentiation.

6. To examine the effect of bone surface topography mimic on osteoimmunomodulation by examining polarization of monocytes/macrophages to M1 or M2 phenotype.

7. To examine the effect of bone surface chemistry mimic on osteoimmunomodulation with immobilization of Col-I and HA on BSM PLA membranes by evaluating polarization of monocytes/macrophages to M1 or M2 phenotype.

8. To observe the synergistic effect of bone surface topography and Col-I and HA immobilization on osteoimmunomodulation by investigating polarization of monocytes/macrophages to M1 or M2 phenotype.

2. BACKGROUND

2.1 Cell Microenvironment

The cell microenvironment is a complicated and dynamic system. It consists of multiple components, including the physicochemical environment, soluble signaling factors, the ECM, and cell-to-cell interactions (Figure 2.1). These components work together to regulate cellular activity and tissue homeostasis. Understanding the cellular response to these variables is critical for developing regenerative medicine strategies and tissue engineering techniques [53, 54]. Furthermore, understanding the significance of the cell microenvironment is pivotal for designing therapeutics for diseases characterized by inappropriate cell activity, such as cancer, tissue degradation, and immunological disorders [55].

The ECM is composed of proteins such as collagen, fibronectin, and laminin. It is also an important part of the cell microenvironment, providing scaffold design as well as pharmacological signals that regulate cell adherence, survival, and differentiation [54, 57]. For example, type-I collagen promotes osteogenic differentiation of MSCs through bone formation-related integrin-mediated signaling pathways [58]. Fibronectin stimulates cell adherence and migration, connecting cells and their ECM through integrin linkage to regulate MSC differentiation into osteoblasts [54]. Finally, laminins play a significant role in stem cell osteogenesis by interacting with receptors in the cell membrane such as integrins and dystroglycans, as well as providing the molecular foundation for cell signaling and cell-ECM interactions [59]. Additionally, the physicochemical factor, mostly represented by oxidative stress mediated by reactive oxygen species (ROS), regulates both adipogenic and osteogenic differentiation of MSCs [60]. One of the major challenges in biomaterial design is replicating the complexity and functionality of the native ECM. The composition and organization of the ECM vary among different tissues, developmental stages, and diseases [61]. Biomaterials must be tailored to mimic specific ECM characteristics to ensure appropriate tissue inte-

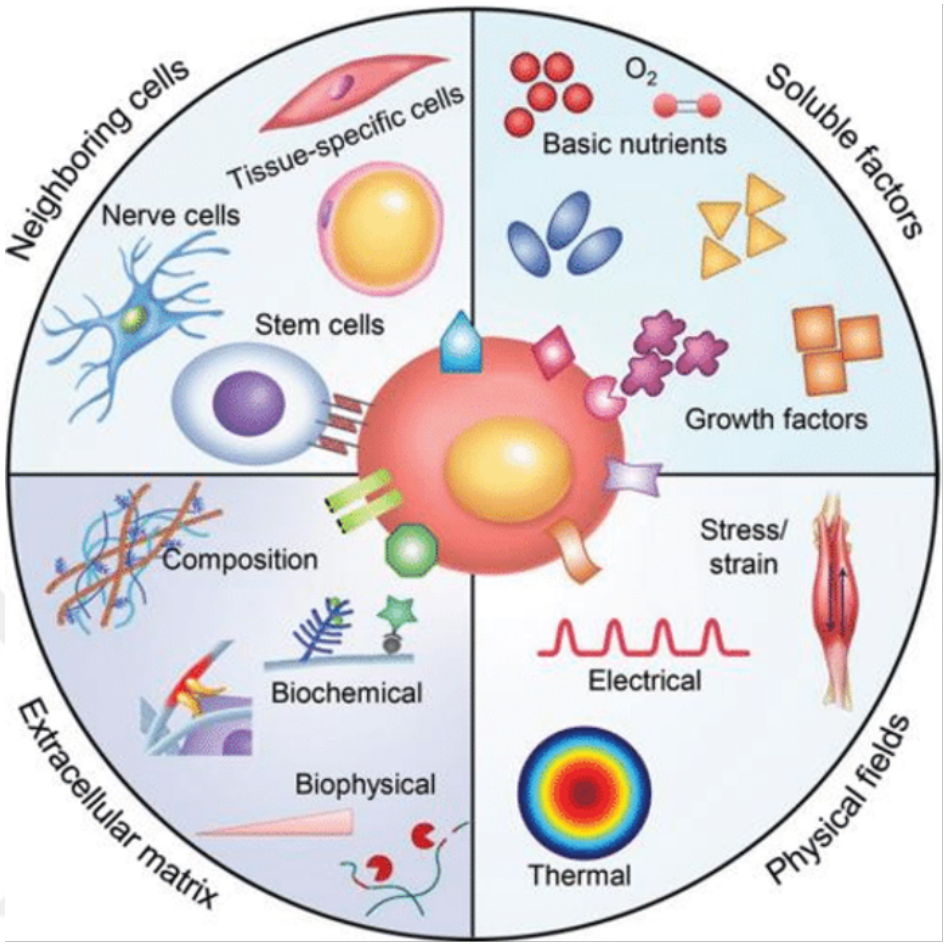


Figure 2.1 Illustration of the key elements of the cellular microenvironment [56].

gration, cellular response, and functionality [62]. Challenges include optimizing the design of biomaterials to provide the right mechanical properties, biochemical cues, and topographical features that govern cell behavior within the specific tissue microenvironment [63]. The ECM is a complex and dynamic network that plays a critical role in tissue development, homeostasis, and regeneration. Understanding its composition, structure, and functions provides valuable insights for designing biomaterials that can mimic its properties and support cellular interactions. Biomaterials that replicate the ECM's features hold great potential for use in regenerative medicine and tissue engineering approaches. Overcoming challenges in biomaterial design, such as mimicking the complexity and the dynamic ECM nature, is vital for developing effective strategies in tissue regeneration and ultimately improving patient outcomes. Soluble signaling factors belong to the group of growth factors, cytokines, morphogens, and peptides. These are responsible for acting as chemical messages in the cell microenvironment,

directing cellular behavior, and determining cell fate, acting through autocrine and paracrine signaling pathways [64]. These factors are essential for directing stem cell self-regeneration or differentiation processes and regulating immune responses, including inflammation and tissue repair [65, 66]. For example, IGF-1 and NGF application following the spinal cord lesion reduces spasticity and improves functional recovery, revealing its neuroprotective effects and problems in neural tissue regeneration [11]. Another of the most important growth factors, FGF, has been revealed to shed light on increased osteogenic differentiation of MSCs in combination with other signaling molecules [67]. A protein cytokine (AIMP1) was identified to induce MSC proliferation via fibroblast growth factor receptor 2 activation and subsequent signaling [68]. TGF-β is known for its dual action in promoting osteogenesis while modulating immune responses, which is important for bone regeneration and osteoimmunomodulation [69]. Besides, VEGF, among many others, has a significant role in angiogenesis and osteogenesis, reflecting one more additional pivotal role of soluble signaling factors in the cell microenvironment [70]. Mechanical properties, topographical cues, pH, and oxygen tension in the microenvironment significantly affect cell behavior and determine cell fate. For instance, stem cells exhibit lineage-specific responses based on the mechanical cues provided by their microenvironment [57]. Furthermore, topographical cues, whether in the ECM or artificially created, impact cell migration, spatial organization, and differentiation processes [71]. Mechanical forces are essential in triggering stem cell fate, illustrating the concept of a stem cell 'mechano-niche' [72]. The stiffness of the polymeric matrices has a decisive impact on the osteogenic differentiation of MSC/PC, and stiffer matrices favor osteogenic lineage commitment [16]. Diverse microtopographies, including microgrooves, micropillars, and micropits, were found to stimulate the osteogenic differentiation of MSCs, highlighting the importance of the physicochemical environment in tissue engineering [73]. Cell to cell interactions within the microenvironment play a vital role in tissue formation, regeneration, and immune regulation. In stem cell niches, neighboring cells provide cues that guide the self-renewal, differentiation, and lineage commitment of stem cells [74]. For example, the interaction between MSCs and endothelial cells by paracrine signaling further empowers the therapeutic potential of MSCs in tissue regeneration [75]. Neighboring cells in the bone marrow niche regulate HSCs, emphasizing that cell to cell interactions within this

niche dictate HSC quiescence while promoting HSC self-renewal [76]. In the context of osteoimmunomodulation, immune cells such as macrophages interact with MSCs, influencing their differentiation and promoting bone regeneration [77]. These immune-cell-modulating nanoparticle-loaded nanoparticles optimize bone-remodeling outcomes and demonstrate the potential of advanced drug-delivery systems in the context of regenerative medicine [78]. Additionally, immune-derived exosomes not only generally promote osseointegration but also regulate the immune environment, further emphasizing the importance of cellâcell interactions for tissue engineering studies [79]. Finally, the microenvironment of a cell is a complex and dynamic system that is composed of the ECM, soluble signaling factors, the physicochemical environment, and cellâcell interactions. These four key parameters work in synergy with each other to support the cells and control their behavior. The ECM provides structural integrity and biochemical cues. Similarly, the soluble signaling factors are the guiding messengers for cellular responses. The mechanical properties and topographical cues of the physicochemical environment guide cell behavior and spatial organization. Additionally, cell to cell interactions also determine cell behavior and regulate cell fate. Comprehending the intricate interconnections among the elements within the cellular microenvironment is crucial for advancing regenerative medicine, tissue engineering, and crafting targeted treatments for various diseases.

2.2 Cell Biomaterial Interaction

The cell-biomaterial interface is one of the most critical bases for new strategies in tissue engineering and regenerative medicine [80]. Cell and biomaterial interaction can be regulated by surface properties of the biomaterials that include topography, chemistry, mechanical features (elastic modulus, strength, etc.), surface charge, wettability, and roughness [81, 82]. These properties regulate cell adhesion, migration, proliferation, differentiation, and polarization on biomaterial surfaces, attributing to the function of engineered tissues [83, 84]. Cellular adhesion is one of the important steps in the tissue regeneration process, playing a role in subsequent cellular behaviors such as migration, proliferation, and differentiation [40]. Biomaterial surface properties

have a significant impact on cell adhesion [85]. For instance, Chen *et al.* analyzed the properties of PLA scaffolds as responsible for favoring adhesion and proliferation of human dermal fibroblasts [40]. Furthermore, Yamada and Cukierman demonstrated that Col-I provides specific binding sites for cell adhesion, promoting the adhesion of cells followed by a spreading phase [86]. Similarly, Ohgushi *et al.* demonstrated that HA promotes excellent cell adhesion because of its biocompatibility and close similarity to minerals found in bone [87]. Moreover, Groth and colleagues found that cells adhere better to PLA scaffolds with specific surface patterns, highlighting the importance of these patterns for cell attachment [88]. Once cells are attached, they migrate to start wound healing and tissue formation [89]. The surface topography and chemistry of biomaterials help guide this cell migration [90]. For instance, Jiang *et al.* observed that PLA-made artificial nerve conduits helped nerve cells move, leading to nerve regeneration [91]. Li *et al.* showed that protein fibers made through electrospinning helped cell migration, which is important for tissue formation [89]. Han *et al.* noticed that mouse induced pluripotent stem cells (iPSCs) migrated well on biomaterials that mimic the body's natural environment, stimulating their differentiation into Schwann cells [92]. He *et al.* demonstrated that the micro/nanotopography of dental implants affected the movement of dental pulp cells, which is important for regenerating dental tissues [93]. The proliferation of cells on biomaterials is crucial to produce enough cells for tissue formation [53]. The properties of these materials, such as their stiffness and surface chemistry, affect cell proliferation [53, 94]. For example, Altankov *et al.* suggested that surface charge affects cell proliferation, with positively charged surfaces encouraging more proliferation [95]. Anselme and Bigerelle found that the texture of titanium surfaces affects human bone cells, enhancing their adherence and proliferation over time [96]. Bacakova *et al.* showed that modifying the surface of implants is crucial to boosting cell proliferation [97]. Hench and Polak discussed advanced biomaterials designed to trigger specific cell responses, including proliferation [80]. Liu and Ma noted that scaffolds made from PLA support the proliferation of bone cells, which is crucial for engineering bone tissue [98]. Differentiating stem cells to specific types of cells is critical for tissue engineering [57]. The surface properties of biomaterials can direct stem cells with the help of physical and chemical cues (Figure 2.2) [99, 100]. For example, Boyan *et al.* found that the surface of materials plays a critical role in how bone and

cartilage cells respond [101]. Curran *et al.* showed that sticking to silane-modified glass surfaces guides MSC differentiation [102]. Discher *et al.* demonstrated that cells are able to feel and react to the stiffness of their microenvironment, which affects stem cell differentiation [57]. Engler *et al.* showed that the elasticity of the material directs stem cell fate, with softer materials promoting neural differentiation and stiffer ones promoting bone differentiation [53]. Hutmacher emphasized the importance of scaffold properties in guiding stem cell differentiation for bone and cartilage engineering [103].

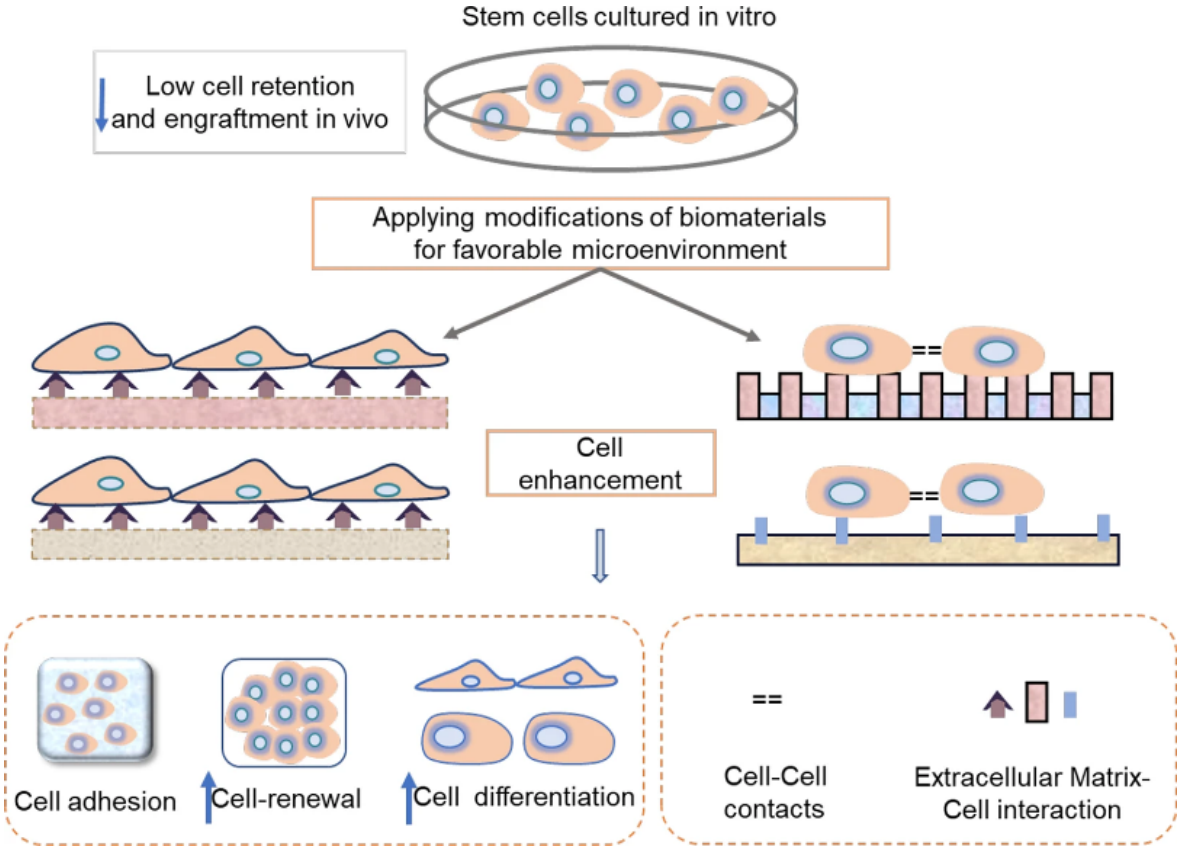


Figure 2.2 Engineered Microenvironment to Regulate Stem Cell Behavior. The engineered scaffolds create a favorable niche by biochemical and biophysical modifications, enhancing cell differentiation, retention, engraftment, and self-renewal through cell-matrix and cell-to-cell interactions. The optimized microenvironment promotes effective tissue repair and regeneration [104].

Finally, macrophage polarization is critical for immune response and tissue repair [105]. The surface properties of biomaterials can modulate macrophage behavior and polarization [35]. For instance, Anderson *et al.* discussed how foreign body reactions to biomaterials are influenced by macrophage activity [83]. Brown *et al.* demonstrated that macrophage polarization can be influenced by the surface chem-

istry of biomaterials, promoting a shift towards the anti-inflammatory M2 phenotype [106]. Chen *et al.* highlighted the role of biomaterials in osteoimmunomodulation, promoting bone regeneration by influencing macrophage polarization [81]. Moreover, Franz *et al.* reviewed the implications of immune reactions to grafts, emphasizing the need for immunomodulatory biomaterials [105]. Spiller *et al.* showed that sequential delivery of immunomodulatory cytokines facilitated the transition of macrophages from the M1 to M2 phenotype, enhancing vascularization and bone healing [35]. To sum up, the interplay between cells and biomaterials is crucial for the effectiveness of regenerative medicine strategies. The surface properties of biomaterials significantly influence cellular responses, including adhesion, migration, proliferation, differentiation, and macrophage polarization. Surface topography, chemical composition, mechanical features, surface charge, wettability, and roughness are examples of surface properties of biomaterials. A thorough understanding and optimization of these interactions are crucial for creating biomaterials that effectively support tissue regeneration and improve clinical outcomes. Advancements in this field will drive the development of next-generation biomaterials designed to enhance tissue repair and regeneration by leveraging these cellular mechanisms.

2.2.1 Surface Topography

The cell-biomaterial interface is an essential feature for the tissue engineering field as well as regenerative medicine approaches. Material surface topography, or its physical features, are key to affecting cell behavior [107]. The adhesion, migration, proliferation, differentiation, and macrophage polarization of cells can all be influenced by various kinds of topographies, such as ordered, random, micro, and nanotopographies [108, 109]. Microtopographies, or surface characteristics with dimensions on the micrometer scale, such as pits, ridges, and grooves, are important for controlling cellular behaviors, shaping the morphology of cells, and regulating cell alignment [110, 111]. For example, microgrooves on titanium surfaces significantly improved the adhesion of human osteoblasts [111]. According to Jiang *et al.*, aligned microgrooves on PLA promoted nerve regeneration by improving nerve cell migration [91]. Additionally,

microtopographies on PLA scaffolds resulted in an increase in cell proliferation [88] and triggered osteogenic differentiation of stem cells [101]. Moreover, Anderson *et al.* suggested that diverse topographies on biomaterials can regulate macrophage activity by promoting a beneficial polarization towards the M2 phenotype [83]. Nanotopographies, defined as surface features with nanometer-scale dimensions like nanopillars, nanogrooves, and nanopores, can interact with cell surface receptors and affect protein adsorption, which may change cell behavior [100, 112]. For example, nanopillars on surfaces improved osteoblast attachment [113]. Polymer surfaces with 13-nm-high islands may increase endothelial cell proliferation [112]. Additionally, nanotopographies with 15 nm length scales on TiO_2 nanotube surfaces may trigger osteoblast differentiation [114]. Random topographies, with irregular features, closely mimic the natural ECM. These topographies are used to observe natural cellular behaviors [57, 81]. Surface roughness on biomaterials improved fibroblast adhesion, increasing implant integration [115]. Random nanoscale roughness also stimulated human mesenchymal stem cell migration, which is important for wound healing [116]. These irregular topographies also promoted osteoblast proliferation and triggered stem cell differentiation by responding to substrate stiffness and roughness [57, 117]. Additionally, they modulated macrophage polarization, promoting bone regeneration [81]. Ordered surface patterns, like rows of pillars or grooves, can be accurately managed and duplicated, making them perfect for examining distinct cell reactions [50, 118]. Kim *et al.* found that arranging nanopillars in arrays improved fibroblast adhesion and spreading [119]. These landscapes also influenced the movement of fibroblasts in a certain direction and enhanced the growth of endothelial cells, which is important for creating vascular tissues. Additionally, structured surface patterns influenced the direction in which stem cells develop, encouraging the formation of bone cells [53]. They also helped switch macrophages from the M1 to M2 phenotype, which improved vascularization and bone healing [35]. In summary, biomaterial surface topography is an important factor that affects different cellular behaviors, including adhesion, migration, proliferation, differentiation, and macrophage polarization. Different topographies such as microtopographies, nanotopographies, random, and ordered topographies provide diverse physical signals, which may increase or inhibit specific cellular functions. By understanding and optimizing these topographical features, it is possible to improve the interaction be-

tween cells and biomaterials. This improvement may lead to an increase in the number of research studies in this area to develop next-generation biomaterials that provide better cellular functions and promote tissue regeneration.

2.2.2 Surface Chemistry

Surface chemistry is crucial in impacting cell activity on biomaterial surfaces. The makeup and characteristics of a material's surface have a significant impact on how cells stick, move, grow, change, and polarize macrophages. Researchers can improve the functionality of engineered tissues by altering surface chemistries, such as functional groups, coatings, and chemical modifications, to enhance specific cellular responses [120]. The presence of functional groups on biomaterials' surfaces can greatly impact cell behavior. Surfaces that have been altered with hydroxyl, carboxyl, or amino groups can improve cell adhesion, proliferation, and differentiation [121]. Chen *et al.* showed that surfaces containing amino and carboxyl functional groups enhanced endothelial cell adhesion, underscoring the significance of chemical functionalities in promoting interactions between cells and surfaces [40]. Likewise, Li and colleagues found that human fibroblasts showed enhanced migration on surfaces treated with carboxyl groups [122]. Therefore, surface chemistry affects directing cell motility. In addition, Altankov *et al.* demonstrated that surfaces containing amino and hydroxyl groups promoted cell proliferation, indicating that surface chemistry can facilitate cell growth [95]. Curran and colleagues showed that MSCs differentiated better into osteoblasts on hydroxyl group surfaces [99]. Moreover, Chen *et al.* found that altering surfaces with functional groups can impact macrophage polarization, favoring an anti-inflammatory phenotype to trigger tissue healing [81]. The change in the surface chemistry of biomaterials by adding bioactive molecules or adjusting surface characteristics to enhance cellular responses [123]. Cooper *et al.* found that applying Col-I to titanium surfaces improved osteoblast adhesion, suggesting that biomimetic coatings have the potential to boost cell attachment [124]. Dalby *et al.* showed that fibronectin-coated surfaces facilitated fibroblast migration [113]. Therefore, protein coatings could direct cell movement. Huang *et al.* demonstrated that HA-coated surfaces promoted the growth of bone

marrow stromal cells, suggesting that bioactive coatings can aid in cell proliferation [125]. Lin *et al.* also stated that HA-coated surfaces help guide the differentiation of MSCs into osteoblasts, showing the efficacy of bioactive coatings in controlling stem cell destiny [126]. Furthermore, Brown and colleagues demonstrated that M2 macrophage polarization, which is advantageous for tissue healing, was enhanced on surfaces treated with anti-inflammatory agents [106]. Changing the surfaces of biomaterials using techniques like plasma treatment, polymer grafting, or chemical etching can add distinct chemical characteristics that impact how cells interact with the surfaces [127]. Cooper and his team discovered that modifying titanium surfaces with plasma caused higher osteoblast adhesion, indicating that changing the chemistry can improve cell interactions [128]. Li *et al.* discovered that modifying polymer surfaces with plasma increased the movement of endothelial cells, proving that chemical changes influence cell migration [89]. Bacakova and colleagues highlighted that cell proliferation was increased by chemically modified surfaces, indicating that surface chemistry has the potential to promote cell growth [97]. Discher *et al.* showed that altering surface chemistry and stiffness can control stem cell differentiation [57]. Additionally, Spiller and colleagues demonstrated that altering surface chemistry could be used to release immunomodulatory cytokines in a specific sequence, which can help shift macrophages from the M1 to M2 phenotype [50]. This process can also improve blood vessel formation and promote bone repair. Overall, the surface chemistry of biomaterials plays a key role in affecting several cellular behaviors, including adhesion, migration, proliferation, differentiation, and macrophage polarization. Alteration of surface chemistries, like functional groups, coatings, and chemical modifications, offers a range of chemical signals that can either boost or hinder certain cellular functions. Through comprehension and fine-tuning of these chemical processes.

2.3 Stem Cells

Stem cells are a comprehensive group of early-stage cells that have a significant capacity to differentiate into a variety of specialized cell types. These cells are important to developmental biology, regenerative medicine, and tissue engineering be-

cause of their ability to differentiate and regenerate themselves [129, 130]. Stem cells are classified into three types: embryonic stem cells (ESCs), induced-pluripotent stem cells (iPSCs), as well as adult stem cells [131–133]. Embryonic Stem Cells (ESCs) are derived from the inner cell mass of early-stage embryos. They can differentiate into any cell type in the body. Because of this capability, they are recognized as pluripotent cells and a crucial asset for studying developmental processes and regenerative treatments [131]. Induced Pluripotent Stem Cells (iPSCs) are adult cells that have been reprogrammed to an embryonic-like state. They are able to differentiate into any cell type. This reprogramming has enormous potential for personalizing medicine and reducing immune rejection in transplants [133]. Adult Stem Cells, such as MSCs, are found in specific tissues like bone marrow and fat. They are multipotent and capable of differentiating into a range of cell types related to their tissue of origin, such as bone, cartilage, and fat cells. These cells are important for tissue maintenance, repair, and regenerative therapies [132]. Various advanced techniques are employed to produce biomaterials that support differentiation to specific lineages. For instance, the interaction between stem cells and biomaterials is heavily influenced by the scaffoldâs physical and chemical properties, which can significantly affect osteogenic differentiation. Liu *et al.* used a freeze-drying technique to prepare HA/collagen composites, enhancing the osteogenic differentiation of MSCs and promoting bone formation in vivo [134]. Similarly, Shim *et al.* utilized solid freeform fabrication (3D printing) to develop PLA scaffolds that enhance the osteogenic differentiation, improving outcomes in bone tissue engineering [135]. Moreover, Agarwal *et al.* incorporated graphene oxide (GO) nanosheets into scaffolds using a layer-by-layer assembly technique, endorsing osteogenic differentiation [136]. In addition to osteogenic differentiation, silk fibroin scaffolds have shown significant potential to promote chondrogenic differentiation. Wang *et al.* prepared silk fibroin scaffolds using a lyophilization method to trigger chondrogenic differentiation of MSCs, demonstrating potential for cartilage tissue engineering [137]. These scaffolds provide a promising environment for chondrocyte development, showing their usefulness in cartilage repair and regeneration. Furthermore, neural differentiation is another serious area where biomaterials play a significant role. Yang *et al.* utilized electrospinning to create PCL scaffolds to direct the differentiation into neural lineages and showed promise for nerve tissue engineering [138]. Additionally, Suri and Schmidt

encapsulated stem cells in polyethylene glycol (PEG) hydrogels using a photopolymerization technique, directing their differentiation into neural cells and aiding in neural tissue engineering [139]. These techniques are crucial for developing treatments for neurological disorders and injuries. Moreover, the vascular differentiation of stem cells is another area of significant research interest. GelMA hydrogels have been utilized effectively to support the stem cell differentiation into vascular endothelial cells. Chen *et al.* used a photo crosslinking technique to prepare GelMA hydrogels, offering a supportive milieu for stem cells to differentiate into vascular endothelial cells, aiding in angiogenesis [140]. This approach has significant implications for vascular tissue engineering. Kong *et al.* employed ionotropic gelation to prepare alginate hydrogels, which were then used to differentiate stem cells into insulin-producing pancreatic cells [141]. This technique showcases the potential for developing functional pancreatic tissues for treating diabetes, demonstrating the versatility of biomaterials in directing stem cell differentiation. Furthermore, Liu *et al.* prepared collagen-based scaffolds using a combination of freeze-drying and crosslinking methods to encourage stem cell differentiation into keratinocytes and fibroblasts, which are essential for skin regeneration [134]. These scaffolds accelerate the healing and regeneration of skin, highlighting their potential in treating skin injuries and conditions. In conclusion, various advanced techniques such as freeze-drying, lyophilization, electrospinning, photo crosslinking, and 3D printing are employed to produce biomaterials that promote stem cell differentiation into specific lineages. These techniques are tailored to create conducive environments for the desired differentiation pathways, enhancing the potential of stem cells in regenerative medicine. The ongoing research and development in this field hold tremendous promise for innovative treatments and therapies, ultimately improving health outcomes and quality of life.

2.3.1 Stem Cells and Osteogenic Differentiation

Osteogenic differentiation is the process by which stem cells transform into osteoblasts, the cells responsible for bone formation. This process is vital in regenerative medicine, especially for repairing bone defects and injuries [142, 143]. Several types of

stem cells, including ESCs [131], iPSCs [133], and MSCs [132], can undergo osteogenic differentiation. However, MSCs are particularly favored for this purpose due to their ease of isolation, low immunogenicity, and inherent capacity to differentiate into bone-forming cells [144, 145]. The properties of biomaterials used as scaffolds play a critical role in the success of this differentiation process. Key properties include surface topography, chemical composition, stiffness, and porosity [146, 147]. Various advanced techniques are employed to produce biomaterials that support stem cell differentiation into specific lineages. The surface topography of biomaterials, which refers to their physical texture and features, can significantly impact stem cell behavior, including adhesion, proliferation, and differentiation. For instance, Camman *et al.* explored scaffolds that mimic the cardiac ECM, demonstrating how varying topographical features can significantly impact cardiomyocyte differentiation from induced pluripotent stem cells (iPSCs). They used electrospinning to create these detailed topographies, highlighting the necessity of replicating the native cardiac environment for effective cell maturation [148]. Similarly, Calore *et al.* emphasized that rough surface topography promotes the osteogenic differentiation of MSCs in scaffolds manufactured using 3D printing. This roughness provides the necessary cues for MSCs to adhere and differentiate efficiently [149]. Furthermore, Prasopthum *et al.* demonstrated that 3D-printed scaffolds with controlled micro- and nanoporous surface topography enhance both chondrogenic and osteogenic differentiation of MSCs. This study underscores the potential of advanced printing techniques to create scaffolds with precise topographical features [150]. Bartolomeu *et al.* explored the surface topography of titanium implants, finding that hydrophilic surfaces enhance cell adhesion, differentiation, and bone integration. Their research utilized additive manufacturing techniques, showing that surface modifications can significantly improve the clinical performance of implants [151]. Chemical composition is another critical factor that influences the osteogenic differentiation of MSCs. The incorporation of specific chemical elements and compounds into biomaterials can create a favorable biochemical environment for bone formation. For instance, Li *et al.* used calcium phosphate coatings on scaffolds to modulate the transition from M1 to M2 macrophage phenotypes, which is essential for successful bone regeneration. This study highlighted the role of chemical composition in guiding cell behavior and improving therapeutic outcomes [152]. Wang *et al.* reviewed how different chemical

compositions of hydrogels influence the differentiation of MSCs into osteoblasts and chondrocytes. Their findings underscored the importance of designing scaffolds with tailored chemical properties to guide specific differentiation pathways [153]. Rahmati *et al.* emphasized that the surface chemical properties of biomaterials significantly affect osteoblast proliferation and differentiation. They showed that modifying the surface chemistry can enhance the biological performance of scaffolds [154]. Dave and Gomes demonstrated that changes in the surface chemistry of scaffolds can direct epidermal stem cell differentiation, highlighting the impact of chemical composition on stem cell behavior [155]. The stiffness of biomaterials plays a significant role in influencing cell behavior by providing physical cues that mimic the rigidity of bone tissue. Haugh *et al.* investigated the effects of stiffness within macro-porous scaffolds created via freeze-drying, finding that varying stiffness directs MSC differentiation into osteogenic and chondrogenic lineages. This study showed that mechanical properties are critical in mimicking the native tissue environment [156]. Xing *et al.* found that stiffer substrates within electrospun scaffolds significantly enhance the differentiation of neural stem cells. This research highlighted the importance of aligning scaffold stiffness with the mechanical properties of neural tissues [157]. Bai *et al.* demonstrated that stiffer substrates with specific topographical patterns promote the osteogenic differentiation of musculoskeletal cells. They used solvent casting techniques to create these structured biomaterials, emphasizing the role of stiffness in cell differentiation [158]. Wang *et al.* studied how vinculin regulates stiffness-induced differentiation in scaffolds embedded into porous chitosan, showing that mechanical cues can direct cell behavior [159]. Porosity of biomaterials affects cell infiltration, nutrient diffusion, and waste removal, which are crucial for successful tissue regeneration. Calore *et al.* highlighted that high porosity in scaffolds, achieved via 3D printing, is crucial for promoting osteogenic differentiation of MSCs. The interconnected porosity provides pathways for nutrient flow and cell migration, which are vital for tissue regeneration [149]. Khajehmohammadi *et al.* demonstrated that varying porosity in bioprinted scaffolds affects both mechanical properties and cellular differentiation. This study showed that controlling scaffold porosity is necessary for optimizing mechanical strength and biological performance [160]. Han *et al.* investigated how scaffold porosity enhances the differentiation of oligodendrocytes, using scaffolds fabricated via 3D printing. They found that opti-

mal porosity supports cell growth and differentiation [161]. Iturriaga and Van Gordon discussed the implications of porosity in 3D-printed scaffolds on tissue regeneration, emphasizing the control of topographical patterns and porosity to guide cell behavior [162]. In conclusion, the osteogenic differentiation of MSCs is profoundly influenced by various properties of biomaterials used as scaffolds. Surface topography, chemical composition, stiffness, and porosity each play a vital role in creating a conducive environment for MSC differentiation into osteoblasts. Through advancements in biomaterial design and fabrication, researchers can optimize these properties to enhance bone regeneration and improve clinical outcomes.

2.4 Immunomodulation

Immunomodulation, the regulation of the immune response, is essential in the field of biomaterials, especially for implants, tissue engineering, and drug delivery systems [105]. The interaction between biomaterials and the immune system can determine the failure and success of medical devices and therapies [83]. The immune response to biomaterials includes several cell types that coordinate a complicated network of interactions influenced by chemical composition, surface topography, degradation products, and biomolecule functionalization [163]. Understanding these interactions and factors is critical for developing biomaterials that improve immune responses for improved therapeutic outcomes [105]. The immune response to biomaterials is characterized by the involvement of a variety of cell types. Macrophages are crucial players in this process, capable of adopting a range of phenotypes from pro-inflammatory (M1) to anti-inflammatory (M2). The dominant phenotype at the biomaterial interface can profoundly influence tissue integration and healing outcomes [106]. Dendritic cells (DCs), serving as professional antigen-presenting cells, bridge innate and adaptive immunity by capturing and presenting antigens, thereby affecting T cell activation and polarization [164]. T cells, which include helper (Th), cytotoxic (Tc), and regulatory (Treg) subsets, are essential in directing immune responses to biomaterials, guided by cytokine environments and antigen presentation [165]. Neutrophils, as the first responders following the insertion of biomaterials, initiate inflammation and impact the recruitment

and activity of other immune cells [166]. Mast cells, known for their role in allergic reactions, release mediators that contribute to inflammation and fibrosis [167]. Natural killer (NK) cells, which identify and eliminate stressed or transformed cells, also play a role in modulating the immune environment at the site of biomaterial implantation [168]. Additionally, fibroblasts, though not classified as immune cells, interact with immune cells and biomaterials, influencing tissue remodeling and immune responses [169]. Several factors influence immunomodulation by biomaterials, including chemical composition, surface topographies, degradation products, and biomolecule functionalization. The chemical composition of materials significantly determines the type of immune response elicited. For instance, titanium and its alloys are renowned for their biocompatibility and minimal immune activation, making them ideal for orthopedic implants [170]. In contrast, some polymers may cause inflammatory responses, which underscores the importance of material selection in biomaterial design [83]. For instance, polylactic-co-glycolic acid (PLGA) is one of the generally used biomaterials because of its biocompatibility and controllable degradation properties; however, the degradation products of PLGA can alter the local pH and activity of immune cells [171]. Another surface property that critically influences the immune responses is the surface topography of the biomaterial, which encompasses surface roughness and specific surface patterns. Surface properties can modulate macrophage behavior and even facilitate a pro-healing phenotype. Previous studies demonstrated that specific surface topographies can increase the adhesion of immunomodulatory cells while minimizing the activation of pro-inflammatory pathways [40, 172]. For example, micro- and nanoscale engineered surfaces have been found to reduce the fibrotic responses and improve tissue integration [173]. Finally, biomaterial degradation products also affect the immune response. Biodegradable polymers, such as PLGA, can degrade to form lactic and glycolic acids, which can control the local pH and activity of immune cells. These degradation products can promote and inhibit inflammation according to their concentration and local tissue environment [171]. Understanding the correlation between degradation products and immune cells is necessary to develop biomaterials that promote tissue healing and integration. Biomaterials that are functionalized with bioactive molecules such as growth factors, cytokines, or peptides can be used to guide particular immune responses. Surface coatings with anti-inflammatory cytokines, such

as IL-10, can greatly decrease inflammation and facilitate healing [174]. Similarly, incorporating immunomodulatory compounds into biomaterial scaffolds might enhance tissue regeneration by controlling local immune responses [175]. In conclusion, the interaction between the immune system and biomaterials is a complicated and multidimensional process, involving several cellular players and impacted by a variety of circumstances. Understanding and controlling these interactions enables the development of prospective biomaterials that optimize immune reactions to observe improved therapeutic outcomes.

2.4.1 Macrophages

Macrophages are a critical component of the innate immune system, playing central roles in tissue homeostasis, inflammation, and wound healing [66, 176, 177]. They are highly versatile immune cells that exhibit remarkable plasticity, enabling them to adapt their functions according to the microenvironment and immune signals they encounter. Macrophages can be found in diverse phenotypes, which are often categorized in a spectrum of activation states [66]. Initially, macrophages are referred to as M0 macrophages, which are known as undifferentiated or resting macrophages [178]. M0 macrophages have not yet polarized into specific phenotypes and are a transitional state capable of adopting M1 or M2 phenotypes depending on the signals they receive [179]. M0 macrophages are characterized by low inflammatory activity and are involved in tissue maintenance [66]. M0 macrophages have an essential role in the initial immune reaction, acting as sentinels to sense alterations in the microenvironment and initiate subsequent immune reactions [180, 181]. Upon exposure to specific stimuli, M0 macrophages can differentiate into M1 or M2 macrophages according to the immune signals present in the local environment [182]. The ability of macrophages to transition between M0, M1, and M2 phenotypes provides them with the flexibility to regulate immune responses and tissue repair processes, contributing to tissue homeostasis and the resolution of inflammation [183]. This plasticity allows macrophages to dynamically respond to changing conditions and play distinct roles in both acute and chronic inflammatory environments [184]. Macrophages are fundamen-

tal to several critical processes, such as pathogen recognition, phagocytosis, antigen presentation, cytokine secretion, tissue remodeling, and wound healing [66, 176]. Their ability to exhibit plasticity allows them to assume different functional states, commonly categorized as M1 and M2 macrophages [66, 176, 184]. M1 macrophages, or classically activated macrophages, are linked with pro-inflammatory responses and the body's defense against infections. They produce pro-inflammatory cytokines like tumor necrosis factor-alpha (TNF-α), interleukin-6 (IL-6), and inducible nitric oxide synthase (iNOS), and generate reactive oxygen species (ROS) to fight pathogens. [66, 176]. M1 macrophages support Th1 responses and have enhanced antigen-presenting capabilities to activate T cells [184]. Conversely, M2 macrophages, known as alternatively activated macrophages, are associated with tissue repair, immune modulation, and anti-inflammatory responses [185–187]. These macrophages are activated by stimuli such as IL-4, IL-13, and glucocorticoids, displaying unique phenotypes influenced by their microenvironment and signals [66, 176]. M2 macrophages are further categorized into subtypes like M2a, M2b, M2c, and M2d, each with distinct characteristics and functions (Figure 2.3) [185–187].

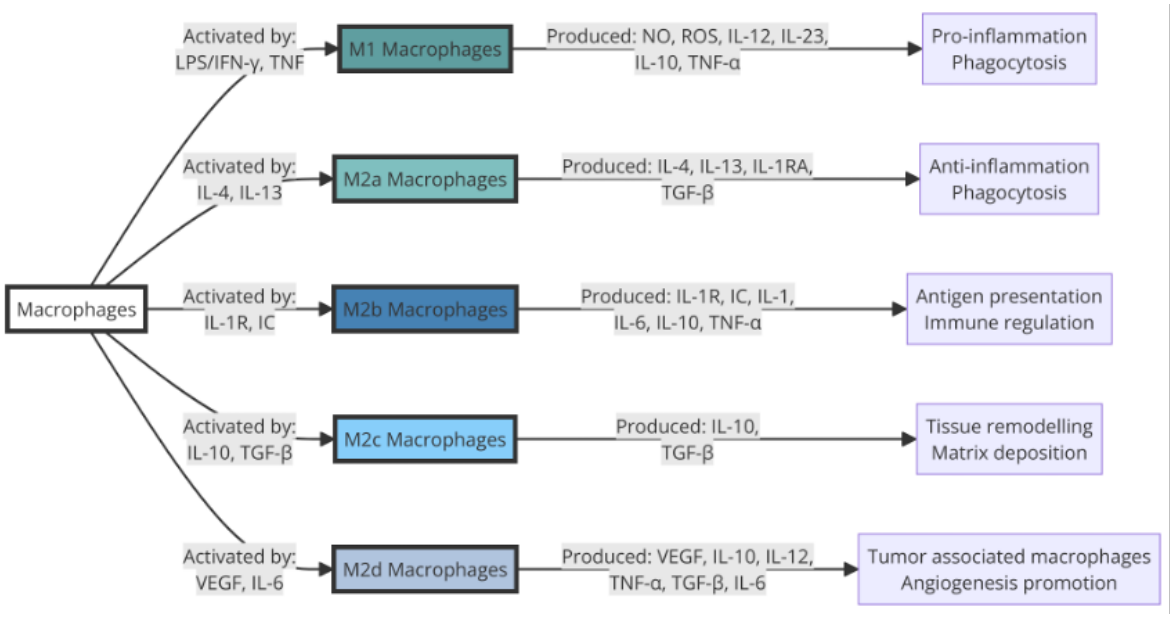


Figure 2.3 Diagram showing macrophage polarization into different phenotypes. Macrophages differentiate into M1 (pro-inflammation and phagocytosis), M2a (anti-inflammation and phagocytosis), M2b (antigen presentation and immune regulation), M2c (tissue remodeling and matrix deposition), and M2d (tumor-associated macrophages and angiogenesis promotion) based on various activating stimuli and cytokine production [188].

The balance between M1 and M2 macrophages and their dynamic interactions is essential for tissue homeostasis and immune response regulation [66, 184]. Disruptions in this balance can lead to various diseases, including chronic inflammation, autoimmune disorders, and tissue fibrosis. In tissue engineering and regenerative medicine, leveraging the immunomodulatory properties of macrophages is highly significant [189]. Techniques involving biomaterials, scaffold-based systems, and cell-based therapies have been designed to influence macrophage function and polarization [190]. By manipulating biochemical and biophysical cues in the microenvironment, it is possible to steer macrophages towards specific phenotypes and modulate inflammatory responses [37, 190].

2.4.2 Osteoimmunomodulation

Osteoimmunomodulation refers to the interaction between the immune system and bone tissue, focusing on how immune responses influence bone healing and regeneration. This concept is crucial for understanding the dynamic relationship between the skeletal and immune systems, playing a noteworthy role in regenerative medicine and tissue engineering. The target is to develop biomaterials to regulate immune reactions to enhance bone repair and integration [83, 191, 192]. Biomaterials used in bone regeneration significantly influence osteoimmunomodulation by interacting with immune cells and modulating their responses. These materials are designed to support the complex process of bone healing, which includes the initial inflammatory response followed by tissue regeneration and remodeling. By tailoring the properties of these biomaterials, researchers aim to improve the efficacy of bone regeneration strategies [192, 193]. The properties of these biomaterials, such as surface topography, chemical composition, and wettability, are critical in determining their effectiveness in bone healing and regeneration [81]. These properties influence how biomaterials interact with cells and tissues, impacting cellular activities like attachment, proliferation, immune modulation, and differentiation. Surface topography is a crucial factor in osteoimmunomodulation, affecting the behavior of immune cells and osteoblasts. Wang *et al.* found that 1D wrinkles that generate grooves and ridges have been shown to promote

M2 polarization, whereas 2D wrinkles that create pits and bumps can stimulate M1 polarization [39]. Chen *et al.* suggested that surface topography can have an impact on macrophage behavior regardless of surface chemistry. Specifically, the increase in topography feature size from 500 nm to 2 μm can restrict macrophage activation and inflammation-related activities [40]. Barth *et al.* also found that macrophages seeded onto rougher surfaces tend to exhibit an M2-like phenotype, which suppresses immune and anti-inflammatory processes and promotes angiogenesis, ECM formation, and tissue repair [41]. Similarly, Damanik *et al.* reported that microporous structures trigger macrophages to exhibit an M2-like phenotype [42]. The chemical composition of biomaterials is another pivotal aspect of osteoimmunomodulation. For example, Laquerriere *et al.* suggested that small-diameter HA particles can activate immune cells to release pivotal cytokines, which favor inflammation [43]. Fernandes *et al.* reported that HA granules activate M2 polarization of THP-1 cells more than M1 [44]. According to Sadowska *et al.*, HA-coated materials have a critical role in starting the production of pro-inflammatory cytokines and controlling osteogenic processes [45]. Moreover, Correia *et al.* found that unmodified PLA activates M1 macrophage polarization, while Col-I modified PLA macrophages with the same surface properties generally prompt M2 macrophage polarization [49]. The effect of surface charge on biomaterials is a critical factor in osteoimmunomodulation, influencing both immune responses and bone regeneration. Research has shown that piezoelectric biomaterials with controllable surface charges can significantly enhance osteogenesis and modulate immune responses. For instance, negatively charged surfaces on $BaTiO_3$/β-TCP ceramics promote protein adsorption and osteogenic differentiation of bone marrow stem cells, while positively charged surfaces inhibit M1 macrophage polarization, reducing inflammation and promoting a pro-healing environment [194]. Similarly, mesoporous silica nanoparticles (MSNs) with appropriate surface charges can establish an immune microenvironment conducive to bone regeneration by activating immune cells and promoting cytokine release [195]. Additionally, surface-modified bioactive glass/graphene oxide (BG/GO) scaffolds have been shown to promote M2 macrophage polarization, enhancing osteogenic differentiation and angiogenesis [196]. These findings highlight the importance of surface charge in designing biomaterials that not only support bone regeneration but also modulate immune responses to create a conducive healing en-

vironment [179, 197]. Wettability, or the ability of a surface to interact with water, is another important factor influencing cell behavior and immune responses. For example, Hotchkiss *et al.* conducted experiments with macrophages cultured on various titanium surfaces with different morphologies and wettability. They found that surface wettability influences macrophage polarization, with hydrophilic rough surfaces inducing an anti-inflammatory M2-like state, while smooth hydrophobic surfaces promoted inflammatory M1-like activation after 3 days of incubation [198]. Similarly, Lv *et al.* demonstrated that hydrophilic TiO_2 surfaces exhibit enhanced anti-inflammatory and pro-healing performance of macrophages compared to hydrophobic ones [199]. Moreover, Gao *et al.* developed super-hydrophilic titania nanotube (TNT) surfaces by hydrogenation, which maintained the nanotubular structure without adding any impurities. Their findings indicated that this super-hydrophilic surface favored the polarization of macrophages towards an anti-inflammatory phenotype under standard conditions [200]. During wound healing, macrophages assume two distinct phenotypes, M1 and M2, which are important for different stages in the process [201–203]. M1 macrophages are present immediately after tissue injury (1-3 days) as they help to control the early inflammatory phase [35]. Additionally, M1 macrophages play a crucial role in initiating angiogenesis and osteogenesis. After the initial 3 days, M1 macrophages are gradually replaced by M2 macrophages, which serve to reduce inflammation and stimulate new tissue formation [35]. Injuries with suboptimal healing outcomes often result from a disruption in the transition of macrophages from the M1 to M2 phenotype. To enhance the healing process, a proposed strategy involves biomaterials that promote the sequential activation of M1 followed by M2 macrophages. This approach is considered more effective in promoting healing compared to activating either phenotype in isolation or concurrently promoting both. A swift transition from M1 to M2 activation accelerates the recovery process. It is well-established that M1 and M2 macrophages play synergistic and sequential roles in tissue repair [50, 202–204]. For instance, He *et al.* demonstrated that proteomic analysis of macrophages revealed a temporal sequence in M1 and M2 activation, critical for macrophage function modulation during inflammation and repair [205]. In bone defect regeneration, a composite BMP-2 and small intestine submucosa hydrogel was shown to sequentially induce M1 and M2 polarization, enhancing bone healing [51]. Similarly, Luo *et*

al. found that IFN-γ/SrBG composite scaffolds stimulate osteogenesis by regulating macrophages from M1 to M2, highlighting the importance of timed polarization in bone regeneration [206]. Additionally, a study by Li *et al.* used 3D-printed IFN-γ-loading scaffolds to sequentially activate M1 and M2 macrophages, promoting vascularization and bone regeneration [207]. These findings are complemented by Qiao *et al.*, who illustrated that biomaterial-induced bone regeneration requires the sequential activation of macrophage polarizations [208]. Moreover, O'Brien *et al.* emphasized that sequential drug delivery could modulate macrophage behavior to enhance implant integration [209]. Alhamdi *et al.* reported that calcium phosphate coatings could control M1-to-M2 transitions in aged macrophages, crucial for bone grafting success [203]. These studies collectively affirm that the sequential polarization of macrophages is pivotal for effective therapeutic outcomes in tissue engineering and immune responses. In conclusion, osteoimmunomodulation represents a critical intersection between the immune system and bone tissue, significantly influencing the success of bone regeneration strategies. The properties of biomaterials, including surface topography, chemical composition, and wettability, are vital in modulating immune responses to enhance bone healing and integration. The research underscores the importance of sequential macrophage polarization, transitioning from M1 to M2 phenotypes, to create an optimal regenerative environment. Advancements in biomaterial design that facilitate this transition have shown promising results in improving bone healing outcomes. Continued research and development in this field are essential to fully harness the potential of biomaterials in promoting effective and efficient bone regeneration, ultimately improving clinical outcomes for patients with bone defects and injuries.

3. PRODUCTION AND CHARACTERIZATION OF BSM PLA MEMBRANES

This chapter describes the procedures for creating and characterizing BSM PLA membranes (Figure 3.1). The manufacturing process begins with the processing of bone samples from bovine femurs, which are cleaned and processed to eliminate any cells, tissues, lipids, and immunologic residue. The cleaned bone fragments are used as templates to create Polydimethylsiloxane (PDMS) molds that mimic the bone surface topography. These molds are then utilized to create BSM PLA membranes by casting a PLA solution onto the PDMS molds.

The chapter delves deeper into the biochemical alterations of the BSM PLA membranes, concentrating on Col-I and HA immobilization. These modifications were performed after the membrane surfaces were activated by oxygen plasma treatment. The membranes were incubated in an EDAC phosphate buffer solution before being treated with Col-I at varied doses. HA modification was accomplished by soaking the membranes in an HA solution. Both modifications attempted to mimic the bone surface structure biochemically.

Modified membranes were characterized using immunohistochemical analysis, Sirius Red staining for collagen concentration, wettability analysis via water contact angle measurements, surface chemistry analysis using FTIR and XPS, and surface topography analysis using AFM and SEM. These procedures aid in evaluating the membranes' physical and chemical characteristics, assuring the effectiveness of bone surface mimicking and chemical modifications.

3.1 Experimental Procedures

3.1.1 Instrumentations and Reagents

Before BSM PLA membranes were modified with HA and Col-I, O_2 plasma treatment (AP-300, Nordson March, Concord, USA) was carried out. The morphology and surface topography of BSM PLA membranes were examined using a SEM (Carl Zeiss EVO 40, Germany), which provided extensive insights into the samples' surface features. AFM (Park Systems, Korea) was used to analyze the surface topography of both modified and unmodified membranes in more detail. The chemical compositions of modified membranes were investigated using FTIR (Perkin Elmer, Spectrum 100, USA), whereas the compositions of unmodified and modified membranes were assessed using XPS (Thermo Scientific K-Alpha, UK). The phase composition of HA-modified membranes was determined by XRD (D/max-2500X, Japan). A digital microscope (HIROX KH-8700) was used to image stained samples during immunohistochemical analysis. The wettability characteristics of the produced membrane surfaces were assessed using a contact angle measuring equipment (CAM 100, KSV, Finland), which provided important data on the surfaces' hydrophilic or hydrophobic nature.

PDMS (Sylgard 184; Dow Corning, Midland, MI) was used to produce PDMS molds, to mimic bone surface topography by using soft lithography technique. BSM PLA membranes were modified with HA (Sigma Aldrich 677418) and rat tail Col-I (Sigma-Aldrich C7661) to mimic bone's biochemical properties.

3.1.2 BSM Membrane Production

3.1.2.1 Bone Surface Cleaning Bovine femur was chosen as a template to prepare BSM membranes. Bone samples were treated according to a xenograft cleaning process [210, 211]. Only the diaphysis part of the cortical bone, at least 10 cm away from the cutting points, was utilized to obtain bone pieces with the dimensions of 2 cm x 2 cm. The bone pieces were first placed in absolute ethanol for 30 minutes and then

transferred into a 10% NaCl solution for 24 hours. During the transfer, the bone pieces were subjected to ultrasonic bath treatment for the first and last 20 minutes to remove any remaining cells and tissue on the bone surface. Subsequently, the bone pieces were immersed in acetone for 20 minutes to eliminate lipids and other possible residues from the surface. Immunologic residues were removed, and prions were inactivated by immersing the samples in 3% H_2O_2, 2 M NaOH, and acetone for 72 hours, 2 hours, and 144 hours, respectively. After chemical cleaning, the bone parts were allowed to dry overnight at room temperature and were kept ready for use in soft lithography.

3.1.2.2 Preparation of PDMS Molds Bone surface topography was mimicked by using soft lithography technique. PDMS (Sylgard 184; Dow Corning, Midland, MI) solution was prepared with a prepolymer cross-linker ratio of 10:1 (w/w). The prepared PDMS solution was degassed and poured onto the pre-treated bone and incubated at 70°C for 4 hours.

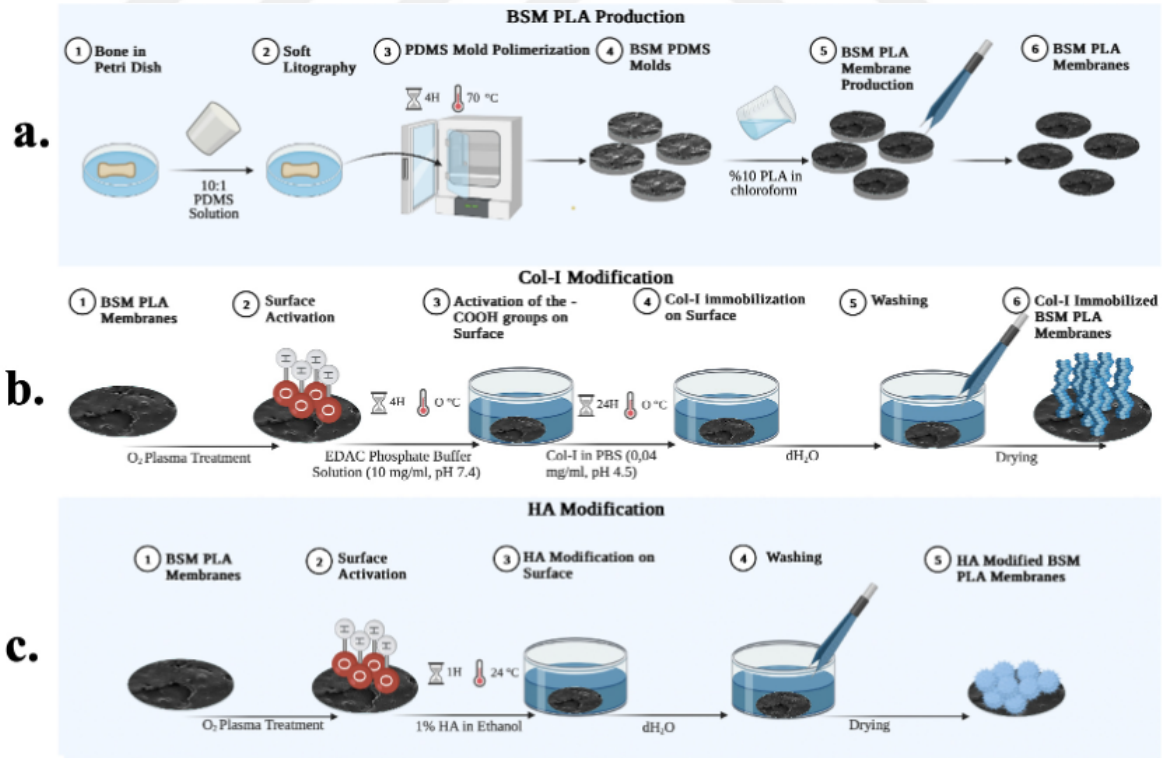


Figure 3.1 Schematic of BSM-PLA membrane production. a. BSM-PLA Membrane Preparation Process, b. Col-I Modification of BSM-PLA Membrane Preparation Process, c. HA Modification of BSM-PLA Membrane Preparation Process.

3.1.2.3 Bone Surface Mimicked PLA Production BSM negative PDMS molds were used to fabricate BSM PLA membranes. PLA (10% (w/v), intrinsic viscosity, 1.8 dL/g, 221.000 g/moL MW) was dissolved in chloroform and cast onto bone surface mimicked negative PDMS molds for 12 hours [212]. As a negative control, plain PLA membranes were also fabricated using plain PDMS molds.

3.1.3 Col-I and HA Immobilization of the BSM PLA Membranes

To mimic bone microstructure biochemically, BSM PLA membranes were modified with HA and Col-I after being activated with O_2 plasma treatment at 100 W Power, 80 Pa Pressure for 10 minutes. For Col-I modification, membranes were incubated with EDAC Phosphate Buffer solution (10 mg/mL, pH 7.4) for 4 hours at 0°C to activate the COOH residues on the surface of the membranes. Finally, these membranes were transferred into the phosphate buffer solution (pH 4.5), containing 0.05, 0.1, 0.25, 0.5 mg/mL Col-I amount for 24 hours, and membranes were kept in deionized water at 37°C for 24 hours to remove unbound collagen from the surface [213]. For HA modification, the membranes were immersed into 50 mL of 1% (w/v) HA in ethanol suspension for 1 hour at room temperature under stirring after O_2 plasma treatment [214]. Plain PLA membranes were modified using the same procedure.

3.1.3.1 Optimization of Col-I Immobilization

Immunohistochemical Analysis for Col-I Immobilized Area Calculation The maximum surface coverage with optimum Col-I amount was analyzed by using immunohistochemical staining, which was performed for unmodified and Col-I modified bone surface mimicked PLA membranes. For blocking, the membranes were incubated into 10% normal goat serum in PBST (PBS + 0.1% Tween 20) for 30 minutes. Blocked membranes were incubated in 1:100 diluted primary antibody (SC-59772, Santa Cruz, CA, USA) overnight at 0°C and then membranes were incubated in 1:200 diluted sec-

ondary antibody [ab97057, Goat Anti-Rat IgG H&L (HRP)] for 10 minutes at room temperature. After incubation in DAB solution (Pierce™ 34002) for 5 minutes, Col-I modified bone surface mimicked PLA membranes were stained. The images of the stained membranes were taken by using a digital microscope (HIROX KH-8700) [215]. Col-I coating area percentage was calculated by using ImageJ software by pixel counting.

Immobilized Col-I Concentration Analysis via Sirius Red The total collagen content on the collagen immobilized biomaterials was measured by Sirius Red/Fast Green Collagen Staining Kit (9046, Chondrex) according to the manufacturerâs instructions. This technique was applied to examine both unmodified and Col-I modified plain, as well as bone surface mimicked PLA membranes. To ensure reliability, all experiments were conducted in triplicates. The unmodified plain PLA membranes were utilized as the designated control group for comparative analysis.

3.1.4 Physicochemical Characterization of the Col-I and HA Modifications

3.1.4.1 Wettability Analysis Sessile drop water contact angle analysis was used to assess wettability properties of unmodified, HA coated, and Col-I modified plain and BSM PLA membranes (CAM 100, KSV, Finland). Deionized water droplets (10 µL) were dropped onto surfaces, and water contact angles were measured by circle fitting. All measurements were performed at room temperature. All water contact angle measurements reported in this thesis are the average of 8 different measurements per experimental group and they were taken from 2 different regions within each experimental group.

3.1.4.2 Fourier Transform Infrared Spectroscopy (FTIR) FTIR spectra were documented over the range of 4000 to 400 cm^{-1} with 32 scans to examine the chemical compositions of the HA-coated and Col-I modified plain and bone surface

mimicked PLA membranes. The FTIR measurements were performed by using Attenuated Total Reflectance (ATR) FTIR spectrophotometer (Perkin Elmer, Spectrum 100, USA) [216].

3.1.4.3 X-ray photoelectron spectroscopy (XPS) To determine the compositions of unmodified and Col-I modified membranes, XPS (Thermo Scientific K-Alpha, UK) was utilized with an Al Kα radiation (photon energy 1000 eV) excitation source. Survey spectra were taken over the range of 1350 to 0 eV with a pass energy of 150 eV [217].

3.1.4.4 X-ray Diffraction (XRD) The phase composition of unmodified and HA modified membranes was characterized by XRD (D/max-2500X, Japan) with monochromated Cu Kα radiation (λ = 1.5405 Ã, 120 mA, 40 kV) in a continuous scan mode and its scanning speed of 8Â°/min as well as the 2θ range was from 10 to 70 [218].

3.1.5 Characterization of the Surface Topography of the BSM Membranes

3.1.5.1 Atomic Force Microscopy (AFM) Sample surface topographies of the HA or Col-I modified and unmodified Plain PLA and BSM PLA membranes (diameter 15.6 mm) were analyzed via AFM (Park Systems, Korea) equipped with NSC36B silicon cantilever in non-contact mode. Scan fields of 12x12 Âμm^2 on all surfaces were processed using the XEI software (1.18).

3.1.5.2 Scanning Electron Microscopy (SEM) To observe bone surface mimicking quality and the possible alteration in surface topography after Col-I or HA modifications, surface topography of modified and unmodified Plain PLA and BSM PLA membranes were analyzed by SEM (Carl Zeiss EVO 40, Germany). Observed areas were pinpointed by creating a reference point on the bone piece prior to preparation

of the PDMS negative mold. All surfaces were coated with a thin layer of platinum (50 nm).

3.1.6 Statistical Analysis

Results were given as mean ± standard deviation and differences were considered as statistically significant for $p < 0.05$. GraphPad Prism 9 (GraphPad Software, USA) was used to perform the statistical analyses. The data were analyzed using two-way ANOVA followed by Tukey's post hoc multiple comparison test. Plain Col-I 0.05 was accepted as a control group for Immunohistochemistry and Sirius Red analyses.

3.2 Results

3.2.1 Optimization of Collagen Immobilization

Immunohistochemistry analysis was conducted to determine the amount of Col-I immobilization, and microscopy images of both unmodified and modified PLA were taken by using digital microscopy and analyzed by using ImageJ software. The results showed that an increase in Col-I concentration in the immobilization solution led to an increase in Col-I coating area percentage. As depicted in Figures 3.2a and 3.2b, 0.05 mg/mL of Col-I concentration covered 51.26 ± 4.22% of the Plain PLA membrane surfaces and 59.43 ± 10.67% of the BSM PLA membrane surfaces. When the Col-I concentration was increased to 0.1 mg/mL, the coating area percentage increased to 66.63 ± 14.96% for Plain PLA membrane surfaces and 71.84 ± 6.88% for BSM PLA membrane surfaces. A concentration of 0.25 mg/mL resulted in a coating area percentage of 84.10 ± 3.15% for Plain PLA membrane surfaces and 92.73 ± 4.31% for BSM PLA membrane surfaces. The highest Col-I coating area percentage was achieved with a concentration of 0.5 mg/mL, which coated 94.36 ± 2.75% of the Plain PLA membrane surface and 98.43 ± 0.43% of the BSM PLA membrane surface.

The maximum immobilized amount of Col-I for each experimental group (0.05 mg/mL, 0.1 mg/mL, 0.25 mg/mL, and 0.5 mg/mL) was analyzed by using Sirius Red staining and is given in Figure 3.2c. 0.353 ± 0.007 $\mu g/cm^2$ of Col-I was immobilized onto BSM membranes after having been incubated with 0.5 mg/mL Col-I solution, and it resulted in the highest immobilized Col-I amount and was significantly statistically different compared to other experimental groups. Then, 0.241 ± 0.017 $\mu g/cm^2$ Col-I was immobilized onto Plain membranes which were incubated in 0.5 mg/mL Col-I solution, and it resulted in being the second highest Col-I amount and significantly statistically different from each experimental group. Therefore, 0.5 mg/mL Col-I concentration was found to be the optimum concentration for the immobilization of Col-I according to immobilized protein amount analysis.

3.2.2 Physicochemical Characterization of the Col-I and HA Modifications

3.2.2.1 Wettability Analysis Biomaterial surface wettability is regulated mainly by chemical properties and surface topography. Hydrophobicity/hydrophilicity affect the protein adsorption behavior on the surface, which in turn affects cell attachment and proliferation [219]. To estimate the effect of the surface topography and the surface chemical modifications on the surface wettability, water contact angle values (WCA) were measured. WCA values of plain PLA and BSM membranes with and without HA and Col-I modified are given in Figure 3.3. Contact angle value of plain PLA was measured at $108.67° \pm 2.2°$ which was similar to the values reported for PLA surfaces by Schaub *et al.* [220]. Ma *et al.* suggested that after Col-I was immobilized on the BSM PLA surface, the WCA reduced from $71.0° \pm 1.6°$ to $35.0° \pm 3.4°$. Contact angle value of Col-I modified PLA was $52.8° \pm 5.3°$. Thereby, the hydrophilic property of the Col-I modified samples was increased two-fold which was parallel to the results of Ma *et al.* [221]. WCA measurement of the unmodified plain PLA was $98.1° \pm 3.2°$. The WCA result of the HA modified plain PLA was $50.1° \pm 5.6°$. According to Ge *et al.*, the WCA measurements of the HA coated PLA membranes dropped from 131.9° to 70.3°, which was in agreement with the obtained results [222]. In addition, unmodified BSM PLA membranes were more hydrophobic than plain PLA membranes ($98.1° \pm 3.2°$ and

108.7° ± 2.3°, respectively). Col-I and HA modified BSM PLA membranes whose WCA values were measured as 38.0° ± 9.2° and 32.4° ± 4.8°, respectively, compared to their plain counterparts, whose WCA values were taken as 52.8° ± 5.3° and 50.1° ± 5.6°, respectively. These results were in line with the Wenzel Theorem, which explains the relation of surface hydrophilicity with material surface roughness. Increased surface roughness on a material will make hydrophobic materials turn into more hydrophobic and hydrophilic materials turn into more hydrophilic [223].

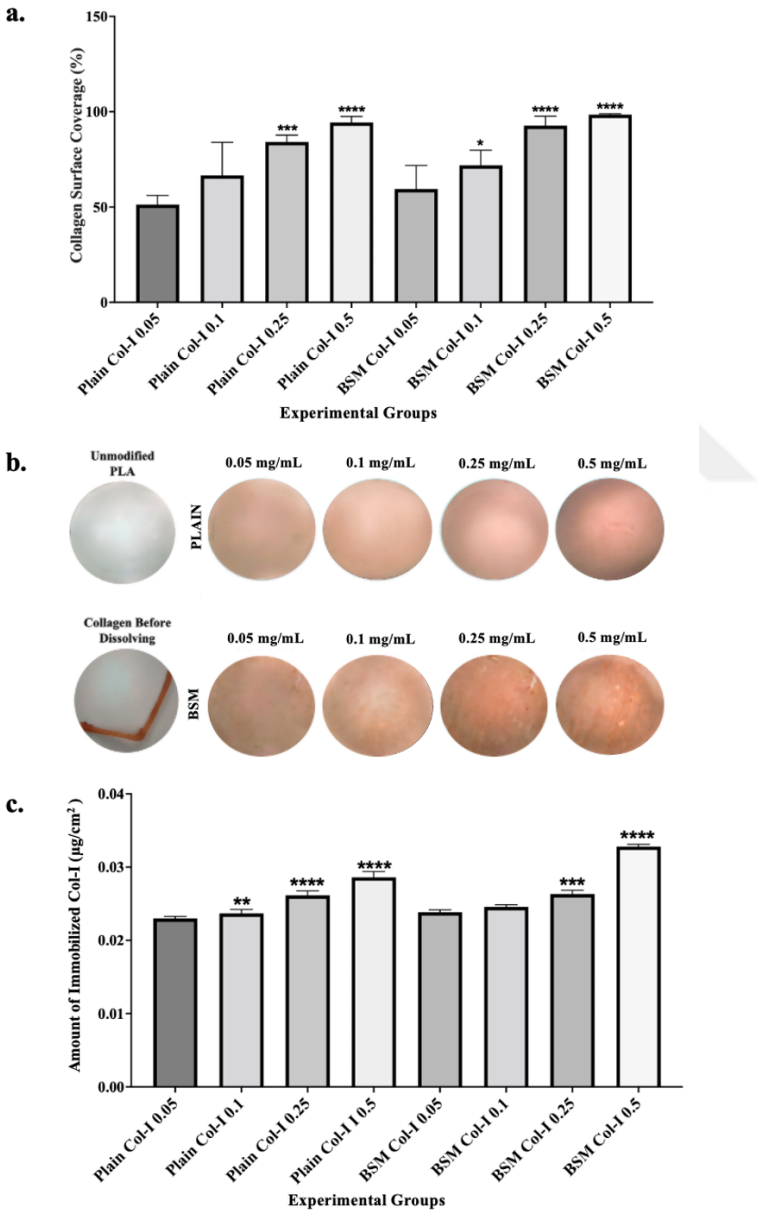


Figure 3.2 a. Immunohistostaining analysis of unmodified and Col-I modified plain and BSM PLA membranes by using ImageJ, b. Immunohistostaining of unmodified and Col-I modified plain and BSM PLA membranes, c. Quantification of Col-I content by Sirius Red assay (* $p < 0.05$, ** $p < 0.01$, *** $p < 0.001$, **** $p < 0.0001$).

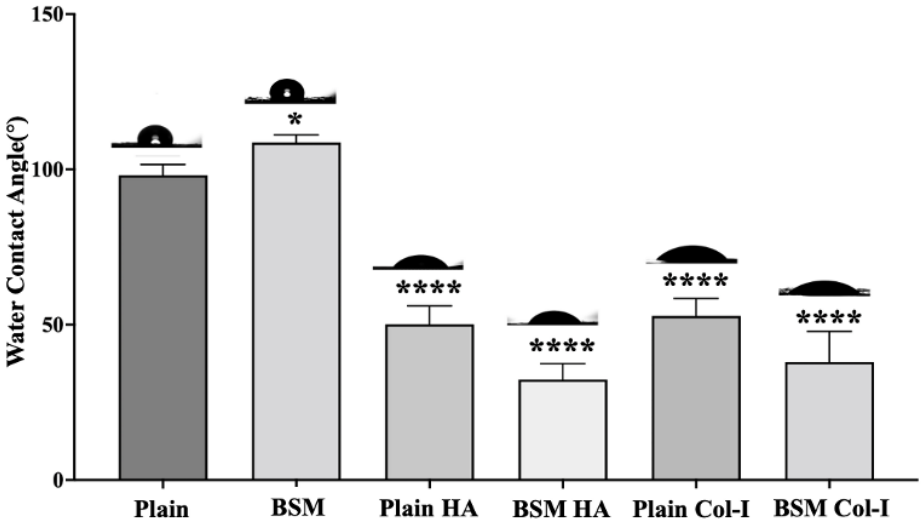


Figure 3.3 Characterization of surface wettability of unmodified and modified plain and BSM membranes by WCA analysis.

3.2.2.2 Fourier Transform Infrared Spectroscopy (FTIR) The composition of Col-I and HA modified PLA membranes was analyzed by FTIR analysis. Col-I modified membranes showed Amide A, Amide I, Amide II and Amide III peaks in their FTIR spectra (Figure 3.4). The peak centered at 3350 cm^{-1} involves a mutual band of hydrogen bonds from the intermolecular water and amide A of collagen related to N-H stretching. The peak around 1650 cm^{-1} was accepted as an amide I band and instigated due to the C=O stretching vibrations coupled with NâH bending vibrations [224]. The peaks around 1545 cm^{-1} and 1238 cm^{-1} were accepted as amide II and amide III bands, respectively [224]. It can be noted that the peak around 1379 cm^{-1} was accepted as a $\delta(CH_2)$ band. Thereby, Col-I modification on the PLA membranes was proven with this data [224]. In IR spectra of the HA deposited membranes, characteristic bands were observed. Peaks observed around 485 cm^{-1}, 1200 cm^{-1}, 524 cm^{-1}, and 627 cm^{-1} were corresponded to a V2 PO_4^{3-}, V3 PO_4^{3-} and V1 PO_4, respectively. HA deposited membranes also exhibited a characteristic carbonate band. The n3 mode of CO_3^{2-} at 1355 cm^{-1} was covered by a broad band because of the occurrence of CO_3^{2-} [225, 226]. The presence of characteristic peaks and bands in the FTIR spectra provided compelling evidence for the successful modifications.

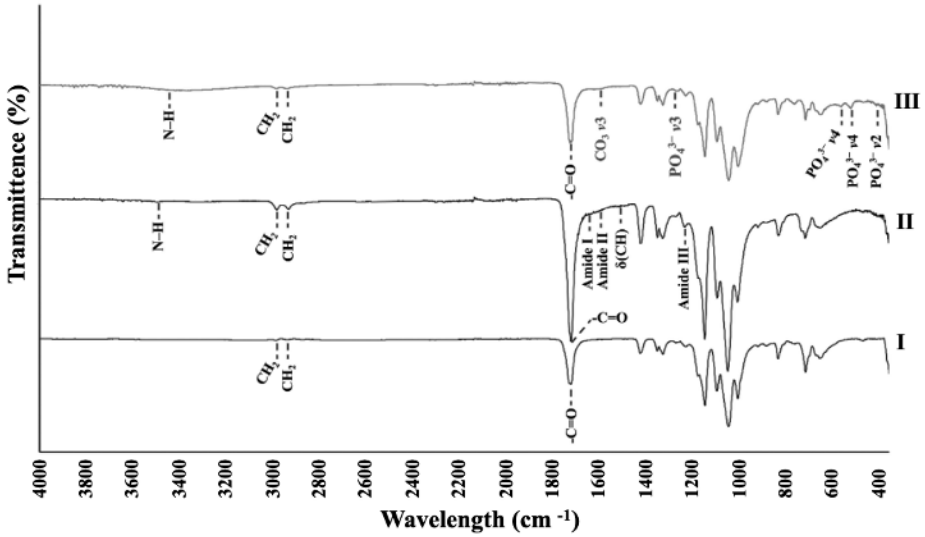


Figure 3.4 Characterization of surface chemical composition by FTIR analysis; I. Unmodified PLA, II. Col-I modified PLA, III. HA modified PLA.

3.2.2.3 X-ray photoelectron spectroscopy (XPS) The surface chemical compositions of unmodified and Col-I modified PLA membranes were evaluated by XPS analysis and the results were given in Figure 3.5. XPS spectra demonstrated that the C1s and O1s peaks of unmodified and Col-I modified PLA membranes were alike to each other. The C1s spectra showed peaks at 284.8 eV, 287.1 eV, and 289.3 eV which related to C-C or C-H, C-O, -CO-O, respectively [227, 228]. O1s peak was adjusted with a single component at 531.8 eV corresponding to O=C-N interactions [229]. Furthermore, although there were not any N1s peaks in the XPS analysis result of the unmodified PLA membranes, Col-I modified PLA membranes had characteristic N1s peak at 410 eV [230]. The results of the XPS analysis provided complementary evidence to the FTIR data, demonstrating the success of the modifications, and enlightening the chemical changes taking place on the surface of the PLA membranes.

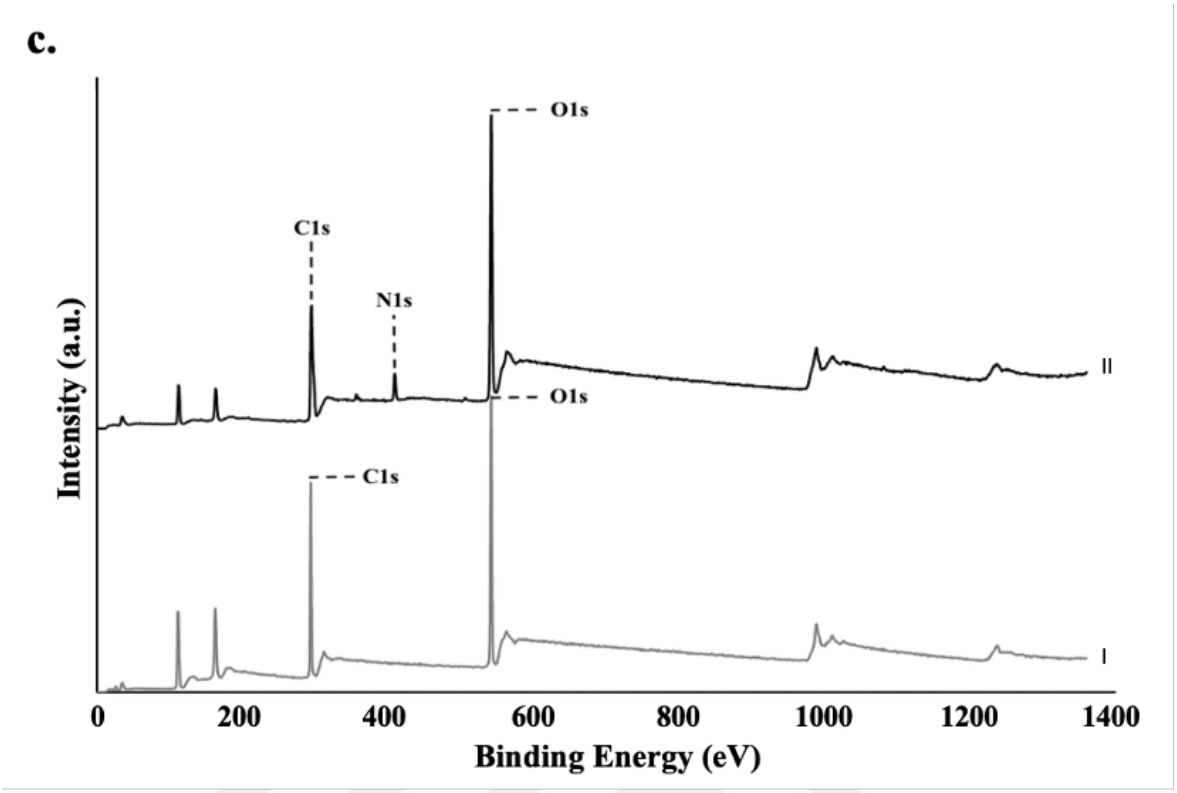


Figure 3.5 Characterization of surface chemical composition by XPS analysis; I. Unmodified PLA, II. Col-I modified PLA.

3.2.2.4 X-ray Diffraction (XRD) To prove the deposition of the HA on the modified membrane surfaces, pure HA powder, HA modified PLA membranes, and unmodified PLA membranes, static XRD analysis was performed. The results were shown in Figure 3.6. Peaks seen in the XRD patterns of HA modified PLA membranes and HA powder can be assigned to the (002), (102), (210), (211), and (310) crystallographic planes of HA [231]. Thereby, the XRD analysis provided valuable insight, underscoring the clear evidence of HA-associated peaks in both the HA powder and the HA-coated PLA membranes. In striking contrast, these distinctive peaks were conspicuously absent in the XRD patterns of the unmodified PLA membranes. This compelling observation serves as robust evidence, strengthening the claim that HA was successfully anchored onto the PLA membrane surfaces.

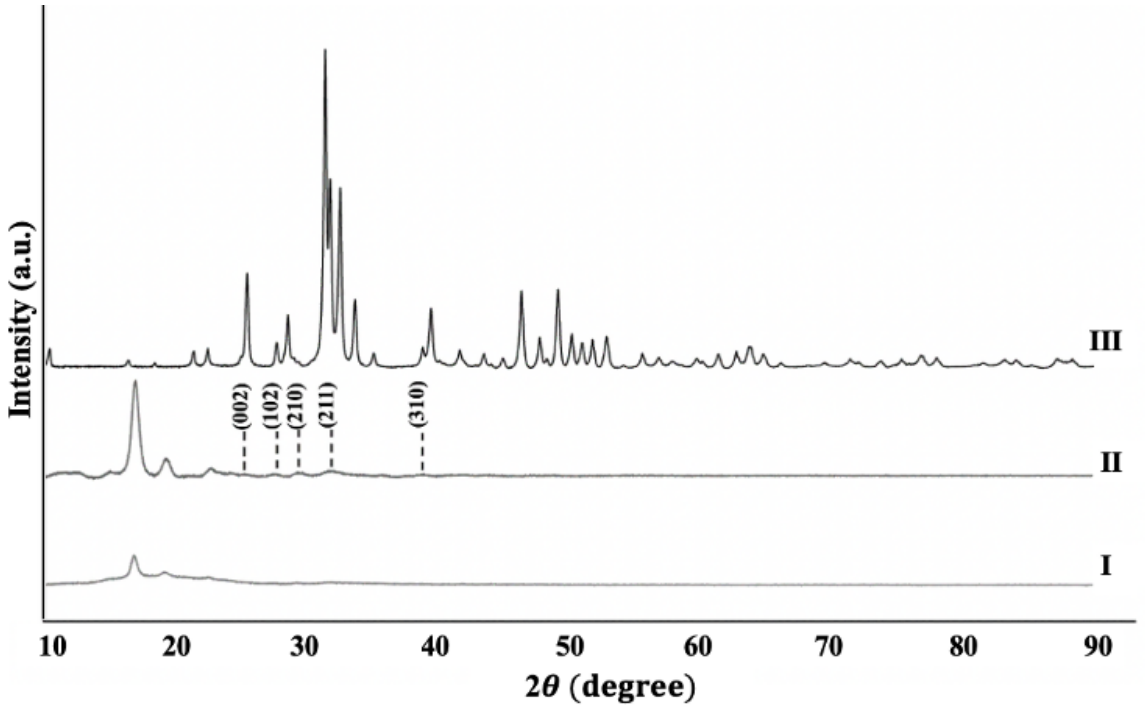


Figure 3.6 Characterization of surface crystallinity by XRD Analysis; I. Unmodified PLA, II. HA modified PLA, III. Pure HA.

3.2.3 Characterization of the Surface Topography of the Unmodified and Modified BSM Membranes

3.2.3.1 Scanning Electron Microscopy (SEM) The quality of mimicking was examined by comparing the SEM images from the same areas on the bone piece, its PDMS negative mold, and its corresponding unmodified and modified BSM PLA membranes. These areas were compared to each other by creating a reference point by making a dent on the bone piece prior to preparation of the PDMS negative mold. The natural bone surface topography comprises microstructures with diverse heights and pits. The surface topography of all protrusions and intrusions of the bone was completely mimicked both onto the PDMS negative mold and, from there, onto the PLA membranes (Figure 3.7). Based on the findings, it can be inferred that the utilization of soft lithography (molding) and solvent casting of PLA offers an effective approach for mimicking bone surface topography, encompassing anisotropic microstructures. After Col-I and HA modifications, the varied heights and pits of the bone surface can still be observed on the BSM membranes produced using the soft lithography technique.

Therefore, it can be said that the modifications did not disrupt the mimicked bone surface microstructure.

3.2.3.2 Atomic Force Microscopy (AFM) To investigate the surface features of the bone, BSM PLA, HA modified, and Col-I modified BSM PLA membranes, non-contact AFM analysis was performed on the samples. As shown in Figure 3.7, the surface features of the bone were a mirror image of the PDMS mold, while the unmodified and Col-I and HA modified BSM PLA surface features were like the bone itself.

The roughness values of the bone and BSM PDMS molds were calculated to be 50.02 nm and 56.36 nm, respectively. The roughness value of the BSM PLA membrane was calculated to be Ra = 64.00 nm, which was higher than that of plain PLA membranes (Ra = 5.88 nm). These results were consistent with the literature, which suggests this is due to the high surface roughness value of the bone surface [28].

Mas *et al.* suggested that collagen had a net-like fibril structure. So, a rise in the roughness of the surface after Col-I modification was expected [229]. The roughness of the Col-I modified BSM PLA membranes (Ra = 70.01 nm) was higher than that of unmodified BSM membranes (Ra = 50.02 nm), confirming the immobilization of collagen on the membranes.

Similarly, according to Bottino *et al.*, HA deposition on the surface led to a rise in the roughness [232]. Comparison of the roughness of the HA modified BSM PLA membranes with the unmodified membranes showed that HA modification increased the surface roughness to Ra = 71.87 nm. Although HA or Col-I modifications did not cause any deformation on the mimicked bone surface structure, these modifications increased surface roughness. Therefore, the results confirmed the mimicking quality and the change in surface features after Col-I immobilization and HA deposition on BSM PLA membranes.

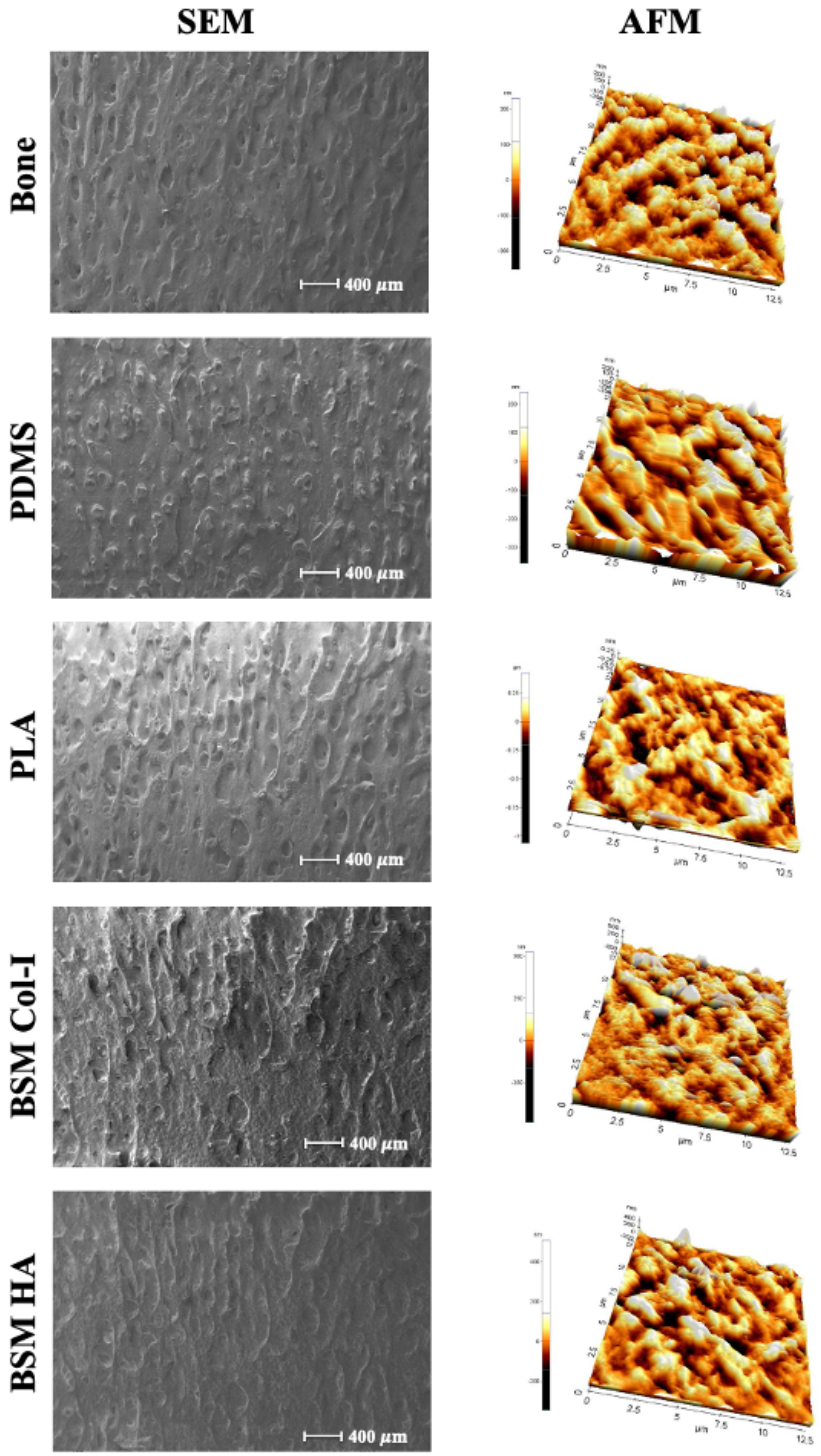


Figure 3.7 SEM and AFM images of the surface 3-D structure of the bone, BSM PDMS mold, unmodified, Col-I and HA modified BSM PLA membranes.

3.3 Discussion

The successful fabrication and characterization of BSMPLA membranes demonstrate significant advancements in replicating both the physical and biochemical properties of natural bone. This thesis meticulously followed a series of steps to ensure the accuracy and effectiveness of the BSM PLA membranes, from the initial processing of bovine femur bones to the final modifications with Col-I and HA.

The first stage involved the thorough cleaning and preparation of bovine femur bones, which were then used to create PDMS molds via soft lithography. This technique proved highly effective in capturing the intricate microstructures of the bone surface, as confirmed by SEM and AFM analyses. The SEM images revealed that the surface topography of the PLA membranes replicated the diverse heights and pits characteristic of natural bone [210, 211]. The AFM results further supported this, showing a roughness value of Ra = 64.00 nm for BSM PLA membranes, significantly higher than the Ra = 5.88 nm for plain PLA membranes. These findings underscore the importance of surface roughness in creating a biomimetic scaffold that can enhance cellular interactions [28].

The thesis further aimed to mimic the biochemical environment of bone by modifying BSM PLA membranes with Col-I and HA following oxygen plasma treatment. This plasma treatment increased the surface energy of the PLA membranes, promoting better attachment and distribution of biomolecules.

The immobilization of Col-I was optimized to enhance the bioactivity of the membranes. Immunohistochemical analysis revealed that increasing Col-I concentrations led to higher coating area percentages. For instance, a 0.5 mg/mL concentration resulted in 98.43±0.43% surface coverage on BSM PLA membranes, the highest among the tested concentrations. Sirius Red staining quantified the immobilized collagen, confirming that the 0.5 mg/mL Col-I concentration yielded the highest protein amount at 0.353 ± 0.007 $\mu g/cm^2$ [213].

Surface chemistry analysis using FTIR confirmed the presence of amide bands in Col-I modified membranes: Amide A at 3350 cm^{-1}, Amide I at 1650 cm^{-1}, Amide II at 1545 cm^{-1}, and Amide III at 1238 cm^{-1} [224]. XPS further supported these findings, with Col-I modified membranes showing characteristic N1s peaks at 400 eV, which were absent in unmodified membranes, indicating successful protein immobilization [230]. The XPS spectra demonstrated that the C1s and O1s peaks of unmodified and Col-I modified PLA membranes were similar, with peaks at 284.8 eV (C-C or C-H), 287.1 eV (C-O), and 289.3 eV (CO-O) for C1s, and a single component at 531.8 eV (O=C-N) for O1s [227, 228].

Wettability analysis indicated that the water contact angle decreased significantly from 71.0°±1.6° for plain PLA to 35.0°±3.4° for Col-I modified surfaces, suggesting increased hydrophilicity [221]. This enhanced hydrophilicity is beneficial for cell adhesion and proliferation, as cells tend to adhere better to hydrophilic surfaces. AFM analysis showed an increase in roughness from Ra = 50.02 nm for unmodified BSM membranes to Ra = 70.01 nm for Col-I modified membranes, consistent with the literature suggesting that collagenâs fibril structure enhances surface roughness [229].

HA modification aimed to replicate the mineral component of bone, supporting osteoblast activity and mineralization. HA deposition involved soaking the membranes in an HA solution, confirmed by characteristic peaks observed in FTIR and XRD analyses.

The FTIR spectra showed bands associated with HA, such as V2 PO_4^{3-} at 485 cm^{-1}, V3 PO_4^{3-} at 1200 cm^{-1}, V4 PO_4 at 524 cm^{-1} and 627 cm^{-1}, as well as CO_3^{2-} at 1355 cm^{-1}, indicating successful modification [225, 226]. The XRD patterns exhibited peaks corresponding to HA crystallographic planes at 25.8° (002), 31.7° (211), 32.2° (112), 32.9° (300), and 49.5° (213), further confirming the presence of HA on the PLA membranes [231].

AFM analysis showed that the surface roughness of HA-modified BSM PLA membranes increased to Ra = 71.87 nm. This increase is consistent with literature re-

ports indicating that HA deposition enhances surface roughness [232]. Water contact angle measurements revealed a decrease to 32.4°±4.8° for HA modified BSM membranes, reflecting increased hydrophilicity [222]. These surface modifications are crucial for improving cell-material interactions, promoting better cell adhesion, proliferation, and differentiation.

In conclusion, this thesis successfully demonstrated the fabrication of BSM PLA membranes that closely mimic the physical and biochemical properties of natural bone. The detailed characterization through SEM, AFM, FTIR, XPS, and water contact angle measurements confirmed the effectiveness of the modifications. These findings suggest that BSM PLA membranes hold great potential for bone tissue engineering applications, providing a biomimetic scaffold that supports cell adhesion, proliferation, and differentiation. Future research should focus on in vivo studies to further validate the clinical applicability and efficacy of these membranes in bone regeneration.

4. EFFECTS OF BONE SURFACE TOPOGRAPHY AND CHEMISTRY ON OSTEOGENIC DIFFERENTIATION

This section investigates the surface properties of bone-mimetic materials that affect ADMSC viability, proliferation, and osteogenic differentiation. Human ADMSCs at passage 1 were procured and cultured in MesenPRO RSTM Basal Medium and then seeded onto the modified and unmodified PLA surfaces.

To analyze cell proliferation on the produced unmodified and modified BSM PLA membranes, the AlamarBlue test was performed at different time points. ADMSC proliferation was measured on days 1, 4, and 7. It was found that ADMSCs have higher rates of proliferation on modified BSM membranes than on unmodified BSM membranes. Greater viability was observed with surfaces modified with Col-I and HA, consistent with literature suggesting that rough and hydrophilic surfaces favor the adhesion and growth of stem cells.

Osteogenic differentiation was measured by Alizarin Red S staining and ALP activity analysis. Increased reddish staining with Alizarin Red S demonstrated the existence of calcified ECM deposits. Additionally, ALP activity, a marker for early osteogenic differentiation, was analyzed colorimetrically. Both markers were higher in cells cultured on modified PLA membranes. These findings show that HA and Col-I modifications significantly improve the osteogenic potential of PLA membranes, making them suitable for bone engineering applications. Additionally, it was observed that the viability, proliferation, and osteogenic differentiation rate of ADMSCs on the HA-deposited BSM membranes were highest among the experimental groups, highlighting the potential benefits of mimicking the bone surface microenvironment to achieve desired osteogenic differentiation of MSCs and the importance of surface topography and chemistry in developing biomaterials for bone tissue engineering applications.

4.1 Experimental Procedures

4.1.1 Instrumentation and Reagents

ADMSCs were utilized to estimate the effects of surface properties on cell viability, proliferation, and osteogenic differentiation (Invitrogen, R7788-115). The ADMSCs were cultured in MesenPRO RSTM Basal Medium supplemented with 2% MesenPRO RSTM Growth Supplement (Invitrogen, 12746-012). Additionally, 2 mM L-glutamine (Invitrogen, 25030-081) and 5 μg/ml gentamicin (Invitrogen, 15710-064) were added to the growth medium to support cell culture. For the passaging of cells, trypsin (Invitrogen, 12604-013) was used to detach the cells. Cell proliferation was quantitatively measured using the AlamarBlue assay (Invitrogen, DAL1100). Absorbance values for this assay were read using a microplate reader (BIO-RAD iMark). To detect calcified ECM deposits, a 2% Alizarin Red S Solution (Sigma-Aldrich, A5533) was employed. Cells were fixed prior to this staining using 10% neutral buffer formalin (Sigma-Aldrich, HT501128). Alkaline phosphatase activity was assessed with the Alkaline Phosphatase Activity Colorimetric Assay Kit (BioVision, Mountain View, CA). For preparing samples for SEM analysis, a 2.5% glutaraldehyde solution (Sigma-Aldrich, G5882) was used to fix the cells. The samples were then dried using hexamethyldisilazane (HMDS, 440191, Sigma-Aldrich). The SEM analysis was conducted using a Carl Zeiss EVO 40 microscope operating at 10 kV to observe cell morphology. The red color intensity was observed and documented using a digital microscope (HIROX KH-8700).

4.1.2 Cell Culture Studies

ADMSCs were utilized to analyze the effects of surface properties on cell viability, proliferation, and osteogenic differentiation (Invitrogen, R7788-115). ADMSCs at passage 1 (frozen sample) were cultured in growth medium, MesenPRO RSTM Basal Medium (Invitrogen, 12746-012), consisting of 2% MesenPRO RSTM Growth Supplement (Invitrogen, 12746-012), 2 mM L-glutamine (Invitrogen, 25030-081), and 5 μg/ml of gentamicin (Invitrogen, 15710-064), at 37°C in a humidified incubator (5% CO_2).

The medium was replaced twice a week. Upon reaching 80-85% confluence, cells were trypsinized using trypsin (Invitrogen, 12604-013). At passage 4, ADMSCs were seeded on modified and unmodified PLA surfaces with growth medium. To ensure cell attachment, a preincubation period of one day in the growth medium was implemented. For all analyses except cell attachment and morphology analysis using SEM, 2×10^4 cells were seeded per well in 24-well plates. For SEM analysis, 5×10^3 cells were seeded per well in 24-well plates (Figure 4.1).

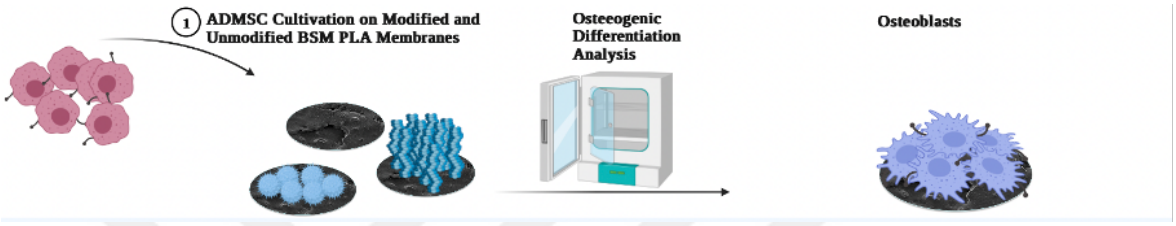


Figure 4.1 Schematic of the experimental procedure for osteogenic differentiation of mesenchymal stem cells. ADMSCs are cultured on modified and unmodified BSM PLA membranes, followed by osteogenic differentiation analysis, leading to the formation of osteoblasts.

4.1.2.1 Cell Proliferation To quantitatively measure cell proliferation, the Alamar Blue (Invitrogen, DAL1100) cell proliferation assay was used. Incubation periods were set for 1 day, 4 days, and 7 days. At each interval, the culture medium was replaced with fresh medium containing 10% AlamarBlue fluorescent dye. The samples were incubated at 37°Cin a 5% CO_2 atmosphere. From each well, 100-μL samples of the culture medium-AlamarBlue mixture were collected to measure absorbance at 570 nm and 595 nm using a microplate reader (BIO-RAD iMark). A 10% AlamarBlue solution in cell-free medium was used as a negative control. Cell proliferation was assessed by calculating the reduction percentage of AlamarBlue with the following Eq. 4.1:

$$Reduced = \frac{C_{RED}TestWell}{C_{OX}NegativeControlWell} = \left(\frac{(\epsilon_{OX})_{\lambda_2} A_{\lambda_1} - (\epsilon_{OX})_{\lambda_1} A_{\lambda_2}}{(\epsilon_{RED})_{\lambda_1} A'_{\lambda_2} - (\epsilon_{RED})_{\lambda_2} A'_{\lambda_1}} \right) \times 100 \quad (4.1)$$

where $\epsilon_{\lambda 1}$ and $\epsilon_{\lambda 2}$ are constants representing the molar extinction coefficients of AlamarBlue. ϵ_{OX} is the oxidized form at 570 nm, and ϵ_{RED} is the reduced form at 595

nm. $A_{\lambda 1}$ and $A_{\lambda 2}$ are the absorbance values at 570 nm and 595 nm for the test wells, respectively. $A'_{\lambda 1}$ and $A'_{\lambda 2}$ are the absorbance values for the negative control wells at 570 nm and 595 nm, respectively [233].

4.1.2.2 Cell Morphology and Attachment Analysis After 7 days of incubation, the medium was removed, scaffolds were rinsed with PBS, and cells were fixed in 2.5% glutaraldehyde (Sigma-Aldrich, G5882) for 20 minutes. Scaffolds were then dehydrated in increasing concentrations of ethanol (30%, 50%, 70%, 90%, and 100%) and dried with hexamethyldisilazane (HMDS, Sigma-Aldrich, 440191). Finally, samples were coated with a 50 nm layer of platinum and examined using a Carl Zeiss EVO 40 microscope operating at 10 kV.

4.1.2.3 Osteogenic Differentiation Analysis

Alizarin Red S Analysis On days 14, 21, and 28, Alizarin Red S staining was used to identify calcified ECM deposits. Samples were fixed in 10% neutral buffered formalin (Sigma-Aldrich, HT501128) for 25 minutes, rinsed with distilled water, and then incubated with 1 mL of 2% Alizarin Red S solution (Sigma-Aldrich, A5533) (pH 4.1-4.3) for 1 hour. After removing the stain, scaffolds were rinsed with deionized water multiple times. Increased calcification turned the scaffolds red. The red color intensity was observed and documented using a digital microscope (HIROX KH-8700) [234].

Alkaline Phosphatase Activity Analysis After 7, 14, and 21 days of incubation, ALP activity was measured using the Alkaline Phosphatase Activity Colorimetric Assay Kit (BioVision, Mountain View, CA). Optical density was measured at 540 nm using a microplate reader (BIO-RAD iMark) [235].

4.1.3 Statistical Analysis

Results were presented as mean ± standard deviation, with $p < 0.05$ considered statistically significant. GraphPad Prism 9 (GraphPad Software, USA) was used for statistical analysis. Data were analyzed using two-way ANOVA followed by Tukeyâs post hoc multiple comparison test. Plain PLA served as the control group for viability and cytokine release analysis.

4.2 Results

4.2.1 Cell Proliferation

Alamar Blue is a cell proliferation assay that utilizes the reduction of resazurin to resorufin by metabolically active cells. This reduction leads to a color change from blue to pink, which is quantitatively measured via fluorescence or absorbance. Alamar Blue is widely used because it is non-toxic and allows continuous monitoring of cell health without harming the cells. It is a reliable measure of cell proliferation and cytotoxicity in various biological and environmental systems [236–238]. The Alamar Blue assay results for the ADMSC cells on the produced unmodified and modified plain and BSM membranes were analyzed at day 1, 4, and 7, showing distinct patterns in cell proliferation and illustrated in Figure 4.2.

On Day 1, all conditions exhibited low levels of Alamar Blue degradation, indicating minimal cell proliferation or attachment. This initial phase reflects the early stage of cell seeding where cells are still adapting to the surfaces. Aging alters the properties of tissue-resident MSCs, leading to a decline in their number and functional characteristics, including reduced proliferative capacity and increased cellular senescence [239]. The early low proliferation observed aligns with this understanding of MSC behavior.

By Day 4, a significant increase in Alamar Blue degradation was observed across most conditions, signifying enhanced cell proliferation and attachment. The conditions with collagen (Plain Col-I and BSM Col-I) demonstrated the highest degradation percentages, suggesting that collagen has a substantial effect on promoting cell proliferation and attachment. This finding aligns with the study by Li *et al.*, where the modification of PLA scaffolds with HA and collagen provided a conducive surface for cell proliferation [46].

On Day 7, most conditions maintained high levels of Alamar Blue degradation, indicating sustained cell proliferation. Plain Col-I and BSM Col-I continued to show the highest degradation percentages, further confirming that collagen significantly supports continuous cell proliferation and attachment. However, a slight decrease or plateau in degradation was observed in some conditions, such as Plain HA and BSM HA. This plateau suggests the onset of differentiation, where cells begin to shift their focus from proliferation to performing specialized functions. This observation is consistent with the study by Ahn *et al.*, which found that ADSCs exhibited higher proliferation on hydrophilic and rough surfaces compared to hydrophobic and smooth surfaces [240].

The decline in proliferation during differentiation is supported by studies showing that MSCs decrease their proliferation rates as they undergo differentiation into specialized cell types, such as osteocytes and adipocytes [241, 242]. This reduction in proliferation is crucial as it indicates that cells are transitioning to a more specialized function, essential for tissue development and repair. The reduced proliferation observed in some conditions by Day 7 supports this understanding and highlights the importance of the stem cell niche in regulating the differentiation process.

In conclusion, results indicate that cell proliferation and attachment are significantly enhanced by Day 4 and maintained at high levels or slightly reduced by Day 7. Col-I appears to enhance cell proliferation more effectively than other conditions. The slight decrease in Alamar Blue degradation by Day 7 suggests the beginning of cell differentiation, highlighting a crucial transition from proliferation to specialization in tissue development and repair. These findings corroborate existing literature, em-

phasizing the importance of surface modifications in supporting stem cell proliferation and function.

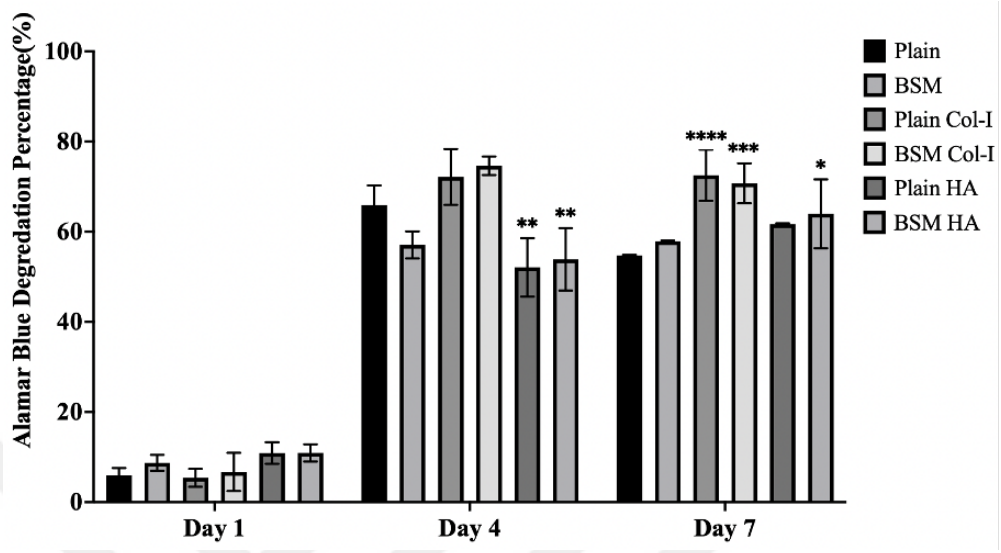


Figure 4.2 The proliferation of the ADMSCs onto unmodified and modified Plain and BSM membranes using the MTT test at day 1, 4, and 7 (* $p < 0.05$, ** $p < 0.01$, *** $p < 0.001$, **** $p < 0.0001$).

4.2.2 Cell Morphology and Attachment Analysis

After 7 days of incubation, MSCs demonstrated differential adhesion across various Poly(Lactic Acid) (PLA) surfaces (Figure 4.3). The cells adhered better to the rough BSM PLA membranes compared to the plain PLA membranes. Furthermore, the attachment of MSCs to the Col-I and HA modified PLA membranes was superior to that on the unmodified PLA membranes. Most notably, the Col-I and HA modified BSM PLA membranes exhibited the highest level of cell attachment.

The enhanced cell adhesion on the rough BSM PLA membranes can be attributed to the increased surface roughness that mimics the natural bone ECM [28]. Studies have shown that surface roughness significantly enhances cell attachment and proliferation by providing physical cues that facilitate cell adhesion. For instance, Lee *et al.* used human mesenchymal stem cells (hMSCs) and demonstrated that PLA nanotopographies created by polymer demixing techniques significantly increased MSC adhesion and proliferation [243]. Similarly, Wan *et al.* used OCT-1 osteoblast-like cells and reported that electrospun nano/micro scale aligned PLA fibers enhanced stem cell

attachment and proliferation [244]. Additionally, Bernardo *et al.* used rat MSCs and found that nano-HA/PLA composite scaffolds significantly promoted MSC adhesion and proliferation compared to pure PLA scaffolds [245].

Biochemical modifications with Col-I and HA further improved cell attachment by introducing binding sites and biochemical signals that interact with cell surface receptors. Col-I serves as a ligand for integrin receptors, facilitating integrin-mediated adhesion and signaling pathways essential for cell attachment and proliferation [246]. Wojak-Cwik *et al.* used human MSCs and showed that Col-I coated PLGA scaffolds promoted the differentiation of MSCs into osteoblasts [247]. Zhou *et al.* used mouse osteoblasts and reported that collagen-incorporated PLA scaffolds improved cell adhesion, proliferation, and differentiation [248]. Moreover, Schofer *et al.* used human MSCs and demonstrated that Col-I incorporated into PLA scaffolds significantly enhanced osteogenic induction and cell adhesion [249].

HA, a primary component of bone mineral, enhances osteoconductivity and provides additional binding sites for cell adhesion molecules. Bernardo *et al.* used rat MSCs and demonstrated that nano-HA/PLA composite scaffolds significantly promoted MSC adhesion and proliferation [245]. Peng *et al.* used hMSCs and reported that HA/chitosan nanofibrous scaffolds enhanced MSC adhesion, proliferation, and osteogenic differentiation through electrospinning techniques [250]. Mansouri *et al.* used human umbilical cord MSCs and reported that HA/chitosan nanofibrous scaffolds enhanced MSC adhesion, proliferation, and osteogenic differentiation through electrospinning techniques [251].

The combined topographical and biochemical modifications in the Col-I and HA modified BSM PLA membranes resulted in the highest level of cell adhesion observed in this thesis. This synergistic effect is likely due to the optimal mimicry of the natural bone environment, providing both the required physical and biochemical cues to observe enhanced cell adhesion and proliferation. Previous research has demonstrated similar enhancements in cell attachment and proliferation with dual modifications. Abagnale *et al.* used hMSCs and found that PLA scaffolds combined with nano-patterns sig-

nificantly improved MSC proliferation and differentiation [20]. Peng *et al.* reported that HA/chitosan nanofibrous scaffolds enhanced MSC adhesion, proliferation, and osteogenic differentiation through electrospinning techniques [250].

In conclusion, the results demonstrate that rough BSM PLA membranes significantly enhance MSC attachment compared to plain PLA membranes. The addition of Col-I and HA further improves cell attachment, with Col-I and HA modified BSM PLA membranes showing the best performance. These findings are well-supported by the literature and highlight the importance of both surface topography and biochemical modifications in optimizing scaffold materials for bone tissue engineering applications.

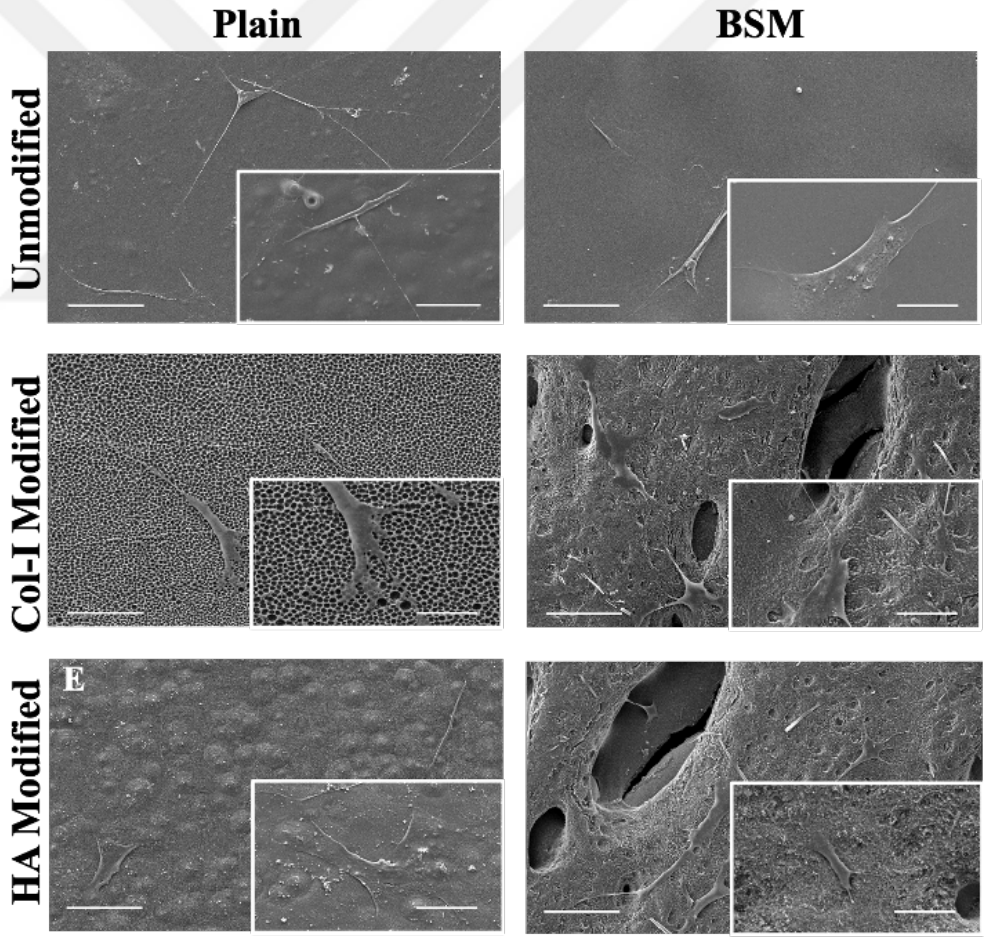


Figure 4.3 The attachment of ADMSCs onto unmodified and modified Plain and BSM membranes observed using SEM (Scale bars: 100 μm, 500x magnification; 50 μm, 1500x magnification (inlet)).

4.2.3 Osteogenic Differentiation Analysis

4.2.3.1 Alkaline Phosphatase Activity Analysis To investigate the osteogenic differentiation of ADMSCs on unmodified and modified plain and BSM membranes, ALP analysis was performed. Increased ALP activity is an indicator of osteogenic differentiation. The results, presented in Figure 4.4, show that the ALP activity of cells increased over time, and all modified PLA membranes exhibited higher ALP activity compared to unmodified PLA membranes.

Among the modified membranes, the HA modified BSM PLA membranes exhibited the highest ALP activity, particularly at days 14 and 21, which was statistically significantly higher than that of plain PLA membranes at day 7. This finding aligns with the results from Ebrahimi *et al.*, who also observed enhanced ALP activity in 3D printed PCL scaffolds coated with collagen and HA, assessed on days 1, 7, and 14 [252]. Their study highlights the role of HA in providing a bioactive surface that promotes osteogenic differentiation.

The consistent enhancement of ALP activity across various studies underscores the effectiveness of surface modifications. Cheng *et al.* reported that collagen-functionalized nanofiber matrices significantly improved ALP activity and osteogenic differentiation of MSCs, with ALP analysis performed on days 4, 7, and 14 [253]. Similarly, Yang *et al.* demonstrated that HA/collagen coatings on PLGA electrospun fibers enhanced ALP activity, measured on days 7 and 14, indicating the beneficial effects of combining HA and collagen [254].

Surface roughness also plays a critical role in enhancing osteogenic differentiation. Hu *et al.* found that nanotopography and Sr ion effects on bone marrow MSCs enhanced ALP activity and mineralized nodule formation, with ALP activity analyzed on days 4, 7, and 10 [255]. This thesis supports the idea that physical cues provided by surface roughness can significantly influence cell behavior and differentiation.

The highest ALP activity observed in HA-modified BSM PLA membranes con-

firms the importance of combined topographical and biochemical modifications in optimizing scaffold materials for bone tissue engineering. The enhanced differentiation observed on rough BSM PLA membranes can be attributed to the increased surface roughness that mimics the natural bone ECM, providing physical cues that facilitate cell adhesion and proliferation.

In conclusion, the results demonstrate that rough BSM PLA membranes significantly enhance MSC differentiation compared to plain PLA membranes. The addition of Col-I and HA further improves osteogenic differentiation, with HA-modified BSM PLA membranes showing the highest ALP activity. These findings are well-supported by the literature and highlight the synergistic effects of surface topography and biochemical modifications in promoting MSC differentiation for bone tissue engineering applications.

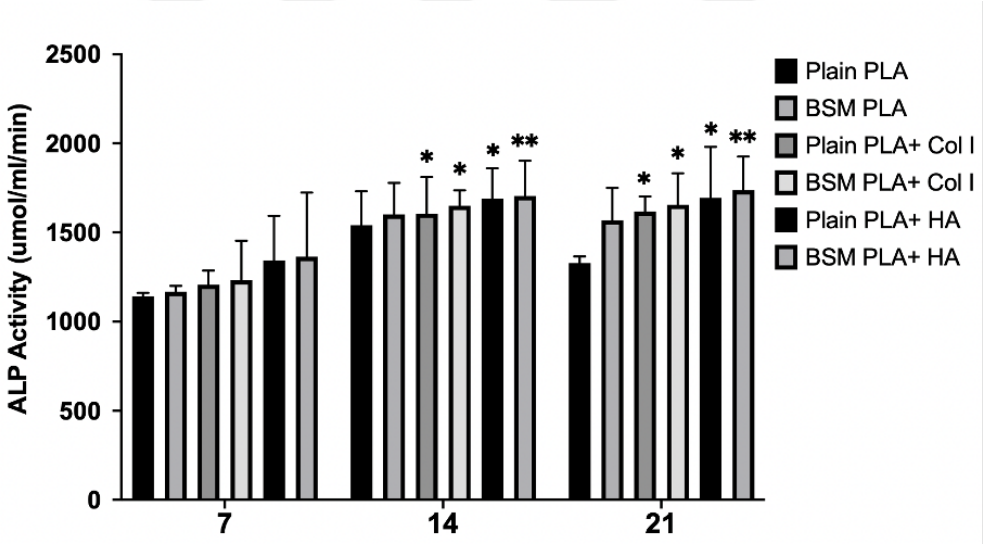


Figure 4.4 The osteogenic differentiation analysis of the ADMSCs onto unmodified and modified Plain and BSM membranes via ALP Analysis at day 7, 14, and 21 (* $p < 0.05$, ** $p < 0.01$, *** $p < 0.001$, **** $p < 0.0001$).

4.2.3.2 Alizarin Red S Analysis In this thesis, the osteogenic differentiation of ADMSCs on both unmodified and modified PLA membranes was investigated by employing Alizarin Red S staining to assess calcium deposition as an indicator of osteogenesis (Figure 4.5). It was found that the modified PLA membranes exhibited significantly more intense reddish staining compared to unmodified membranes, sug-

gesting enhanced osteogenic differentiation.

The significant increase in Alizarin Red S staining on HA-modified PLA membranes is consistent with previous findings in the literature. For example, Wu *et al.* reported that HA/collagen/PLA scaffolds significantly enhanced the osteogenic differentiation of human amnion MSCs, which was demonstrated by increased Alizarin Red S staining on day 21 [256]. Similarly, Martinez *et al.* found that HA structures supported the osteogenesis of human MSCs, confirmed by Alizarin Red S staining on day 14 [257]. These findings support the observation that HA modification significantly boosts osteogenic activity.

Col-I modification was also demonstrated to positively impact osteogenic differentiation. Calabrese *et al.* found that collagen/HA scaffolds accelerated the osteogenic differentiation of human ADSCs, with increased Alizarin Red S staining observed at various time points (7, 14, 21, and 28 days) [258]. Similarly, Rabadan-Ros *et al.* showed that Nurseâs A-phase ceramic modified with HA and collagen enhanced Alizarin Red S staining in mesenchymal stem cells on PLA, indicating improved osteogenic differentiation in vitro at days 14, 21, and 28 [259]. These studies align with the results, confirming that Col-I modification enhances osteogenic differentiation.

Surface roughness was identified as another critical factor influencing osteogenic differentiation. Hu *et al.* demonstrated that nanotopography and Sr ion effects on bone marrow MSCs enhanced ALP activity and mineralized nodule formation, with Alizarin Red S staining analyzed on days 4, 7, and 10 [255]. Bou Assaf *et al.* found that gelatin scaffold-embedded MSCs showed increased Alizarin Red S staining and osteogenic differentiation on days 7 and 14 [260]. Hild *et al.* reported that the modification of double-layer membranes with calcium phosphate/collagen/PLGA nanofibers significantly enhanced biomineralization and osteogenic differentiation of human MSCs, confirmed by Alizarin Red S staining on day 28 [261]. These findings are consistent with the observations that modified surfaces with specific topographies improve osteogenic outcomes.

The combined effect of surface roughness and Col-I modification was found to further enhance osteogenic differentiation. Calabrese *et al.* demonstrated that collagen and HA scaffolds significantly enhanced the osteogenic differentiation of human ADSCs, evidenced by Alizarin Red S staining at multiple time points (7, 14, 21, and 28 days). Similarly, Rabadan-Ros *et al.* showed enhanced Alizarin Red S staining in MSCs on PLA modified with Nurseâs A-phase ceramic, HA, and collagen, indicating potential for improved osteogenic differentiation at days 14, 21, and 28 [259]. Thein-Han and Xu *et al.* also reported significant mineralization on collagen-calcium phosphate cement scaffolds seeded with umbilical cord stem cells, confirmed by Alizarin Red S staining on days 14 and 21 [262].

When combining surface roughness with HA modification, osteogenic differentiation was markedly enhanced. Wu *et al.* observed that HA/collagen/PLA scaffolds significantly increased Alizarin Red S staining in human amnion mesenchymal stem cells on day 21 [216]. Martinez *et al.* confirmed that HA structures supported osteogenesis of human MSCs on day 14 [257]. Favi *et al.* found that HA modification on bacterial cellulose composites supported osteogenic differentiation of equine mesenchymal stem cells, confirmed by positive Alizarin Red S staining on day 8 [263]. These results reinforce the findings that the synergistic effects of surface roughness and HA modification significantly enhance osteogenic differentiation.

This thesis demonstrated that modifying PLA membranes with HA and Col-I, along with specific surface roughness, significantly enhances the mineralization and osteogenic differentiation of MSCs. This enhancement was shown by the increased rate of Alizarin Red S staining. These findings are supported by extensive literature, highlighting the importance of surface modifications in promoting osteogenesis. It was found that among all the modifications tested, the HA-modified rough BSM PLA membranes exhibited the most intense Alizarin Red S staining, highlighting their superior efficacy in promoting osteogenic differentiation. Future studies should continue to explore the synergistic effects of various modifications and optimize biomaterial properties to enhance bone tissue engineering outcomes. Comprehensive analyses at multiple time points will provide deeper insights into the dynamic process of osteogenic

differentiation and the role of biomaterial surface properties.

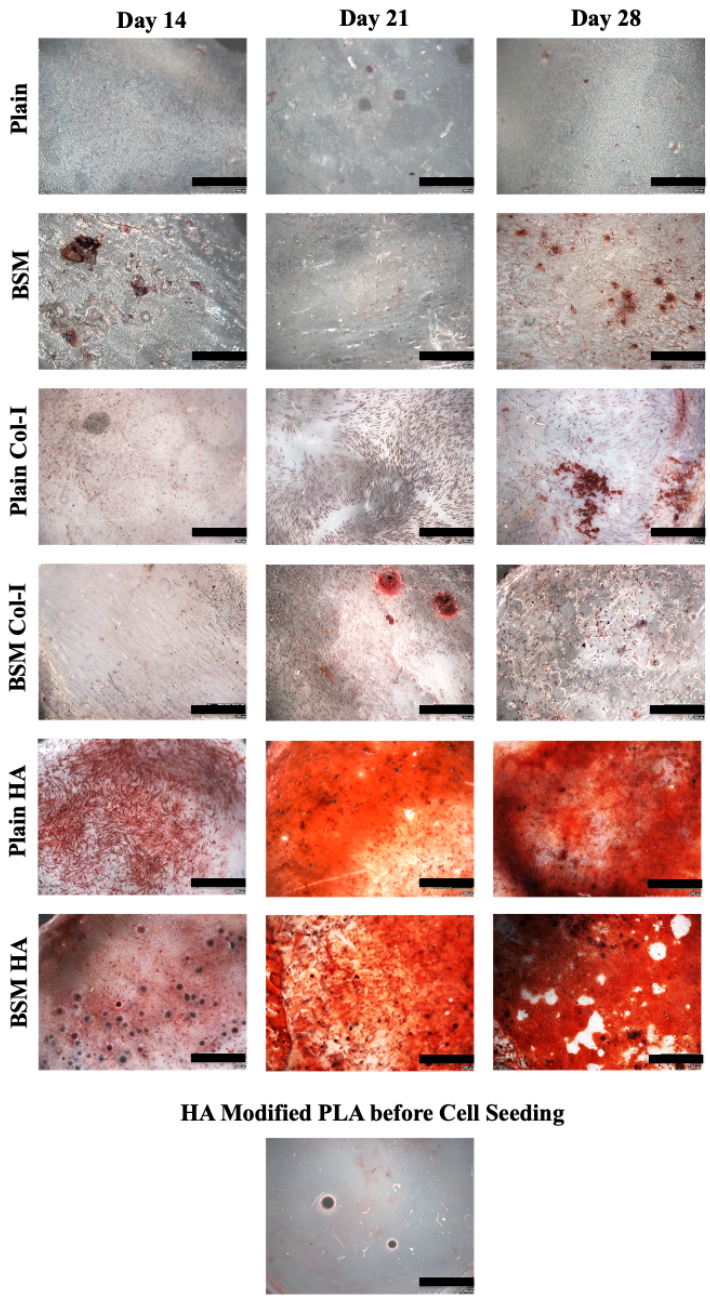


Figure 4.5 The osteogenic differentiation analysis of the ADMSCs onto unmodified and modified Plain and BSM membranes via Alizarin Red Analysis (Scale bars: 2000 μm).

4.3 Discussion

The proliferation of ADMSCs on unmodified and modified plain and BSM membranes were evaluated using the Alamar Blue assay at days 1, 4, and 7. The prolifera-

tion results align with the literature, showing that initial cell proliferation was minimal across all conditions on Day 1, indicating an early adaptation phase. This observation is consistent with studies suggesting that early stages involve cell attachment and adaptation rather than active proliferation.

By Day 4, a significant increase in Alamar Blue degradation was noted, especially in collagen-modified conditions (Plain Col-I and BSM Col-I), indicating enhanced cell proliferation. This supports previous research by Li *et al.*, where collagen-modified scaffolds showed improved cell viability [46]. The results suggest that collagen provides a conducive surface for cell attachment and proliferation. Additionally, by Day 7, the sustained high levels of Alamar Blue degradation in collagen-modified conditions further highlight collagen's role in supporting continuous cell proliferation. However, a slight decrease in proliferation in some conditions, such as Plain HA and BSM HA, suggests the onset of differentiation, which is a crucial transition in tissue development and repair. These observations align with findings that MSCs reduce proliferation rates as they begin to differentiate [241, 242].

After 7 days of incubation, SEM analysis demonstrated differential adhesion of MSCs across various scaffold surfaces. Consistent with the literature, rough BSM PLA membranes showed superior cell attachment compared to plain PLA membranes. The enhanced cell adhesion on rough surfaces can be attributed to increased surface roughness that mimics the natural bone ECM, providing physical cues for cell attachment. Studies, such as those by Lee *et al.* and Wan *et al.*, have shown that surface roughness significantly enhances cell attachment and proliferation [243, 244].

Biochemical modifications with Col-I and HA further improved cell attachment by introducing binding sites and biochemical signals that interact with cell surface receptors. Col-I, serving as a ligand for integrin receptors, facilitates integrin-mediated adhesion and signaling pathways essential for cell attachment and proliferation. Similarly, HA, a primary component of bone mineral, enhances osteoconductivity and provides additional binding sites for cell adhesion molecules. This synergistic effect of topographical and biochemical modifications resulted in the highest level of cell attach-

ment on Col-I and HA modified BSM PLA membranes. Previous research, including studies by Bernardo *et al.* and Peng *et al.*, supports these findings, demonstrating enhanced cell attachment and proliferation with dual modifications [245, 250].

The osteogenic differentiation of ADMSCs on unmodified and modified plain and BSM membranes was investigated using ALP activity analysis. Increased ALP activity, a marker for osteogenic differentiation, was observed over time across all modified PLA membranes, with HA-modified BSM PLA membranes showing the highest ALP activity at days 14 and 21. This significant enhancement in osteogenic differentiation is consistent with studies by Ebrahimi *et al.* and Cheng *et al.*, highlighting the role of HA in providing a bioactive surface that promotes osteogenic differentiation [252, 253].

Surface roughness also plays a critical role in enhancing osteogenic differentiation. Hu *et al.* found that nanotopography and Sr ion effects on bone marrow MSCs enhanced ALP activity and mineralized nodule formation [255]. The highest ALP activity observed in HA-modified BSM PLA membranes confirms the importance of combined topographical and biochemical modifications in optimizing scaffold materials for bone tissue engineering.

Further supporting these findings, Alizarin Red S staining revealed enhanced calcium deposition on modified PLA membranes, with HA-modified membranes exhibiting the most intense staining, indicating superior osteogenic differentiation. These results are consistent with studies by Wu *et al.* and Martinez *et al.*, demonstrating that HA modification significantly boosts osteogenic activity [256, 257]. The combined effect of surface roughness and biochemical modifications, particularly with collagen and HA, further enhances osteogenic differentiation, as supported by studies from Calabrese *et al.* and Rabadan-Ros et al [258, 259].

In conclusion, the results of this chapter demonstrate that rough BSM PLA membranes significantly enhance MSC attachment and differentiation compared to plain PLA membranes. The addition of Col-I and HA further improves cell attachment and osteogenic differentiation, with HA-modified BSM PLA membranes showing

the highest ALP activity and calcium deposition. These findings are well-supported by the literature and highlight the synergistic effects of surface topography and biochemical modifications in promoting MSC differentiation for bone tissue engineering applications. However, the analysis could be further strengthened by supporting osteogenic differentiation with additional methods such as RT-PCR and Western Blot.

5. EFFECTS OF BONE SURFACE TOPOGRAPHY AND CHEMISTRY ON MACROPHAGE POLARIZATION

In this section, the influence of the surface properties of bone surface mimicking materials on the behavior of macrophages, especially their polarization, is investigated. The RAW 264.7 cell line, which is used in this thesis to investigate how various surface modifications affect cell survival, morphology, and cytokine production. RAW 264.7 cells were cultured onto plain PLA and BSM, modified and unmodified membranes.

The WST-1 assay was used to determine cell viability on days 1, 3, and 6 after inoculation. The results revealed substantial differences in cell viability between altered and unmodified membranes, with HA and Col-I alterations promoting cell proliferation on unmodified surfaces. In addition, cell morphology was examined by SEM after cell fixation and dehydration. SEM analysis revealed distinct differences in cell attachment and morphology between the differently modified surfaces, indicating that surface chemistry and topography significantly influence macrophage behavior.

To gain a better understanding of the immune response, cytokine concentration in culture supernatants was evaluated using ELISA kits. To determine the dominant macrophage phenotype, the analysis focused on both pro-inflammatory (IL-6 and IL-1β) and anti-inflammatory (IL-1ra and IL-10) cytokines. Samples were collected on days 1, 3, and 6 and stored until analysis. The results showed that surface modifications, especially HA and Col-I, significantly affected cytokine release profiles, thereby promoting a more balanced immune response. Statistical analyses confirmed that these effects were significant, highlighting the potential of these modified surfaces to modulate macrophage polarization and improve their biocompatibility for biomedical applications.

5.1 Experimental Procedures

5.1.1 Instrumentation and Reagents

The RAW 264.7 cell line was purchased from the American Type Culture Collection (ATCC® TIB-71™). For culturing the cells, high glucose DMEM (D5796, Sigma-Aldrich) was employed, supplemented with 10% FBS (F9665, Sigma-Aldrich) and 1% penicillin/streptomycin (P4333, Sigma-Aldrich).

To assess cell viability, the WST-1 assay kit (ab65473; Abcam, Cambridge, MA) was utilized consistent with the manufacturerâs instructions. For cell morphology analysis, cells were fixed using 2.5% glutaraldehyde (Sigma-Aldrich, G5882) and dehydrated with hexamethyldisilazane (HMDS, 440191, Sigma-Aldrich). Then the cells were analyzed using a SEM (Carl Zeiss EVO 40, Germany).

For cytokine content analysis in the cell culture supernatants, double antibody sandwich ELISA kits from R&D Systems (Gymea, NSW, Australia) were used. This allowed for the colorimetric assessment of proinflammatory and anti-inflammatory factors via a microplate reader (BIO-RAD iMark, Microplate Reader).

5.1.2 Cell Culture Studies

The RAW 264.7 cell line, acquired from the American Type Culture Collection (ATCC® TIB-71™), was cultured in high glucose DMEM (D5796, Sigma-Aldrich) supplemented with 10% FBS (F9665, Sigma-Aldrich) and 1% penicillin/streptomycin. The cells were maintained in a 5% CO_2 and 95% humidity environment at 37°C. Upon reaching 80% confluence, cells were detached using a cell scraper and passaged at a 1:6 ratio in T-75 flasks, continuing this process up to passage number 5. For experiments, 4×10^4 RAW 264.7 cells were seeded on both modified and unmodified plain PLA and BSM PLA membranes (Figure 5.1). The culture medium used consisted of high glucose DMEM (D5796, Sigma-Aldrich), 10% FBS (F9665, Sigma-Aldrich), and 1%

penicillin/streptomycin (P4333, Sigma-Aldrich).

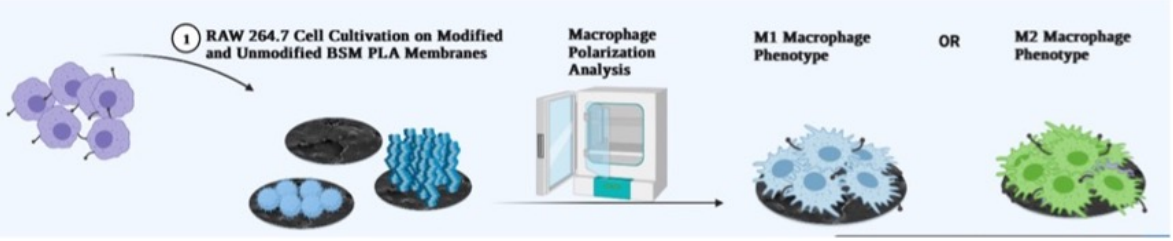


Figure 5.1 Schematic of the experimental procedure for macrophage polarization. RAW 264.7 cells are cultured on modified and unmodified BSM PLA membranes. The polarization analysis determines whether the macrophages adopt an M1 (pro-inflammatory) or M2 (anti-inflammatory) phenotype.

5.1.2.1 Cell Viability The effect of plain and BSM modified and unmodified membranes on the viability of the RAW 264.7 cells was analyzed via the WST-1 assay using a commercial kit according to the manufacturerâs instructions (ab65473; Abcam, Cambridge, MA) on day 1, day 3, and day 6. Experiments were conducted in triplicates, and plain PLA membranes were accepted as a control group.

5.1.2.2 Cell Morphology Analysis After incubation, the RAW 264.7 cells were fixed with 2.5% glutaraldehyde (Sigma-Aldrich, G5882). Then, fixed cells were dehydrated by incubating them in graded ethanol series (30%, 50%, 70%, 90%, and 100%). Finally, the cells were dried with a hexamethyldisilazane (HMDS, 440191, Sigma-Aldrich) solution for 5 minutes [264, 265]. Before analysis, the samples were sputter-coated with a thin layer of gold (Au) and observed under SEM (Carl Zeiss EVO 40, Germany) at 10 kV.

5.1.2.3 Cytokine Content Analysis in the Supernatant To determine the dominant macrophage phenotype in osteoimmunomodulation regulation, we utilized double antibody sandwich ELISA kits for the colorimetric assessment of the ratio of proinflammatory and anti-inflammatory factors of monocytes/macrophages. RAW 264.7 cells were incubated on unmodified and modified, plain PLA and BSM PLA membranes for 1 day, 3 days, and 6 days, and then the media were collected. Super-

natants were obtained from the collected medium by centrifugation at 210 g and stored at -80°C until use. The presence and amount of proinflammatory (IL-6 and IL-1β) and anti-inflammatory (IL-1ra and IL-10) factors in the stored supernatants were analyzed using appropriate ELISA kits (R&D Systems, Gymea, NSW, Australia), according to the manufacturer's instructions. A calibration curve was obtained for each cytokine to determine unknown concentrations. Calibration curves are provided in the appendices part as Figure A1. Experiments were conducted in triplicates [266, 267].

5.1.2.4 Statistical Analysis Results were given as mean ± standard deviation and differences were considered statistically significant for $p < 0.05$. GraphPad Prism 9 (GraphPad Software, USA) was used to perform the statistical analyses. The data were analyzed using two-way ANOVA followed by Tukeyâs post hoc multiple comparison test. Plain PLA was accepted as a control group for viability and cytokine release analysis.

5.2 Results

5.2.1 Cell Viability

To investigate the impact of surface topography and chemical modifications on immune cells, we assessed the viability of RAW 264.7 cells on unmodified and modified plain and BSM membranes for 6 days (Figure 5.2). The viability of cells was measured on day 1, day 3, and day 6. The results showed that surface chemical modifications of the membranes significantly influenced cell viability. HA modification on BSM PLA membranes significantly increased adherent cell viability compared to plain PLA membranes without HA modification ($p < 0.01$). Additionally, the Col-I modification of BSM membranes improved cell viability at day 3 ($p < 0.0001$) compared to the HA-coated plain and BSM membranes (OD 1.23 ± 0.13, 1.82 ± 0.09, respectively). Moreover, HA-coated plain and BSM membranes showed the lowest viability rate on day 3 ($p < 0.0001$) compared to the other groups.

The initial high viability observed on day 1 with HA-deposited BSM membranes suggests enhanced cell adhesion and spreading due to surface modification. Conversely, the sustained viability observed on day 3 with Col-I modified BSM membranes may be attributed to Col-I's role as a ligand for integrin receptors, facilitating integrin signaling pathways crucial for cell proliferation and differentiation [268, 269].

Previous studies have highlighted HA surface modifications influence immune cell behavior, affecting macrophage activation and inflammation. Jha *et al.* reported reduced M1 macrophage activation with DGEA, a Col-I-derived peptide, suggesting a potential mechanism for the improved viability observed with Col-I modification [270], and Viji *et al.* demonstrated anti-inflammatory effects of a collagen sheet impregnated with neem extract [271]. Additionally, the observed reduction in viability on the 3rd and 6th days for the HA-coated BSM membranes can be attributed to the differentiation of M0 macrophages into M1 or M2 phenotypes, which have distinct roles in the immune response. For instance, Laquerriere *et al.* demonstrated that small-diameter HA particles can stimulate immune cells to release cytokines that promote inflammation [43]. Similarly, Sadowska *et al.* found that HA-coated materials contribute to the production of pro-inflammatory cytokines and regulate osteogenic processes [45].

Surface topography alone appears to have minimal initial impact on viability, as observed by Schaub *et al.* with PLA electrospun fibers, Majidi *et al.* with PDMS surfaces, and Wang *et al.* with smooth and rough titanium. In these studies, no significant differences in viability were noted at day 1, regardless of topography, after a day of incubation [272–274]. These findings suggest that initial cell adhesion and spreading may be less influenced by surface topography compared to surface chemistry. However, Wang *et al.* observed increased viability on rough surfaces by day 3, suggesting topographical influence over time [273]. This delayed effect might be due to changes in cell morphology, cytoskeletal organization, or mechano-transduction pathways triggered by surface features. Kim *et al.* reported no significant effect on cell morphology with collagen-incorporated PEG hydrogels, indicating collagen alone may not affect viability through topographical cues [275]. Li *et al.* observed no difference in viability at days 1 and 2 with Col-I modified samples, but noted changes in cytoskeleton and

focal adhesion at day 3, suggesting delayed effects of surface properties on these aspects of cell behavior that could ultimately influence viability and macrophage polarization [185]. Finally, Neacsu *et al.* found that the addition of the M1 macrophage phenotype stimulator LPS resulted in decreased viability of macrophages on TiO_2 nanotubes, while Schaub *et al.* reported similar findings with LPS-stimulated macrophages on PLA electrospun fibers [272, 276]. Therefore, changes in viability observed on day 3 may be related to polarization, reflecting the complex interaction between surface properties, inflammatory stimuli, and cell behavior.

In summary, surface chemical modifications, such as HA or Col-I addition, significantly impact immune cell viability, with variations attributed to surface properties. While surface topography alone minimally affects viability initially, alterations in both topography and surface chemistry can synergistically enhance viability over time. These findings underscore the collective influence of surface topography, material composition, and macrophage polarization status on cell viability.

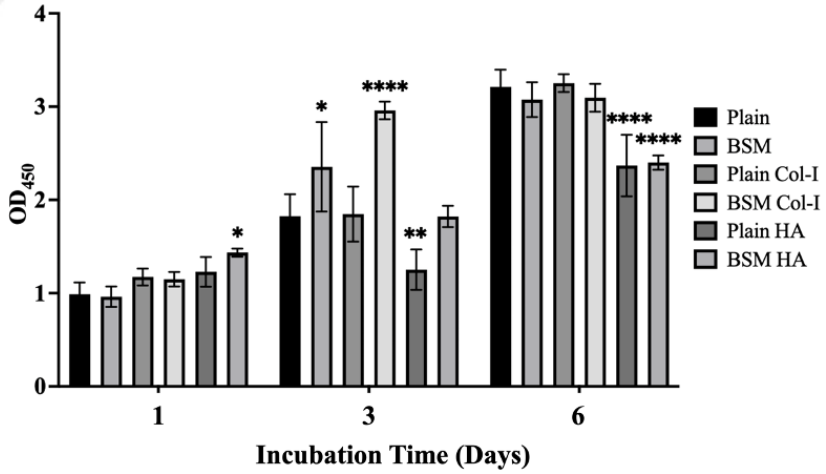


Figure 5.2 Viability of RAW 264.7 cells adherent on unmodified, Col-I modified, and HA modified plain PLA and BSM PLA surfaces measured at day 1, day 3, and day 6 (* $p < 0.05$, ** $p < 0.01$, *** $p < 0.001$, **** $p < 0.0001$).

5.2.2 Cell Morphology Analysis

To investigate the effect of surface topography and Col-I and HA modifications on macrophage polarization, the morphology of RAW 264.7 cells on unmodified and

modified plain and BSM membranes was examined on day 1, day 3, and day 6. The cells on the samples were observed by SEM (Zeiss EVO HD) and presented in Figure 5.3.

According to Heinrich *et al.*, M0-macrophages were predominantly observed as compact, circular cells, with an average diameter of around 8 μm. These cells displayed minimal to no cytoplasmic extensions, occasionally reaching a length of up to 1 μm [277]. On the first day, the cell morphology on each sample resembled that of M0 macrophages as described in existing literature. In all samples, cells were observed to be attached and displayed a small, rounded morphology with limited cytoplasmic extensions.

By day 3, if the produced membranes were osteoimmunomodulatory, the M1 macrophage phenotype was expected to be observed. The cells seeded on HA coated plain and BSM membranes showed an expanded amoeboid cell shape with rounded cell bodies and several fragile cytoplasmic extensions on the surface similar to the reported phenotype of M1 macrophages in the literature [277, 278].

The M2 macrophage phenotype consists of two distinct cell types: the first type includes large "spindeloid" macrophages characterized by an elongated cell body with cytoplasmic extensions at the ends, while the second type encompasses giant multinucleated cells that have numerous cytoplasmic projections on their surfaces [277, 278]. By day 6, all cells on both unmodified and modified membranes exhibited a large "spindeloid" morphology, indicative of the M2 phenotype. Moreover, the M2 macrophage phenotype comprises four subtypes, each with distinct morphological features and functional roles: M2a, M2b, M2c, and M2d. M2a macrophages show elongated and narrowed morphologies. On the other hand, M2b macrophages are elongated and granular, whereas M2c macrophages are smaller and more circular. Finally, M2d macrophages are identified by their flattened and elongated morphology [185–187]. Macrophages on unmodified membranes resembled M2a macrophages, displaying an elongated and narrowed shape. In contrast, cells on modified membranes did not exhibit elongation and showed characteristics more akin to both M2b and M2c subtypes.

Consequently, sequential M1 and M2 macrophage polarizations were only observed in the cells adherent to HA-deposited plain and BSM PLA membranes. These observations suggest that HA-deposited plain and BSM PLA membranes might promote initial M1 polarization at day 3, followed by a shift towards M2b or M2c polarization by day 6. However, conclusive evidence for sequential M1 and M2 polarization is limited to HA-deposited plain and BSM PLA membranes and requires further investigation.

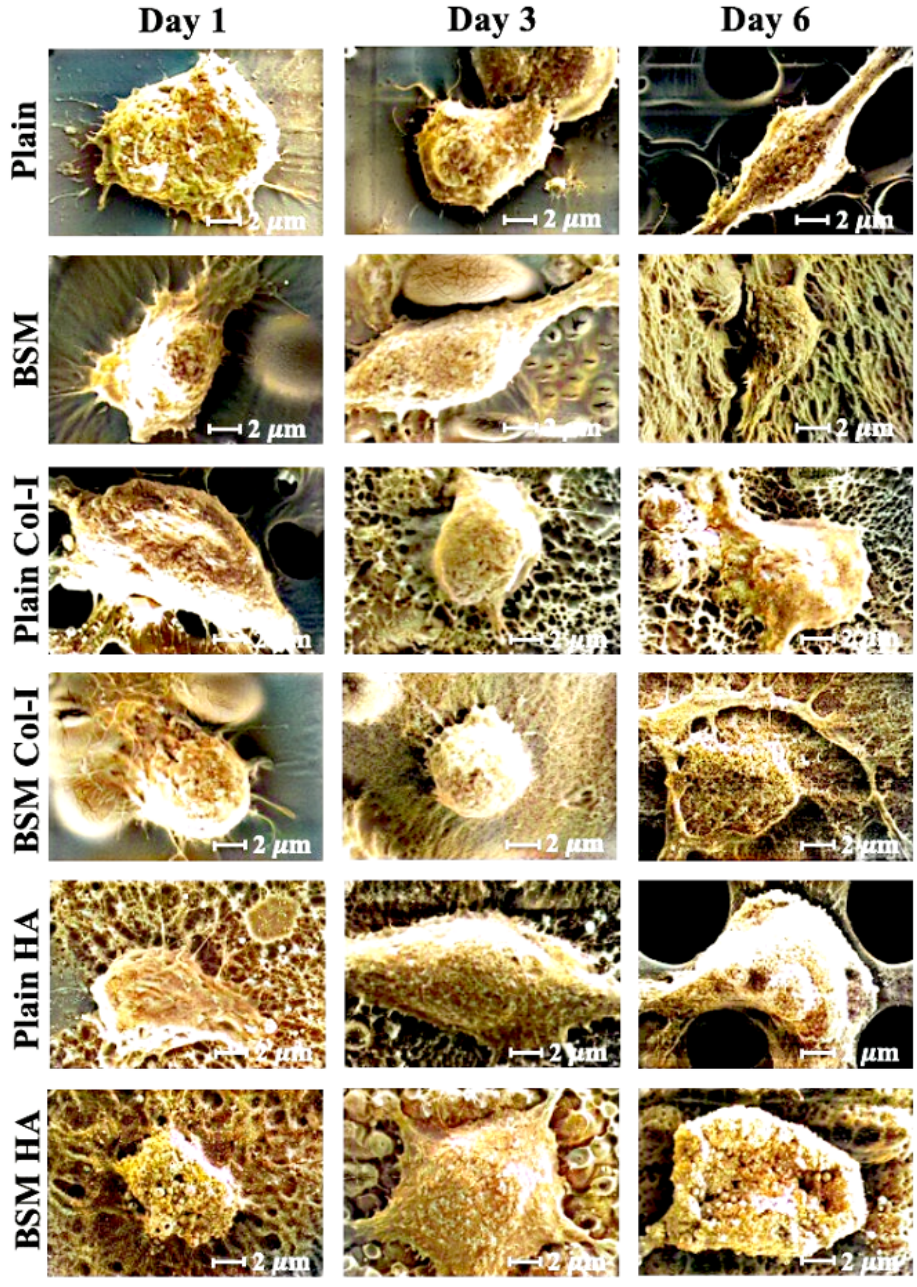


Figure 5.3 SEM images of unmodified, and Col-I and HA modified, plain and BSM membranes on day 1, day 3, and day 6 (Scale bars: 2 μm).

5.2.3 Cytokine Content Analysis in the Supernatant

To understand the dominant macrophage phenotype in the regulation of osteoimmunomodulation, the ratio of proinflammatory and anti-inflammatory factors of monocytes/macrophages was determined colorimetrically with double antibody sandwich ELISA kits. Cells seeded on unmodified and modified, plain PLA and BSM PLA membranes were incubated for 1 day, 3 days, 6 days, and the presence of proinflammatory (IL-6 and IL-1β) and anti-inflammatory (IL-1ra and IL-10) factors in the medium and the amount of these cytokines were analyzed using ELISA [266, 267]. For the analysis, first, a calibration curve was obtained to find the concentration of each cytokine. Concentration calculations were made for each cytokine and the results are presented in Figure 5.4.

Wound healing challenges often arise from disruptions in transitioning from M1 to M2 macrophages. Biomaterials facilitating sequential M1-to-M2 macrophage activation are proposed to enhance healing [50, 202–204]. Typically, M1 macrophages dominate early wound healing (days 1-3) before transitioning to M2 macrophages (days 4-7) [35]. Thus, it was expected that the highest levels of proinflammatory cytokines IL-6 and IL-1β would be observed on the 3rd day, followed by a decrease, while anti-inflammatory cytokines IL-1ra and IL-10 would steadily increase, peaking on the 6th day. This pattern would demonstrate the immunomodulatory effect of the produced biomaterial.

Regarding the observations, first, IL-6 cytokine, which is known as proinflammatory, was released in all samples the most on the 3rd day, and then the rate of release increased in the control group (TCP) on the 6th day but decreased in all other samples. The IL-6 release rate of HA deposited samples was statistically different on days 1 and 6 compared to TCP. On the 6th day, the cytokine release of all samples was statistically different from the cells seeded on the TCP. When it comes to the analysis of the second proinflammatory, IL-1β cytokines, the amount of cytokine released from the HA-deposited BSM membranes was significantly statistically different from the adherent cells on the cell culture dish on all days. For IL-1ra and IL-10, which

are anti-inflammatory cytokines, the release increased day by day in all samples and this increase is consistent with the literature. For IL-10, the groups that were most statistically different from the cell culture dish on all days were HA and Col-I modified BSM membranes, while for IL-1ra, the group that was most statistically different from the cell culture dish when all days were considered was HA coated BSM membranes.

Despite differences in surface morphology between plain and BSM PLA surfaces, the Col-I and HA-modified BSM PLA surfaces exhibit hydrophilic properties. This distinction highlights a significant contrast: while plain and BSM PLA membranes are hydrophobic, the modifications make them hydrophilic. This indicates that the variations in immune responses observed among unmodified and modified samples are likely influenced more by changes in their surface chemistry and topography, which collectively affect surface wetting properties, rather than differences in surface topography alone. This perspective finds support in several studies demonstrating that alterations in surface chemistry, along with morphology, notably impact macrophage behavior and polarization. Under standard culture conditions, Neacsu *et al.* observed that surface texture alone did not significantly affect macrophage inflammatory activity. They examined the interactions between commercially pure titanium and titania nanotubes with macrophages under both normal and pro-inflammatory conditions [276]. Hotchkiss *et al.* conducted experiments with macrophages cultured on various titanium surfaces with different morphologies and wettability. They found that surface wettability influences macrophage polarization, with hydrophilic rough surfaces inducing an anti-inflammatory M2-like state, while smooth hydrophobic surfaces promoted inflammatory M1-like activation after 3 days of incubation [198]. Similarly, Lv *et al.* demonstrated that hydrophilic TiO_2 surfaces exhibit enhanced anti-inflammatory and pro-healing performance of macrophages compared to hydrophobic ones [199]. Additionally, Gao *et al.* developed super-hydrophilic TNT surfaces through hydrogenation, which maintained the nanotubular topography without introducing impurities. They found that these super-hydrophilic nanotubular surfaces preferentially induced macrophages to adopt an anti-inflammatory phenotype under standard conditions [200]. Furthermore, it was observed that HA-deposited samples, being the most hydrophilic, demonstrated M1 polarization on day 3 and M2 polarization on day

6. This suggests a dynamic interaction between surface chemistry, morphology, and immune response over time. These results align with existing literature, suggesting that HA-deposited BSM samples, considering their SEM images, appear to be the most osteoimmunomodulatory samples. Thus, in this thesis, the regulation of immune responses is primarily driven by the synergistic effect of modifications and surface morphology due to surface hydrophilicity.

To gain a deeper understanding and achieve more precise classification of the M1/M2 phenotypes, future studies should incorporate additional techniques such as flow cytometry and RT-PCR to evaluate the effect of HA-deposited BSM membranes on osteoimmunomodulation. However, these results show the potential advantages of bone surface mimic biomaterials on osteoimmunomodulation.

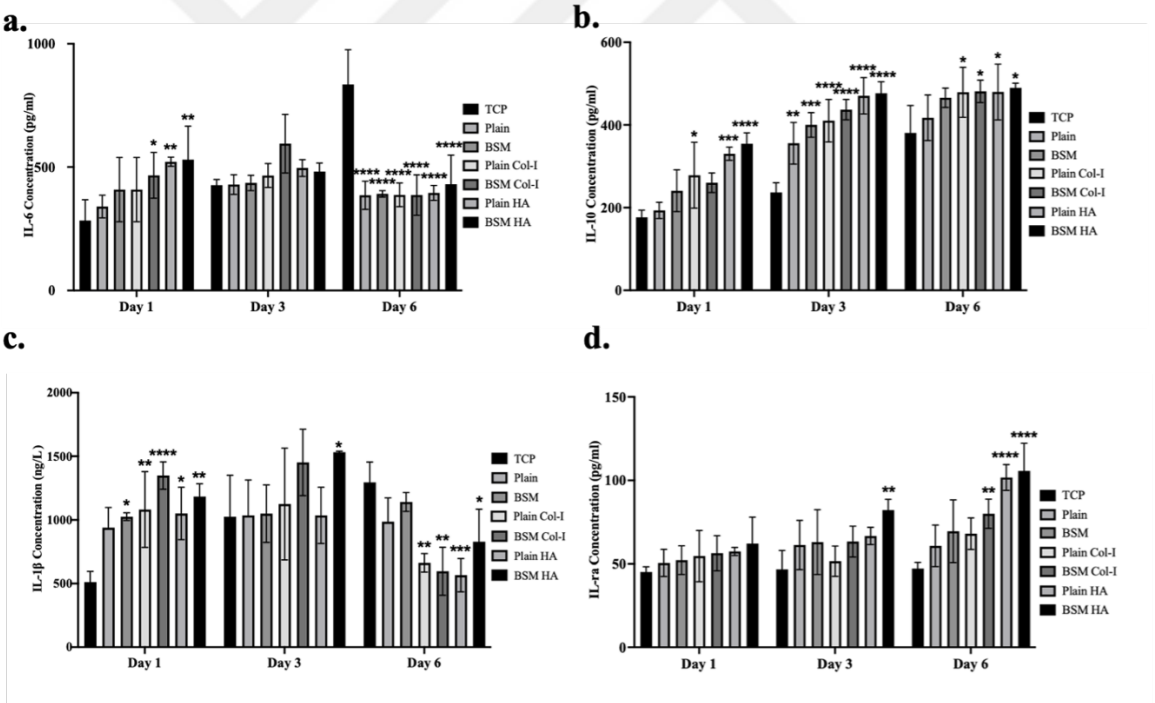


Figure 5.4 Pro-Inflammatory and Anti-Inflammatory factor content and amount analysis on unmodified and Col-I and HA modified, plain PLA and BSM PLA membranes by days. (a) IL-6 Concentration, (b) IL-10 Concentration, (c) IL-1β Concentration, (d) IL-1ra Concentration (* $p < 0.05$, ** $p < 0.01$, *** $p < 0.001$, **** $p < 0.0001$).

5.3 Discussion

The section investigated the impact of surface topography and chemical modifications on the viability of RAW 264.7 cells cultured on unmodified and modified plain and BSM PLA membranes over six days. Cell viability was assessed on days 1, 3, and 6. The results showed that surface chemical modifications significantly influenced cell viability. Specifically, HA modification on BSM PLA membranes significantly increased cell viability compared to plain PLA membranes without HA modification ($p < 0.01$). Moreover, Col-I modification of BSM membranes improved cell viability notably on day 3 ($p < 0.0001$) compared to the HA-coated plain and BSM membranes (OD 1.23 ± 0.13, 1.82 ± 0.09, respectively). Interestingly, HA-coated plain and BSM membranes showed the lowest viability rate on day 3 ($p < 0.0001$) compared to other groups.

The high initial viability observed on day 1 with HA-deposited BSM membranes suggests enhanced cell adhesion and spreading due to surface modification. Conversely, the sustained viability observed on day 3 with Col-I modified BSM membranes may be attributed to Col-I's role as a ligand for integrin receptors, facilitating integrin signaling pathways crucial for cell proliferation and differentiation [225, 227]. Previous studies have highlighted HA surface chemical modifications influence immune cell behavior, affecting macrophage activation and inflammation. Jha *et al.* reported reduced M1 macrophage activation with DGEA, a Col-I-derived peptide, suggesting a potential mechanism for the improved viability observed with Col-I modification [270]. Viji *et al.* demonstrated anti-inflammatory effects of a collagen sheet impregnated with neem extract [271]. Additionally, the observed delay in viability on the 3rd and 6th days for the HA-coated BSM membranes can be linked to the differentiation of M0 macrophages into M1 or M2 phenotypes, each with distinct functions in the immune response. For instance, Laquerriere *et al.* demonstrated that small-diameter HA particles can stimulate immune cells to release cytokines that promote inflammation [43], whereas Sadowska *et al.* found that HA-coated materials contribute to the production of pro-inflammatory cytokines and regulate osteogenic processes [45].

Surface topography alone appeared to have minimal initial impact on viability, as observed by Schaub *et al.* with PLA electrospun fibers, Majidi *et al.* with PDMS surfaces, and Wang *et al.* with smooth and rough titanium. In these studies, no significant differences in viability were noted at day 1, regardless of topography, after a day of incubation [272–274]. These findings suggest that initial cell adhesion and spreading may be less influenced by surface topography compared to surface chemistry. However, Wang *et al.* observed increased viability on rough surfaces by day 3, suggesting topographical influence over time [273]. This delayed effect might be due to changes in cell morphology, cytoskeletal organization, or mechano-transduction pathways triggered by surface features. Kim *et al.* reported no significant effect on cell morphology with collagen-incorporated PEG hydrogels, indicating collagen alone may not affect viability through topographical cues [275]. Li *et al.* observed no difference in viability at days 1 and 2 with Col-I modified samples but noted changes in cytoskeleton and focal adhesion at day 3, suggesting delayed effects of surface properties on these aspects of cell behavior that could ultimately influence viability and macrophage polarization [185]. Finally, Neacsu *et al.* found that the addition of the M1 macrophage phenotype stimulator LPS resulted in decreased viability of macrophages on TiO_2 nanotubes, while Schaub *et al.* reported similar findings with LPS-stimulated macrophages on PLA electrospun fibers [272, 276]. Therefore, changes in viability observed on day 3 may be related to polarization, reflecting the complex interaction between surface properties, inflammatory stimuli, and cell behavior.

Examining the morphology of RAW 264.7 cells on the different membranes provided further insights into macrophage polarization influenced by surface modifications. On day 1, cells exhibited a compact, circular morphology characteristic of M0 macrophages, with minimal cytoplasmic extensions, aligning with findings by Heinrich *et al.* [277]. By day 3, cells on HA-coated plain and BSM membranes showed expanded amoeboid shapes with multiple cytoplasmic extensions, indicative of M1 macrophages [277, 278]. By day 6, cells on both unmodified and modified membranes exhibited a large "spindeloid" morphology, indicative of M2 macrophages. M2 macrophages, classified into subtypes M2a, M2b, M2c, and M2d, exhibit distinct morphological features and functional roles [185–187]. Cells on unmodified membranes resembled M2a

macrophages, displaying an elongated and narrowed shape, while those on modified membranes displayed characteristics more akin to M2b and M2c subtypes.

Cytokine content analysis using ELISA kits further elucidated the macrophage phenotype transitions. The presence and amount of proinflammatory (IL-6 and IL-1β) and anti-inflammatory (IL-1ra and IL-10) factors were determined in the medium after incubating cells on unmodified and modified plain and BSM PLA membranes for 1, 3, and 6 days. Typically, M1 macrophages dominate early wound healing (days 1-3) before transitioning to M2 macrophages (days 4-7) [35]. Thus, it was expected that the highest levels of proinflammatory cytokines IL-6 and IL-1β would be observed on the 3rd day, followed by a decrease, while anti-inflammatory cytokines IL-1ra and IL-10 would steadily increase, peaking on the 6th day. These observations confirmed this pattern: IL-6 release peaked on the 3rd day, with a decrease observed on the 6th day in all samples except the control group. IL-6 release was statistically different in HA-deposited samples compared to the TCP control on days 1 and 6. IL-1β release from HA-deposited BSM membranes was significantly different from cells on the cell culture dish on all days. For anti-inflammatory cytokines IL-1ra and IL-10, release increased consistently over time in all samples. Notably, HA and Col-I modified BSM membranes exhibited the most statistically significant differences in IL-10 release compared to the cell culture dish on all days, while HA-coated BSM membranes showed the most significant differences in IL-1ra release.

Despite differences in surface morphology between plain and BSM PLA surfaces, the Col-I and HA-modified BSM PLA surfaces exhibited hydrophilic properties, in contrast to the hydrophobic nature of unmodified membranes. This indicates that variations in immune responses are likely influenced more by changes in surface chemistry and topography, affecting surface wetting properties, rather than differences in surface topography alone. Several studies support this perspective, demonstrating that alterations in surface chemistry, along with morphology, notably impact macrophage behavior and polarization. For instance, Neacsu *et al.* observed that under standard culture conditions, surface topography alone did not significantly influence macrophage inflammatory activity [276]. Hotchkiss *et al.* found that surface

wettability influences macrophage polarization, with hydrophilic rough surfaces inducing an anti-inflammatory M2-like state [198]. Similarly, Lv *et al.* demonstrated enhanced anti-inflammatory and pro-healing performance of macrophages on hydrophilic TiO_2 surfaces compared to hydrophobic ones [199]. Gao *et al.* observed that superhydrophilic nanotubular surfaces preferentially activated macrophages toward an anti-inflammatory phenotype [200]. These observations indicate that HA-deposited samples, being the most hydrophilic, demonstrated M1 polarization on day 3 and M2 polarization on day 6. Thereby, there is a dynamic interaction between surface chemistry, morphology, and immune response over time. The results align with existing literature, suggesting that HA-deposited BSM samples appear to be the most osteoimmunomodulatory, as indicated by their SEM images. The regulation of immune responses in this thesis is primarily driven by the synergistic effect of surface modifications and morphology, influenced by surface hydrophilicity.

In summary, surface chemical modifications, such as HA or Col-I addition, significantly affect immune cell viability, with variations attributed to surface properties. While surface topography alone minimally affects viability initially, alterations in both topography and surface chemistry can synergistically enhance viability over time. These findings underscore the collective influence of surface topography, material composition, and macrophage polarization status on cell viability. The results show the potential advantages of bone surface mimic biomaterials on osteoimmunomodulation.

6. CONCLUSION

This thesis successfully demonstrated the fabrication and characterization of BSM PLA membranes, showcasing significant advancements in replicating the physical and biochemical properties of natural bone. The thesis was divided into three main parts: the topographical and biochemical replication of the bone surface, the investigation of osteoimmunomodulatory effects, and the evaluation of osteogenic differentiation. In the first part, the thesis concentrates replicating the topographical and biochemical properties of the bone surface. Bovine femur bones were thoroughly cleaned and prepared to create PDMS molds via soft lithography. This technique effectively captured the intricate microstructures of the bone surface, as confirmed by SEM and AFM analyses. SEM images showed that the surface topography of the PLA membranes closely replicated the diverse heights and pits characteristic of natural bone, while AFM results showed a roughness value of Ra = 64.00 nm for BSM PLA membranes, significantly higher than the Ra = 5.88 nm for plain PLA membranes. Additionally, chemical analyses using FTIR, XPS and XRD confirmed the successful immobilization of Col-I and HA on the PLA membranes, enhancing their biochemical properties. The second part focused on evaluating the osteogenic differentiation of ADMSCs on unmodified and modified plain and BSM membranes. ALP analysis, a key indicator of osteogenic differentiation, revealed that all modified PLA membranes exhibited higher ALP activity compared to unmodified PLA membranes. At days 14 and 21, the HA modified BSM PLA membranes demonstrated the highest ALP activity, indicating the most significant enhancement in osteogenic differentiation. These findings were consistent with Alizarin Red S staining results, which showed increased mineralization on HA-modified membranes. This enhanced differentiation can be attributed to the increased surface roughness that mimics the natural bone ECM, providing physical cues that facilitate cell adhesion and proliferation. Biochemical modifications with Col-I and HA further improved cell attachment and differentiation by introducing binding sites and biochemical signals that interact with cell surface receptors. These findings align with literature, emphasizing the importance of combined topographical and biochemical modifications

in optimizing scaffold materials for bone tissue engineering. The third part investigated the effect of surface topography and chemical modifications on the viability and immune modulation of RAW 264.7 cells seeded on unmodified and modified plain and BSM PLA membranes over six days. Cell viability assessments on days 1, 3, and 6 demonstrated that surface chemical modifications significantly influenced cell viability. Specifically, HA modification on BSM PLA membranes significantly increased cell viability compared to plain PLA membranes without HA modification. Col-I modification of BSM membranes notably improved cell viability on day 3, likely due to Col-I's role as a ligand for integrin receptors, facilitating integrin signaling pathways crucial for cell proliferation and differentiation. The thesis also examined the morphology of RAW 264.7 cells, revealing insights into macrophage polarization influenced by surface modifications. On day 1, cells exhibited a compact, circular morphology characteristic of M0 macrophages. By day 3, cells on HA-coated plain and BSM membranes showed expanded amoeboid shapes with multiple cytoplasmic extensions, indicative of M1 macrophages, and by day 6, cells exhibited a large "spindeloid" morphology, indicative of M2 macrophages. Cytokine content analysis using ELISA kits further elucidated macrophage phenotype transitions, with proinflammatory (IL-1β and IL-6) and anti-inflammatory (IL-10 and IL-1ra) cytokine levels measured at different time points. The results indicated that HA-deposited BSM membranes were particularly effective in modulating immune responses, demonstrating pro- inflammatory and anti-inflammatory cytokine manufacture at different stages. These findings indicate that HA-modified BSM PLA membranes are highly effective in promoting balanced osteoimmunomodulation. In conclusion, this thesis clearly demonstrated that the combined topographical and biochemical modifications significantly enhance mesenchymal stem cell differentiation and modulate the immune response. HA-modified BSM PLA membranes proved to be the most effective group in terms of both osteogenic differentiation and osteoimmunomodulation. Supported by the literature, these findings highlight the potential of HA-modified BSM PLA membranes in bone tissue engineering. Nevertheless, the analysis could benefit from further supporting osteoimmunomodulation and osteogenic differentiation with additional techniques such as Flow Cytometry, Western Blot, and RT-PCR. Future research will emphasize co-culture experiments with mesenchymal stem cells and macrophages, along with *in vivo* studies, to further assess the

clinical applicability and effectiveness of these membranes in bone regeneration and immune response modulation.

APPENDIX A. CALIBRATION CURVES

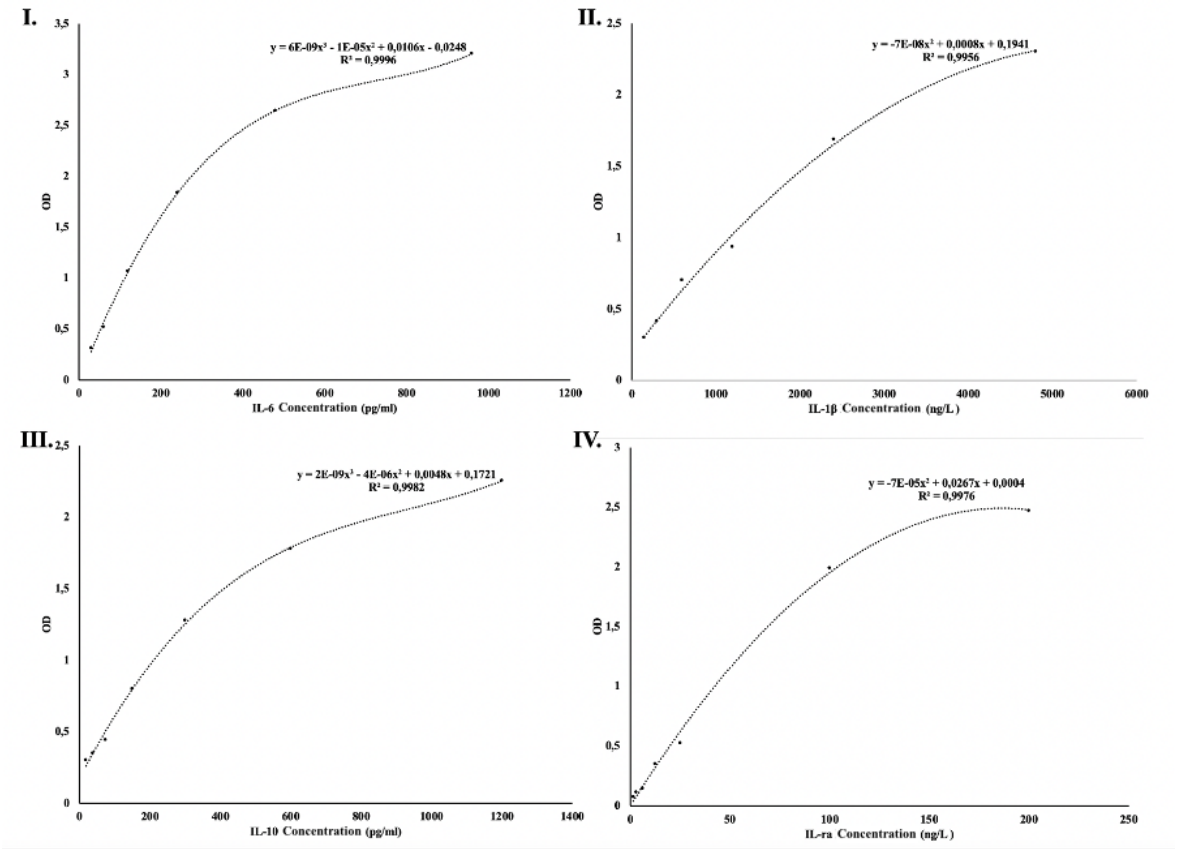


Figure A.1 Calibration Curves. I. IL-6 Calibration Curve, II. IL-1β Calibration Curve, III. IL-10 Calibration Curve, IV. IL-1ra Calibration Curve.

REFERENCES

1. Bedogni, B., and M. Powell, "Hypoxia, melanocytes and melanoma: survival and tumor development in the permissive microenvironment of the skin," *Pigment Cell & Melanoma Research*, 2009.

2. Biteau, B., H. C. E., and H. Jasper, "Maintaining tissue homeostasis: dynamic control of somatic stem cell activity," *Cell Stem Cell*, Vol. 9, no. 5, pp. 402–411, 2011.

3. Kim, S.-H., T. J., and S. Guimond, "Extracellular matrix and cell signalling: the dynamic cooperation of integrin, proteoglycan and growth factor receptor," *The Journal of Endocrinology*, Vol. 209, no. 2, pp. 139–151, 2011.

4. Mathews, S., B. R. G. P. K., and S. Totey, "Extracellular matrix protein mediated regulation of the osteoblast differentiation of bone marrow derived human mesenchymal stem cells," *Differentiation; Research in Biological Diversity*, Vol. 84, no. 2, pp. 185–192, 2012.

5. Singh, P., and J. E. Schwarzbauer, "Fibronectin and stem cell differentiation: lessons from chondrogenesis," *Journal of Cell Science*, Vol. 125, no. 16, pp. 3703–3712, 2012.

6. Chen, C., Z. Jiang, and G. Yang, "Laminins in osteogenic differentiation and pluripotency maintenance," *Differentiation*, Vol. 114, pp. 13–19, 2020.

7. Costa, P., F. V. M. Almeida, and J. T. Connelly, "Biophysical signals controlling cell fate decisions: how do stem cells really feel?," *The International Journal of Biochemistry Cell Biology*, Vol. 44, no. 12, pp. 2233–2237, 2012.

8. Gasiorowski, J. Z., C. J. Murphy, and P. F. Nealey, "Biophysical cues and cell behavior: the big impact of little things," *Annual Review of Biomedical Engineering*, Vol. 15, pp. 155–176, 2013.

9. Robinson, S. C., and L. Coussens, "Soluble mediators of inflammation during tumor development," *Advances in Cancer Research*, Vol. 93, pp. 159–187, 2005.

10. Zhao, Y., W. Zhang, Q. Lan, H. Liu, and Y. Zhang, "Osteoimmunomodulation for the development of advanced bone biomaterials," *Materials Science and Engineering: C*, Vol. 59, pp. 1181–1191, 2016.

11. Talifu, Z., C. Qin, Z. Xin, Y. Chen, J. Liu, S. Dangol, X. Ma, H. Gong, Z. Pei, and Y. Yu, "The overexpression of insulin-like growth factor-1 and neurotrophin-3 promote functional recovery and alleviate spasticity after spinal cord injury," *Frontiers in Neuroscience*, Vol. 16, p. 863793, 2022.

12. Ornitz, D. M., and P. J. Marie, "Fibroblast growth factor signaling in skeletal development and disease," *Genes Development*, Vol. 29, no. 14, pp. 1463–1486, 2015.

13. Ruprecht, V., P. Monzo, A. Ravasio, Z. Yue, E. Makhija, P. O. Strale, N. Gauthier, G. V. Shivashankar, V. Studer, and C. Albiges-Rizo, "How cells respond to environmental cues: insights from bio-functionalized substrates," *Journal of Cell Science*, Vol. 130, no. 1, pp. 51–61, 2017.

14. Vining, K. H., and D. J. Mooney, "Mechanical forces direct stem cell behaviour in development and regeneration," *Nature Reviews Molecular Cell Biology*, Vol. 18, no. 12, pp. 728–742, 2017.

15. Sun, M., G. Chi, P. Li, S. Lv, J. Xu, Z. Xu, Y. Xia, Y. Tan, J. Xu, and L. Li, "Effects of matrix stiffness on the morphology, adhesion, proliferation and osteogenic differentiation of mesenchymal stem cells," *International Journal of Medical Sciences*, Vol. 15, no. 3, p. 257, 2018.

16. El-Rashidy, A. A., S. E. Moshy, I. Radwan, D. Rady, M. M. S. Abbass, C. DÂrfer, and K. F. F. El-Sayed, "Effect of polymeric matrix stiffness on osteogenic differentiation of mesenchymal stem/progenitor cells: Concise review," *Polymers*, Vol. 13, no. 8, p. 1236, 2021.

17. McNamara, L. E., R. J. McMurray, M. J. P. Biggs, F. Kantawong, R. O. C. Oreffo, and M. J. Dalby, "Nanotopographical control of stem cell differentiation," *Journal of Tissue Engineering*, Vol. 1, no. 1, p. 120623, 2010.

18. Keselowsky, B. G., D. M. Collard, and A. J. GarcÂa, "Integrin binding specificity regulates biomaterial surface chemistry effects on cell differentiation," *Proceedings of the National Academy of Sciences*, Vol. 102, no. 17, pp. 5953–5957, 2005.

19. Chen, Z., X. Mao, L. Tan, S. Lin, and B. Shi, "Hydroxyapatite nanoparticle-modified scaffold induces osteogenic differentiation of mesenchymal stem cells," *Journal of the Mechanical Behavior of Biomedical Materials*, Vol. 81, pp. 195–201, 2018.

20. Abagnale, G., M. Steger, V. H. Nguyen, N. Hersch, A. Sechi, S. Joussen, B. Denecke, R. Merkel, B. Hoffmann, and A. Dreser, "Surface topography enhances differentiation of mesenchymal stem cells towards osteogenic and adipogenic lineages," *Biomaterials*, Vol. 61, pp. 316–326, 2015.

21. Zhao, L., L. Liu, Z. Wu, Y. Zhang, and P. K. Chu, "Effects of micropitted/nanotubular titania topographies on bone mesenchymal stem cell osteogenic differentiation," *Biomaterials*, Vol. 33, no. 9, pp. 2629–2641, 2012.

22. Chen, L., R. Coleman, R. Leang, H. Tran, A. Kopf, C. M. Walsh, I. Sears-Kraxberger, O. Steward, W. B. Macklin, J. F. Loring, and T. E. Lane, "Human neural precursor cells promote neurologic recovery in a viral model of multiple sclerosis," *Stem Cell Reports*, Vol. 2, no. 6, pp. 825–837, 2014.

23. Ohata, Y., and K. Ozono, "Bone and stem cells. the mechanism of osteogenic differentiation from mesenchymal stem cell," *Clinical Calcium*, Vol. 24, no. 4, pp. 501–508, 2014.

24. Gou, Y., Y. Huang, W. Luo, Y. Li, P. Zhao, J. Zhong, X. Dong, M. Guo, A. Li, and A. Hao, "Adipose-derived mesenchymal stem cells (mscs) are a superior cell source for bone tissue engineering," *Bioactive Materials*, Vol. 34, pp. 51–63, 2024.

25. Kim, H. S., S. G. Kumbar, and S. P. Nukavarapu, "Biomaterial-directed cell behavior for tissue engineering," *Current Opinion in Biomedical Engineering*, Vol. 17, p. 100260, 2021.

26. Ventura, R., P. A. K. B. P. M., and B.-T. Lee, "Evaluation of bone regeneration potential of injectable extracellular matrix (ecm) from porcine dermis loaded with biphasic calcium phosphate (bcp) powder," *Materials Science & Engineering. C, Materials for Biological Applications*, Vol. 110, p. 110663, 2020.

27. Zhu, M., R. Zhang, Z. Mao, J. Fang, and F. Ren, "Topographical biointerface regulating cellular functions for bone tissue engineering," *Biosurface and Biotribology*, Vol. 8, no. 3, pp. 165–187, 2022.

28. Palin, E., H. Liu, and T. J. Webster, "Mimicking the nanofeatures of bone increases bone-forming cell adhesion and proliferation," *Nanotechnology*, Vol. 16, no. 9, p. 1828, 2005.

29. Webster, T. J., C. Ergun, R. H. Doremus, R. W. Siegel, and R. Bizios, "Enhanced functions of osteoblasts on nanophase ceramics," *Biomaterials*, Vol. 21, no. 17, pp. 1803–1810, 2000.

30. Dimitrievska, S., M. N. Bureau, J. Antoniou, F. Mwale, A. Petit, R. S. Lima, and B. R. Marple, "Titania-hydroxyapatite nanocomposite coatings support human mesenchymal stem cells osteogenic differentiation," *Journal of Biomedical Materials Research Part A*, Vol. 98, no. 4, pp. 576–588, 2011.

31. Qin, D., N. Wang, X.-G. You, A.-D. Zhang, X.-G. Chen, and Y. Liu, "Collagen-based biocomposites inspired by bone hierarchical structures for advanced bone regeneration: Ongoing research and perspectives," *Biomaterials Science*, Vol. 10, no. 2, pp. 318–353, 2022.

32. Krtolica, A., "Role of microenvironment in regulating stem cell and tumor initiating cancer cell behavior and its potential therapeutic implications," *Tumor Dormancy, Quiescence, and Senescence, Volume 2: Aging, Cancer, and Noncancer Pathologies*, pp. 301–312, 2014.

33. Qazi, T. H., D. J. Mooney, G. N. Duda, and S. Geissler, "Biomaterials that promote cell-cell interactions enhance the paracrine function of mscs," *Biomaterials*, Vol. 140, pp. 103–114, 2017.

34. May, M., A. Slaughter, and D. Lucas, "Dynamic regulation of hematopoietic stem cells by bone marrow niches," *Current Stem Cell Reports*, Vol. 4, pp. 201–208, 2018.

35. Spiller, K. L., R. R. Anfang, K. J. Spiller, J. Ng, K. R. Nakazawa, J. W. Daulton, and G. Vunjak-Novakovic, "The role of macrophage phenotype in vascularization of tissue engineering scaffolds," *Biomaterials*, 2014.

36. Gong, F., T. Groth, C. Tu, M. Zhao, X. Huang, and J. Chu, "Crosstalk between macrophages and mesenchymal stem cells regulated by biomaterials and its role in bone regeneration," *Advances in Materials Science and Engineering*, Vol. 2021, pp. 1–21, 2021.

37. Sridharan, R., A. R. Cameron, D. J. Kelly, C. J. Kearney, and F. J. O'Brien, "Biomaterial based modulation of macrophage polarization: A review and suggested design principles," *Materials Today*, Vol. 18, no. 6, pp. 313–325, 2015.

38. Zhang, Y., T. BÂse, R. E. Unger, J. A. Jansen, C. J. Kirkpatrick, and J. J. J. P. van den Beucken, "Macrophage type modulates osteogenic differentiation of adipose tissue mscs," *Cell and Tissue Research*, Vol. 369, no. 2, pp. 273–286, 2017.

39. Wang, H., G. Wu, J. Zhang, K. Zhou, B. Yin, X. Su, G. Qiu, G. Yang, X. Zhang, G. Zhou, and Z. Wu, "Osteogenic effect of controlled released rhbmp-2 in 3d printed porous hydroxyapatite scaffold," *Colloids and Surfaces B: Biointerfaces*, Vol. 141, pp. 491–498, 2016.

40. Chen, S., J. A. Jones, Y. Xu, H. Y. Low, J. M. Anderson, and K. W. Leong, "Characterization of topographical effects on macrophage behavior in a foreign body response model," *Biomaterials*, 2010.

41. Barth, K. A., J. D. Waterfield, and D. M. Brunette, "The effect of surface roughness on raw 264.7 macrophage phenotype," *Journal of Biomedical Materials Research - Part A*, Vol. 101, no. 9, pp. 2679–2688, 2013.

42. Damanik, F. F., T. C. Rothuizen, C. V. Blitterswijk, J. I. Rotmans, and L. Moroni, "Towards an in vitro model mimicking the foreign body response: Tailoring the surface properties of biomaterials to modulate extracellular matrix," *Scientific Reports*, Vol. 4, 2014.

43. Laquerriere, P., A. Grandjean-Laquerriere, E. Jallot, G. Balossier, P. Frayssinet, and M. Guenounou, "Importance of hydroxyapatite particles characteristics on cytokines production by human monocytes in vitro," *Biomaterials*, Vol. 24, no. 16, pp. 2739–2747, 2003.

44. Fernandes, K. R., Y. Zhang, A. M. Magri, A. C. Renno, and J. J. V. D. Beucken, "Biomaterial property effects on platelets and macrophages: An in vitro study," *ACS Biomaterials Science and Engineering*, Vol. 3, no. 12, pp. 3318–3327, 2017.

45. Sadowska, J. M., F. Wei, J. Guo, J. Guillem-Marti, M. P. Ginebra, and Y. Xiao, "Effect of nano-structural properties of biomimetic hydroxyapatite on osteoimmunomodulation," *Biomaterials*, 2018.

46. Li, J., Y. Chen, A. F. T. Mak, R. S. Tuan, L. Li, and Y. Li, "A one-step method to fabricate plla scaffolds with deposition of bioactive hydroxyapatite and collagen using ice-based microporogens," *Acta Biomaterialia*, Vol. 6, no. 6, pp. 2013–2019, 2010.

47. Bennett, C. N., K. A. Longo, W. S. Wright, L. J. Suva, T. F. Lane, K. D. Hankenson, and O. A. MacDougald, "Regulation of osteoblastogenesis and bone mass by wnt10b," *Proceedings of the National Academy of Sciences*, 2005.

48. Wend, P., K. Wend, S. A. Krum, and G. A. Miranda-Carboni, "The role of wnt10b in physiology and disease," *Acta Physiologica (Oxf)*, Vol. 204, pp. 34–51, Jan 2012. Epub 2011 May 7.

49. Correia, C. R., J. Gaifem, M. B. Oliveira, R. Silvestre, and J. F. Mano, "The influence of surface modified poly(l-lactic acid) films on the differentiation of human monocytes into macrophages," *Biomaterials Science*, 2017.

50. Spiller, K. L., D. O. Freytes, and G. Vunjak-Novakovic, "Macrophages modulate engineered human tissues for enhanced vascularization and healing," *Annals of Biomedical Engineering*, Vol. 43, no. 3, pp. 616–627, 2015.

51. Tan, J., Q. Y. Zhang, Y. T. Song, K. Huang, Y. L. Jiang, and Others, "Accelerated bone defect regeneration through sequential activation of the m1 and m2 phenotypes of macrophages by a composite bmp-2@sis hydrogel," *Composites Part B*, 2022.

52. Spiller, K. L., S. Nassiri, C. E. Witherel, R. R. Anfang, J. Ng, K. R. Nakazawa, T. Yu, and G. Vunjak-Novakovic, "Sequential delivery of immunomodulatory cytokines to facilitate the m1-to-m2 transition of macrophages and enhance vascularization of bone scaffolds," *Biomaterials*, 2015.

53. Engler, A. J., and Others, "Matrix elasticity directs stem cell lineage specification," *Cell*, Vol. 126, pp. 677–689, 2006.

54. Hynes, A., "Extracellular matrix: an important regulator of cell functions and skeletal muscle development," *Cell & Bioscience*, Vol. 8, no. 4, pp. 255–266, 2009.

55. Bissell, M. J., and W. C. Hines, "Why don't we get more cancer? a proposed role of the microenvironment in restraining cancer progression," *Nature Medicine*, Vol. 17, no. 3, pp. 320–329, 2011.

56. Thatikonda, N., *Functionalization of spider silk with affinity and bioactive domains via genetic engineering for in vitro disease diagnosis and tissue engineering.* Doctoral dissertation, KTH Royal Institute of Technology, 2018.

57. Discher, D. E., and Others, "Biomechanics: Stem cells in development," *Nature*, Vol. 430, pp. 41–49, 2005.

58. Santos, A., A. D. Bakker, B. Zandieh-Doulabi, C. M. Semeins, and J. Klein-Nulend, "Pulsating fluid flow modulates gene expression of proteins involved in wnt signaling pathways in osteocytes," *Journal of Orthopaedic Research*, Vol. 27, no. 10, pp. 1280–1287, 2009.

59. Domogatskaya, A., S. Rodin, and K. Tryggvason, "Functional diversity of laminins," *Annual Review of Cell and Developmental Biology*, Vol. 28, pp. 523–553, 2012.

60. Atashi, F., A. Modarressi, and M. Pepper, "The role of reactive oxygen species in mesenchymal stem cell adipogenic and osteogenic differentiation: A review," *Stem Cells and Development*, Vol. 24, no. 10, pp. 1150–1163, 2015.

61. Bonnans, C., J. Chou, and Z. Werb, "Remodelling the extracellular matrix in development and disease," *Nature Reviews Molecular Cell Biology*, Vol. 15, no. 12, pp. 786–801, 2014.

62. Gattazzo, F., A. Urciuolo, and P. Bonaldo, "Extracellular matrix: a dynamic microenvironment for stem cell niche," *Biochimica et Biophysica Acta (BBA)-General Subjects*, Vol. 1840, no. 8, pp. 2506–2519, 2014.

63. Nguyen, L. H., N. Annabi, M. Nikkhah, H. Bae, L. Binan, S. Park, Y. Kang, Y. Yang, and A. Khademhosseini, "Vascularized bone tissue engineering: approaches for potential improvement," *Tissue Engineering Part B: Reviews*, Vol. 18, no. 5, pp. 363–382, 2012.

64. Rajnicek, A. M., L. E. Foubister, and C. D. McCaig, "Growth cone steering by a physiological electric field requires dynamic microtubules, microfilaments and rac-mediated filopodial asymmetry," *Journal of Cell Science*, Vol. 119, no. 9, pp. 1736–1745, 2006.

65. Lutolf, M. P., and H. M. Blau, "Artificial stem cell niches," *Advanced Materials*, Vol. 21, no. 32-33, pp. 3255–3268, 2009.

66. Murray, P. J., J. E. Allen, S. K. Biswas, E. A. Fisher, D. W. Gilroy, S. Goerdt, S. Gordon, J. A. Hamilton, L. B. Ivashkiv, and T. Lawrence, "Macrophage activation and polarization: nomenclature and experimental guidelines," *Immunity*, Vol. 41, no. 1, pp. 14–20, 2014.

67. Zhang, T., M. Jiang, X. Yin, P. Yao, and H. Sun, "Mechanism of exosomes involved in osteoimmunity promoting osseointegration around titanium implants with small-scale topography," *Frontiers in Bioengineering and Biotechnology*, Vol. 9, p. 682384, 2021.

68. Kim, S. Y., W. S. Son, M. C. Park, C. M. Kim, B. H. Cha, K. J. Yoon, S.-H. Lee, and S. G. Park, "Ars-interacting multi-functional protein 1 induces proliferation of human bone marrow-derived mesenchymal stem cells by accumulation of ?-catenin via fibroblast growth factor receptor 2-mediated activation of akt," *Stem Cells and Development*, Vol. 22, no. 19, pp. 2630–2640, 2013.

69. Vigetti, D., M. GÂtte, M. S. G. PavÂo, and A. D. Theocharis, "Cellular microenvironment in human pathologies," 2013.

70. Diomede, F., G. D. Marconi, L. Fonticoli, J. Pizzicanella, I. Merciaro, P. Bramanti, E. Mazzon, and O. Trubiani, "Functional relationship between osteogenesis and angiogenesis in tissue regeneration," *International Journal of Molecular Sciences*, Vol. 21, no. 9, p. 3242, 2020.

71. Lai, H., B. Gong, J. Yin, and J. Qian, "3d printing topographic cues for cell contact guidance: A review," *Materials Design*, Vol. 218, p. 110663, 2022.

72. Lee, K., E. A. Silva, and D. J. Mooney, "Growth factor delivery-based tissue engineering: general approaches and a review of recent developments," *J Royal Soc Interface*, Vol. 8, 2011.

73. Chen, C. Y., P. H. Tsai, Y. H. Lin, C. Y. Huang, J. H. Chung, and G. Y. Chen, "Controllable graphene oxide-based biocompatible hybrid interface as an anti-fibrotic coating for metallic implants," *Materials Today Bio*, Vol. 15, p. 100326, 2022.

74. Fuchs, E., T. Tumbar, and G. Guasch, "Socializing with the neighbors: stem cells and their niche," *Cell*, Vol. 116, no. 6, pp. 769–778, 2004.

75. Kusuma, G. D., J. Carthew, R. Lim, and J. E. Frith, "Effect of the microenvironment on mesenchymal stem cell paracrine signaling: opportunities to engineer the therapeutic effect," *Stem Cells and Development*, Vol. 26, no. 9, pp. 617–631, 2017.

76. Mann, Z., M. Sengar, Y. K. Verma, R. Rajalingam, and P. K. Raghav, "Hematopoietic stem cell factors: their functional role in self-renewal and clinical aspects," *Frontiers in Cell and Developmental Biology*, Vol. 10, p. 664261, 2022.

77. Yang, F., and Others, "Osteoblastic lineage cells and the vasculature in bone regeneration," *Bone Research*, Vol. 11, pp. 789–800, 2023.

78. Wen, J., D. Cai, W. Gao, R. He, Y. Li, Y. Zhou, T. Klein, L. Xiao, and Y. Xiao, "Osteoimmunomodulatory nanoparticles for bone regeneration," *Nanomaterials*, Vol. 13, no. 2, p. 215, 2023.

79. Xiao, Y., Y. Ding, J. Zhuang, R. Sun, H. Sun, and L. Bai, "Osteoimmunomodulation role of exosomes derived from immune cells on osseointegration," *Frontiers in Bioengineering and Biotechnology*, Vol. 10, p. 831627, 2022.

80. Hench, L. L., and J. M. Polak, "Third-generation biomedical materials," *Science*, Vol. 295, no. 5557, pp. 1014–1017, 2002.

81. Chen, C., S. Bang, Y. Cho, S. Lee, I. Lee, S. Zhang, and I. Noh, "Research trends in biomimetic medical materials for tissue engineering: 3d bioprinting, surface modification, nano/micro-technology and clinical aspects in tissue engineering of cartilage and bone," *Biomaterials Research*, Vol. 20, no. 1, p. 10, 2016.

82. Zhang, Y., S. E. Chen, J. Shao, and J. J. J. P. van den Beucken, "Combinatorial surface roughness effects on osteoclastogenesis and osteogenesis," *ACS Applied Materials Interfaces*, Vol. 10, no. 43, pp. 36652–36663, 2018.

83. Anderson, J. M., A. Rodriguez, and D. T. Chang, "Foreign body reaction to biomaterials," *Seminars in Immunology*, Vol. 20, pp. 86–100, 2008.

84. Galli, S., and Others, "Surface modifications for enhancing the osseointegration of titanium implants," *International Journal of Oral Maxillofacial Implants*, Vol. 32, no. 5, pp. 919–930, 2017.

85. Gristina, A. G., P. Naylor, and Q. Myrvik, "Infections from biomaterials and implants: a race for the surface," *Medical Progress Through Technology*, Vol. 14, no. 3-4, pp. 205–224, 1987.

86. Yamada, K. M., and E. Cukierman, "Modeling tissue morphogenesis and cancer in 3d," *Cell*, Vol. 130, no. 4, pp. 601–610, 2007.

87. Ohgushi, H., T. Yoshikawa, M. Okumura, S. Tamai, E. C. Shors, and D. T. Davy, "Biomechanical properties of hydroxyapatite ceramics and its osteogenic potential," *Journal of Biomedical Materials Research Part A*, Vol. 29, no. 12, pp. 1527–1536, 2005.

88. Groth, T., G. Altankov, and K. Klosz, "Adhesion of human endothelial cells and smooth muscle cells on modified polymers," *Journal of Biomedical Materials Research Part A*, Vol. 67, no. 2, pp. 960–969, 2004.

89. Li, J., T. Tan, and Y. Zhang, "Effects of surface-treated hydroxyapatite on the ultrastructure and function of human endothelial cells," *Journal of Biomedical Materials Research Part A*, Vol. 101, no. 3, pp. 691–698, 2013.

90. Teixeira, A. I., G. A. Abrams, P. J. Bertics, C. J. Murphy, and P. F. Nealey, "Epithelial contact guidance on well-defined micro-and nanostructured substrates," *Journal of Cell Science*, Vol. 116, no. 10, pp. 1881–1892, 2003.

91. Jiang, X., J. Mi, X. Li, H. Li, T. Zhang, and W. Sun, "Enhanced migration of nerve cells facilitated by aligned nanofibrous scaffolds in nerve conduits," *Journal of Biomedical Materials Research Part A*, Vol. 93, no. 3, pp. 1035–1042, 2010.

92. Han, S.-H., Y. Chen, J. Shin, and Y.-K. Chung, "The migration and differentiation of mouse induced pluripotent stem cells toward a schwann cell fate," *Biomaterials*, Vol. 30, no. 26, pp. 4993–5001, 2009.

93. He, F.-M., G.-L. Yang, Y.-N. Li, and X.-X. Wang, "The role of the micro/nanotopography of dental implants in osseointegration: A review of recent findings," *Journal of Biomedical Materials Research Part B: Applied Biomaterials*, Vol. 99, no. 2, pp. 150–160, 2011.

94. Buxboim, A., I. L. Ivanovska, and D. E. Discher, "Matrix elasticity, cytoskeletal forces and physics of the nucleus: how deeply do cells ÃfeelÃ outside and in?," *Journal of Cell Science*, Vol. 123, no. 3, pp. 297–308, 2010.

95. Altankov, G., F. Grinnell, and T. Groth, "Studies on the biocompatibility of materials: fibroblast reorganization of substratum-bound fibronectin on surfaces varying in wettability," *Journal of Biomedical Materials Research Part A*, Vol. 67, no. 2, pp. 736–745, 2003.

96. Anselme, K., and M. Bigerelle, "Topography effects of pure titanium substrates on human osteoblast long-term adhesion," *Acta Biomaterialia*, Vol. 2, no. 4, pp. 347–357, 2006.

97. Bacakova, L., E. Filova, M. Parizek, T. Ruml, and V. Svorcik, "Modulation of cell adhesion, proliferation and differentiation on materials designed for body implants," *Biotechnology Advances*, Vol. 29, no. 6, pp. 739–767, 2011.

98. Liu, X., J. Y. Lim, H. J. Donahue, R. Dhurjati, A. M. Mastro, E. A. Vogler, and C. T. Laurencin, "Influence of substratum surface chemistry/energy and topography on the human fetal osteoblastic cell line," *Journal of Biomedical Materials Research Part A*, Vol. 69, no. 2, pp. 301–311, 2004.

99. Curran, J. M., R. Chen, and J. A. Hunt, "The guidance of human mesenchymal stem cell differentiation in vitro by controlled modifications to the cell substrate," *Biomaterials*, Vol. 26, no. 4, pp. 705–714, 2005.

100. Dalby, M. J., G. N., and C. D. W. Wilkinson, "Nanoscale symmetry and disorder: control of human mesenchymal cell differentiation," *Nature Nanotechnology*, Vol. 2, pp. 232–236, 2007.

101. Boyan, B. D., and Others, "Role of surface chemistry in mediating osteoblast behavior on titanium biomaterials," *Journal of Biomedical Materials Research*, Vol. 32, pp. 639–649, 1996.

102. Curran, J. M., R. Chen, and J. A. Hunt, "Controlling the phenotype and function of mesenchymal stem cells in vitro by adhesion to silane-modified clean glass surfaces," *Biomaterials*, Vol. 26, no. 34, pp. 7057–7067, 2005.

103. Hutmacher, D. W., "Scaffolds in tissue engineering bone and cartilage," *Biomaterials*, Vol. 21, no. 24, pp. 2529–2543, 2001.

104. Zhao, X., Q. Li, Z. Guo, and Z. Li, "Constructing a cell microenvironment with biomaterial scaffolds for stem cell therapy," *Stem Cell Research Therapy*, Vol. 12, pp. 1–13, 2021.

105. Franz, S., S. Rammelt, D. Scharnweber, and J. C. Simon, "Immune responses to implants: A review of the implications for the design of immunomodulatory biomaterials," *Biomaterials*, Vol. 32, no. 28, pp. 6692–6709, 2011.

106. Brown, B. N., B. D. Ratner, S. B. Goodman, S. Amar, and S. F. Badylak, "Macrophage polarization: an opportunity for improved outcomes in biomaterials and regenerative medicine," *Biomaterials*, Vol. 33, no. 15, pp. 3792–3802, 2012.

107. Khang, D., J. Carpenter, Y. W. Chun, R. Pareta, and T. J. Webster, "Nanotechnology for regenerative medicine," *Biomedical Microdevices*, Vol. 12, pp. 575–587, 2010.

108. Zinger, O., K. Anselme, A. Denzer, P. Habersetzer, M. Wieland, J. Jeanfils, and P. Hardouin, "Time-dependent morphology and adhesion of osteoblastic cells on titanium model surfaces featuring scale-resolved topography," *Biomaterials*, Vol. 25, no. 14, pp. 2695–2711, 2004.

109. Lord, M. S., M. Foss, and F. Besenbacher, "Influence of nanoscale surface topography on protein adsorption and cellular response," *Nano Today*, Vol. 5, no. 1, pp. 66–78, 2010.

110. Bettinger, C. J., R. Langer, and J. T. Borenstein, "Engineering substrate topography at the micro- and nanoscale to control cell function," *Angewandte Chemie International Edition*, Vol. 48, no. 30, pp. 5406–5415, 2009.

111. Anselme, K., M. Bigerelle, L. Ploux, and A. Ponche, "Cell/material interfaces: influence of surface chemistry and surface topography on cell adhesion," *Journal of Adhesion Science and Technology*, Vol. 24, no. 5, pp. 831–852, 2010.

112. Dalby, M. J., S. J. Yarwood, M. O. Riehle, H. J. H. Johnstone, S. Affrossman, and A. S. G. Curtis, "Increasing fibroblast response to materials using nanotopography: morphological and genetic measurements of cell response to 13-nm-high polymer demixed islands," *Experimental Cell Research*, Vol. 276, no. 1, pp. 1–9, 2002.

113. Dalby, M. J., M. O. Riehle, H. Johnstone, S. Affrossman, and A. S. G. Curtis, "Investigating the limits of filopodial sensing: a brief report on filopodial interaction with nanotopography," *Journal of Biomedical Materials Research Part A*, Vol. 84, no. 3, pp. 973–979, 2007.

114. Park, J.-H., S. Bauer, K. A. Schlegel, F. W. Neukam, K. von der Mark, and P. Schmuki, "Tio2 nanotube surfaces: 15 nm-an optimal length scale of surface topography for cell adhesion and differentiation," *Small*, Vol. 5, no. 6, pp. 666–671, 2009.

115. Schakenraad, J. M., H. J. Busscher, C. R. H. Wildevuur, and J. Arends, "The influence of substratum surface free energy on growth and spreading of human fibroblasts in the presence and absence of serum proteins," *Journal of Biomedical Materials Research*, Vol. 25, no. 4, pp. 453–464, 1991.

116. Yim, E. K. F., S. W. Pang, and K. W. Leong, "Synthetic nanostructures inducing differentiation of human mesenchymal stem cells into neuronal lineage," *Experimental Cell Research*, Vol. 311, no. 2, pp. 371–377, 2005.

117. Fink, J., and Others, "Nanostructured surfaces cause severe but reversible non-genomic dysfunction in human adipose-derived stem cells," *Biomaterials*, Vol. 32, no. 9, pp. 3275–3284, 2011.

118. Gittens, R. A., T. McLachlan, R. Olivares-Navarrete, Y. Cai, S. Berner, R. Tannenbaum, Z. Schwartz, K. H. Sandhage, and B. D. Boyan, "The effects of combined micron-/submicron-scale surface roughness and nanoscale features on cell proliferation and differentiation," *Biomaterials*, Vol. 32, no. 13, pp. 3395–3403, 2011.

119. Kim, Y.-C., J.-H. Park, and M. R. Prausnitz, "Microneedles for drug and vaccine delivery," *Advanced Drug Delivery Reviews*, Vol. 64, no. 14, pp. 1547–1568, 2012.

120. Vladkova, T. G., "Surface engineered polymeric biomaterials with improved bio contact properties," *International Journal of Polymer Sciences (Print)*, Vol. 2009, 2009.

121. Nouri, A., and C. Wen, "Introduction to surface coating and modification for metallic biomaterials," *Surface Coating and Modification of Metallic Biomaterials*, pp. 3–60, 2015.

122. Li, W. J., R. Tuli, C. Okafor, A. Derfoul, K. G. Danielson, D. J. Hall, and R. S. Tuan, "A three-dimensional nanofibrous scaffold for cartilage tissue engineering using human mesenchymal stem cells," *Biomaterials*, Vol. 26, 2005.

123. Amani, H., H. Arzaghi, M. Bayandori, A. S. Dezfuli, H. Pazoki-Toroudi, A. Shafiee, and L. Moradi, "Controlling cell behavior through the design of biomaterial surfaces: a focus on surface modification techniques," *Advanced Materials Interfaces*, Vol. 6, no. 13, p. 1900572, 2019.

124. Cooper, L. F., T. Masuda, P. K. Yliheikkila, and D. A. Felton, "Generalizations regarding the process and phenomenon of osseointegration. part ii. in vivo studies," *The International Journal of Oral & Maxillofacial Implants*, Vol. 21, no. 1, pp. 35–46, 2006.

125. Huang, Z., E. R. Nelson, R. L. Smith, and S. B. Goodman, "The sequential expression profiles of growth factors from osteoprogenitors [correction of osteroprogenitors] to osteoblasts in vitro.," *Tissue Engineering*, Vol. 13, no. 9, pp. 2311–20, 2007.

126. Lin, K., L. Xia, H. Li, X. Jiang, H. Pan, Y. Xu, and Z. Zhang, "Enhanced osteoporotic bone regeneration by strontium-substituted calcium silicate bioactive ceramics," *Biomaterials*, Vol. 34, no. 38, pp. 10028–10039, 2012.

127. Rana, D., K. Ramasamy, M. Leena, C. JimÂnez, J. Campos, P. Ibarra, Z. S. Haidar, and M. Ramalingam, "Surface functionalization of nanobiomaterials for application in stem cell culture, tissue engineering, and regenerative medicine," *Biotechnology Progress*, Vol. 32, no. 3, pp. 554–567, 2016.

128. Cooper, L. F., T. Masuda, S. W. Whitson, P. K. Yliheikkila, and D. A. Felton, "Formation of mineralizing osteoblast cultures on machined, titanium oxide grit-blasted, and plasma-sprayed titanium surfaces," *International Journal of Oral and Maxillofacial Implants*, Vol. 14, no. 1, pp. 37–47, 1999.

129. Weissman, I. L., "Stem cells: units of development, units of regeneration, and units in evolution," *Cell*, Vol. 100, no. 1, pp. 157–168, 2000.

130. Orkin, S. H., and L. I. Zon, "Hematopoiesis: an evolving paradigm for stem cell biology," *Cell*, Vol. 132, no. 4, pp. 631–644, 2008.

131. Thomson, J. A., J. Itskovitz-Eldor, S. S. Shapiro, M. A. Waknitz, J. J. Swiergiel, V. S. Marshall, and J. M. Jones, "Embryonic stem cell lines derived from human blastocysts," *Science*, Vol. 282, no. 5391, pp. 1145–1147, 1998.

132. Pittenger, M. F., A. M. Mackay, S. C. Beck, R. K. Jaiswal, R. Douglas, J. D. Mosca, M. A. Moorman, D. W. Simonetti, S. Craig, and D. R. Marshak, "Multilineage potential of adult human mesenchymal stem cells," *Science*, Vol. 284, no. 5411, pp. 143–147, 1999.

133. Takahashi, K., K. Tanabe, M. Ohnuki, M. Narita, T. Ichisaka, K. Tomoda, and S. Yamanaka, "Induction of pluripotent stem cells from adult human fibroblasts by defined factors," *Cell*, Vol. 131, 2007.

134. Liu, Y., J. Lim, and S. H. Teoh, "Review: development of clinically relevant scaffolds for vascularised bone tissue engineering," *Biotechnology Advances*, Vol. 31, no. 5, pp. 688–705, 2011.

135. Shim, J. H., J. Y. Kim, M. Park, J. Park, and D. W. Cho, "Development of a hybrid scaffold with synthetic biomaterials and hydrogel using solid freeform fabrication technology," *Biofabrication*, Vol. 4, no. 1, p. 15002, 2012.

136. Agarwal, S., X. Zhou, F. Ye, Q. He, and G. Q. Chen, "The performance of graphene oxide as a nanocarrier for the in vitro delivery of dexamethasone to induce osteogenic differentiation of human mesenchymal stem cells," *Biomaterials*, Vol. 35, no. 17, pp. 6112–6118, 2016.

137. Wang, Y., D. J. Blasioli, H. J. Kim, H. S. Kim, and D. L. Kaplan, "Cartilage tissue engineering with silk scaffolds and human articular chondrocytes," *Biomaterials*, Vol. 27, no. 25, pp. 4434–4442, 2006.

138. Yang, F., R. Murugan, S. Wang, and S. Ramakrishna, "Electrospinning of nano/micro scale poly (l-lactic acid) aligned fibers and their potential in neural tissue engineering," *Biomaterials*, Vol. 26, no. 15, pp. 2603–2610, 2005.

139. Suri, S., and C. E. Schmidt, "Cell-laden hydrogel constructs of hyaluronic acid, collagen, and laminin for neural tissue engineering," *Tissue Engineering Part A*, Vol. 16, no. 5, pp. 1703–1716, 2010.

140. Chen, Y. C., R. Z. Lin, H. Qi, Y. Yang, H. Bae, J. M. Melero-Martin, and A. Khademhosseini, "Functional human vascular network generated in photocrosslinkable gelatin methacrylate hydrogels," *Advanced Functional Materials*, Vol. 22, no. 10, pp. 2027–2039, 2012.

141. Kong, H. J., E. S. Kim, and D. J. Mooney, "Electrospun fibrous scaffolds for engineering the development of 3-dimensional heterotypic cellular interactions," *Biomedical Microdevices*, Vol. 5, no. 4, pp. 317–322, 2003.

142. Khan, Y., M. J. Yaszemski, A. G. Mikos, and C. T. Laurencin, "Tissue engineering of bone: material and matrix considerations," *Journal of Bone and Joint Surgery*, Vol. 90, no. Supplement_1, pp. 36–42, 2008.

143. Pham, Q. P., U. Sharma, and A. G. Mikos, "Electrospinning of polymeric nanofibers for tissue engineering applications: a review," *Tissue Engineering*, Vol. 12, no. 5, pp. 1197–1211, 2008.

144. Barry, F. P., and J. M. Murphy, "Mesenchymal stem cells: clinical applications and biological characterization," *International Journal of Biochemistry Cell Biology*, Vol. 36, no. 4, pp. 568–584, 2004.

145. Borciani, G., G. Montalbano, N. Baldini, G. Cerqueni, C. Vitale-Brovarone, and G. Ciapetti, "Co-culture systems of osteoblasts and osteoclasts: Simulating in vitro bone remodeling in regenerative approaches," *Acta Biomaterialia*, Vol. 108, pp. 22–45, 2020.

146. Langer, R., and J. P. Vacanti, "Tissue engineering," *Science (New York, N.Y.)*, Vol. 260, no. 5110, pp. 920–926, 1993.

147. Bhat, S., and A. Kumar, "Biomaterials and bioengineering tomorrow's healthcare," *Biomaterials*, Vol. 34, no. 34, pp. 9203–9211, 2013.

148. Camman, M., P. Joanne, O. Agbulut, and C. Hélary, "3d models of dilated cardiomyopathy: Shaping the chemical, physical and topographical properties of biomaterials to mimic the cardiac extracellular matrix," *Bioactive Materials*, 2022.

149. Calore, A. R., V. Srinivas, L. Groenendijk, A. Serafim, and Others, "Manufacturing of scaffolds with interconnected internal open porosity and surface roughness," *Acta Biomaterialia*, 2023.

150. Prasopthum, A., M. Cooper, and Others, "Three-dimensional printed scaffolds with controlled micro-/nanoporous surface topography direct chondrogenic and osteogenic differentiation of mesenchymal stem cells," *ACS Applied Materials & Interfaces*, 2019.

151. Bartolomeu, F., N. Dourado, F. Pereira, N. Alves, and Others, "Additive manufactured porous biomaterials targeting orthopedic implants: A suitable combination of mechanical, physical and topological properties," *Materials Science and Engineering: C*, 2020.

152. Li, Z., and et al., "Exosomes derived from m2 macrophages facilitate osteogenesis and reduce adipogenesis of bmscs," *Frontiers in Endocrinology*, Vol. 12, p. 680328, 2021.

153. Wang, L., C. Wang, S. Wu, Y. Fan, and X. Li, "Influence of the mechanical properties of biomaterials on degradability, cell behaviors and signaling pathways: current progress and challenges," *Biomaterials Science*, 2020.

154. Rahmati, M., E. A. Silva, J. E. Reseland, and Others, "Biological responses to physicochemical properties of biomaterial surface," *Chemical Society Reviews*, 2020.

155. Dave, K., and V. G. Gomes, "Interactions at scaffold interfaces: Effect of surface chemistry, structural attributes and bioaffinity," *Materials Science and Engineering: C*, 2019.

156. Haugh, M. G., T. J. Vaughan, C. M. Madl, R. M. Raftery, and Others, "Investigating the interplay between substrate stiffness and ligand chemistry in directing mesenchymal stem cell differentiation within 3d macro-porous substrates," *Biomaterials*, 2018.

157. Xing, F., L. Li, C. Zhou, C. Long, L. Wu, H. Lei, and Others, "Regulation and directing stem cell fate by tissue engineering functional microenvironments: scaffold physical and chemical cues," *Stem Cells International*, 2019.

158. Bai, M., L. Cai, X. Li, L. Ye, and J. Xie, "Stiffness and topography of biomaterials dictate cell-matrix interaction in musculoskeletal cells at the bio-interface: a concise progress review," *Journal of Biomedical Materials Research Part B: Applied Biomaterials*, 2020.

159. Wang, S., S. Hashemi, S. Stratton, and Others, "The effect of physical cues of biomaterial scaffolds on stem cell behavior," *Advanced Healthcare Materials*, 2021.

160. Khajehmohammadi, M., R. A. Tafti, and Others, "Effect of porosity on mechanical and biological properties of bioprinted scaffolds," *Journal of Biomedical Materials Research Part A*, 2023.

161. Han, P., G. A. Gomez, G. N. Duda, S. Ivanovski, and P. S. P. Poh, "Scaffold geometry modulation of mechanotransduction and its influence on epigenetics," *Acta Biomaterialia*, 2023.

162. Iturriaga, L., and K. D. V. Gordon, "Strategies to introduce topographical and structural cues in 3d-printed scaffolds and implications in tissue regeneration," *Advanced NanoBiomed Research*, 2021.

163. Veiseh, O., J. C. Doloff, M. Ma, A. J. Vegas, H. H. Tam, A. R. Bader, and Others, "Size- and shape-dependent foreign body immune response to materials implanted in rodents and non-human primates," *Nature Materials*, Vol. 14, no. 6, pp. 643–651, 2015.

164. Mildner, A., and S. Jung, "Development and function of dendritic cell subsets," *Immunity*, Vol. 40, no. 5, pp. 642–656, 2014.

165. Zhu, J., H. Yamane, and W. E. Paul, "Differentiation of effector cd4 t cell populations," *Annual Review of Immunology*, Vol. 28, pp. 445–489, 2010.

166. Amulic, B., C. Cazalet, G. L. Hayes, K. D. Metzler, and A. Zychlinsky, "Neutrophil function: from mechanisms to disease," *Annual Review of Immunology*, Vol. 30, pp. 459–489, 2012.

167. Theoharides, T. C., K. D. Alysandratos, A. Angelidou, D. A. Delivanis, N. Sismanopoulos, B. Zhang, and Others, "Mast cells and inflammation," *Biochimica et Biophysica Acta (BBA)-Molecular Basis of Disease*, Vol. 1822, no. 1, pp. 21–33, 2012.

168. Vivier, E., D. H. Raulet, A. Moretta, M. A. Caligiuri, L. Zitvogel, L. L. Lanier, and Others, "Innate or adaptive immunity? the example of natural killer cells," *Science*, Vol. 331, no. 6013, pp. 44–49, 2011.

169. Darby, I. A., and T. D. Hewitson, "Fibroblast differentiation in wound healing and fibrosis," *International Review of Cytology*, Vol. 257, pp. 143–179, 2007.

170. Geetha, M., A. K. Singh, R. Asokamani, and A. K. Gogia, "Ti based biomaterials, the ultimate choice for orthopaedic implants: A review," *Progress in Materials Science*, Vol. 54, no. 3, pp. 397–425, 2009.

171. Lu, L., C. A. Garcia, and A. G. Mikos, "In vitro degradation of thin poly (dl-lactic-co-glycolic acid) films," *Journal of Biomedical Materials Research*, Vol. 46, no. 2, pp. 236–244, 1999.

172. Zhang, M., X. Li, L. Bai, K. Uchida, W. Bai, B. Wu, W. Xu, H. Zhu, and H. Huang, "Effects of low frequency electromagnetic field on proliferation of human epidermal stem cells: An in vitro study," *Bioelectromagnetics*, Vol. 34, no. 1, pp. 74–80, 2013.

173. Roohani-Esfahani, S.-I., P. Newman, and H. Zreiqat, "Design and fabrication of 3d printed scaffolds with a mechanical strength comparable to cortical bone to repair large bone defects," *Scientific Reports*, Vol. 6, p. 19468, 2016.

174. Pradhan, S., J. M. Clary, D. Seliktar, and E. A. Lipke, "A three-dimensional spheroidal cancer model based on peg-fibrinogen hydrogel microspheres," *Biomaterials*, Vol. 115, pp. 141–154, 2017.

175. Brown, B. N., J. E. Valentin, A. M. Stewart-Akers, G. P. McCabe, and S. F. Badylak, "Macrophage phenotype and remodeling outcomes in response to biologic scaffolds with and without a cellular component," *Biomaterials*, 2009.

176. Mosser, D. M., and J. P. Edwards, "Exploring the full spectrum of macrophage activation," *Nature Reviews Immunology*, Vol. 8, no. 12, pp. 958–969, 2008.

177. Eljarrah, A., M. Gergues, P. W. Pobiarzyn, O. A. Sandiford, and P. Rameshwar, "Therapeutic potential of mesenchymal stem cells in immune-mediated diseases," *Stem Cells: Therapeutic Applications*, pp. 93–108, 2019.

178. Orekhov, A. N., V. A. Orekhova, N. G. Nikiforov, V. A. Myasoedova, A. V. Grechko, E. B. Romanenko, D. Zhang, and D. A. Chistiakov, "Monocyte differentiation and macrophage polarization," *Vessel Plus*, Vol. 3, no. 10, pp. 1209–2574, 2019.

179. Chen, Z., F. Xing, Y. Zhou, P. Yu, J. Xu, R. Luo, C. Zhou, Z. Xiang, P. M. Rommens, and M. Liu, "Integrated osteoimmunomodulatory strategies based on designing scaffold surface properties in bone regeneration," *Journal of Materials Chemistry B*, 2023.

180. Ta, W., A. Chawla, and J. Pollard, "Origins and hallmarks of macrophages: development, homeostasis, and disease," *Nature*, Vol. 496, no. 7446, pp. 445–455, 2013.

181. Sheu, K. M., and A. Hoffmann, "Functional hallmarks of healthy macrophage responses: their regulatory basis and disease relevance," *Annual Review of Immunology*, Vol. 40, pp. 295–321, 2022.

182. Colin, S., G. Chinetti-Gbaguidi, and B. Staels, "Macrophage phenotypes in atherosclerosis," *Immunological Reviews*, Vol. 262, no. 1, pp. 153–166, 2014.

183. RodrÂguez-Morales, P., and R. A. Franklin, "Macrophage phenotypes and functions: resolving inflammation and restoring homeostasis," *Trends in Immunology*, Vol. 44, no. 12, pp. 986–998, 2023.

184. Sica, A., and A. Mantovani, "Macrophage plasticity and polarization: in vivo veritas," *The Journal of Clinical Investigation*, Vol. 122, no. 3, pp. 787–795, 2012.

185. Li, P., C. Ma, J. Li, S. You, L. Dang, J. Wu, Z. Hao, J. Li, Y. Zhi, L. Chen, and S. Sun, "Proteomic characterization of four subtypes of m2 macrophages derived from human thp-1 cells," *Journal of Zhejiang University: Science B*, Vol. 23, no. 5, pp. 407–422, 2022.

186. Hourani, T., A. Perez-Gonzalez, K. Khoshmanesh, R. Luwor, A. A. Achuthan, S. Baratchi, N. M. OÃBrien-Simpson, and A. Al-Hourani, "Label-free macrophage phenotype classification using machine learning methods," *Scientific Reports*, Vol. 13, no. 1, pp. 1–15, 2023.

187. Selig, M., L. Poehlman, N. C. Lang, M. VÂlker, B. Rolauffs, and M. L. Hart, "Prediction of six macrophage phenotypes and their il-10 content based on single-cell morphology using artificial intelligence," *Frontiers in Immunology*, Vol. 14, no. January, pp. 1–18, 2023.

188. Antmen, E., N. E. Vrana, and V. Hasirci, "The role of biomaterials and scaffolds in immune responses in regenerative medicine: macrophage phenotype modulation by biomaterial properties and scaffold architectures," *Biomaterials science*, Vol. 9, no. 24, pp. 8090–8110, 2021.

189. Niu, Y., Z. Wang, Y. Shi, L. Dong, and C. Wang, "Modulating macrophage activities to promote endogenous bone regeneration: Biological mechanisms and engineering approaches," *Bioactive materials*, Vol. 6, no. 1, pp. 244–261, 2021.

190. He, J., G. Chen, M. Liu, Z. Xu, H. Chen, L. Yang, and Y. Lv, "Scaffold strategies for modulating immune microenvironment during bone regeneration," *Materials Science and Engineering: C*, Vol. 108, p. 110411, 2020.

191. Lorenzo, J., M. Horowitz, Y. Choi, and H. Takayanagi, "Osteoimmunology: interactions of the bone and immune system," *Endocrine Reviews*, Vol. 29, no. 4, pp. 403–440, 2008.

192. Mountziaris, P. M., and A. G. Mikos, "Modulation of the inflammatory response for enhanced bone tissue regeneration," *Tissue Engineering Part B: Reviews*, Vol. 14, no. 2, pp. 179–186, 2008.

193. Schmidt-Bleek, K., A. Petersen, A. Dienelt, C. Schwarz, and G. N. Duda, "Initiation and early control of tissue regeneration: bone healing as a model system for tissue regeneration," *Expert Opinion on Biological Therapy*, Vol. 15, no. 9, pp. 1175–1189, 2015.

194. Mao, L., L. Bai, X. Wang, X. Chen, D. Zhang, F. Chen, and C. Liu, "Enhanced cell osteogenesis and osteoimmunology regulated by piezoelectric biomaterials with controllable surface potential and charges," *ACS Applied Materials Interfaces*, Vol. 14, no. 39, pp. 44111–44124, 2022.

195. Hosseinpour, S., L. J. Walsh, and C. Xu, "Modulating osteoimmune responses by mesoporous silica nanoparticles," *ACS Biomaterials Science Engineering*, Vol. 8, no. 10, pp. 4110–4122, 2021.

196. Qi, X., Y. Liu, X. Yin, R. Zhao, W. Zhang, J. Cao, W. Wang, and W. Jia, "Surface-based modified 3d-printed bg/go scaffolds promote bone defect repair through bone immunomodulation," *Composites Part B: Engineering*, Vol. 257, p. 110673, 2023.

197. Xie, Y., C. Hu, Y. Feng, D. Li, T. Ai, Y. Huang, X. Chen, L. Huang, and J. Tan, "Osteoimmunomodulatory effects of biomaterial modification strategies on macrophage polarization and bone regeneration," *Regenerative biomaterials*, Vol. 7, no. 3, pp. 233–245, 2020.

198. Hotchkiss, K. M., G. B. Reddy, S. L. Hyzy, Z. Schwartz, B. D. Boyan, and R. Olivares-Navarrete, "Titanium surface characteristics, including topography and wettability, alter macrophage activation," *Acta Biomaterialia*, Vol. 31, pp. 425–434, 2016.

199. Lv, L., Y. Xie, K. Li, T. Hu, X. Lu, Y. Cao, and X. Zheng, "Unveiling the mechanism of surface hydrophilicity-modulated macrophage polarization," *Advanced Healthcare Materials*, Vol. 7, no. 19, pp. 1–11, 2018.

200. Gao, S., R. Lu, X. Wang, J. Chou, N. Wang, X. Huai, C. Wang, Y. Zhao, and S. Chen, "Immune response of macrophages on super-hydrophilic tio2 nanotube arrays," *Journal of Biomaterials Applications*, Vol. 34, no. 9, pp. 1239–1253, 2020.

201. Gutman, J., "In vitro culture of human monocyte-derived macrophages with regards to m1/m2 polarization," *Chalmers University of Technology*, 2016.

202. Spiller, K. L., and T. J. Koh, "Macrophage-based therapeutic strategies in regenerative medicine," *Advanced Drug Delivery Reviews*, Vol. 122, pp. 74–83, Dec 2017. Epub 2017 May 16.

203. Alhamdi, J. R., T. Peng, I. M. Al-Naggar, K. L. Hawley, K. L. Spiller, and L. T. Kuhn, "Controlled m1-to-m2 transition of aged macrophages by calcium phosphate coatings," *Biomaterials*, 2019.

204. Graney, P. L., E. B. Lurier, and K. L. Spiller, "Biomaterials and bioactive factor delivery systems for the control of macrophage activation in regenerative medicine," *ACS Biomaterials Science & Engineering*, Vol. 4, no. 4, pp. 1137–1148, 2017.

205. He, X., and Others, "Osteoimmunomodulation: the immunology of bone regeneration," *Nature Reviews Materials*, Vol. 6, pp. 928–944, 2021.

206. Luo, M., F. Zhao, L. Liu, Z. Yang, T. Tian, X. Chen, and Others, "Ifn-γ/ srbg composite scaffolds promote osteogenesis by sequential regulation of macrophages from m1 to m2," *Journal of Materials*, 2021.

207. Li, T., M. Peng, Z. Yang, X. Zhou, Y. Deng, C. Jiang, M. Xiao, and Others, "3d-printed ifn-γ -loading calcium silicate-β-tricalcium phosphate scaffold sequentially activates m1 and m2 polarization of macrophages to promote vascularization of tissue engineering bone," *Acta Biomaterialia*, 2018.

208. Qiao, W., H. Xie, J. Fang, J. Shen, W. Li, D. Shen, J. Wu, and Others, "Sequential activation of heterogeneous macrophage phenotypes is essential for biomaterials-induced bone regeneration," *Biomaterials*, 2021.

209. OÃBrien, E. M., G. E. Risser, and K. L. Spiller, "Sequential drug delivery to modulate macrophage behavior and enhance implant integration," *Advanced Drug Delivery Reviews*, 2019.

210. Erenay, B., A. S. Y. SaÂlam, B. Garipcan, K. D. Jandt, and S. OdabaÂ, "Bone surface mimicked pdms membranes stimulate osteoblasts and calcification of bone matrix," *Biomaterials Advances*, Vol. 142, p. 213170, 2022.

211. Puza, F., S. Rostami, B. ÂzÂolak Aslan, S. OdabaÂ, K. D. Jandt, and B. Garipcan, "Anisotropic bone surface topography mimicked chitosan/graphene oxide membranes," *Advanced Engineering Materials*, Vol. 25, no. 1, pp. 1–10, 2023.

212. Ozcolak, B., B. Erenay, S. OdabaÂ, K. D. Jandt, and B. Garipcan, "Effects of bone surface topography and chemistry on macrophage polarization," *Scientific Reports*, Vol. 14, no. 1, p. 12721, 2024.

213. Wen, F., S. Chang, Y. C. Toh, S. H. Teoh, and H. Yu, "Development of poly (lactic-co-glycolic acid)-collagen scaffolds for tissue engineering," *Materials Science and Engineering C*, Vol. 27, no. 2, pp. 285–292, 2007.

214. Mima, Y., S. Fukumoto, H. Koyama, M. Okada, S. Tanaka, T. Shoji, M. Emoto, T. Furuzono, Y. Nishizawa, and M. Inaba, "Enhancement of cell-based therapeutic angiogenesis using a novel type of injectable scaffolds of hydroxyapatite-polymer nanocomposite microspheres," *PLoS ONE*, Vol. 7, no. 4, 2012.

215. Marks, J., N. J. Carvou, E. S. Debnam, S. K. Srai, and R. J. Unwin, "Diabetes increases facilitative glucose uptake and glut2 expression at the rat proximal tubule brush border membrane," *Journal of Physiology*, Vol. 553, no. 1, pp. 137–145, 2003.

216. Wu, F., J. Wei, C. Liu, B. OÃNeill, and Y. Ngothai, "Fabrication and properties of porous scaffold of zein/pcl biocomposite for bone tissue engineering," *Composites Part B: Engineering*, 2012.

217. Ma, H., W. Su, Z. Tai, D. Sun, X. Yan, B. Liu, and Q. Xue, "Preparation and cytocompatibility of polylactic acid/hydroxyapatite/graphene oxide nanocomposite fibrous membrane," *Chinese Science Bulletin*, Vol. 57, no. 23, pp. 3051–3058, 2012.

218. Nejati, E., V. Firouzdor, M. B. Eslaminejad, and F. Bagheri, "Needle-like nano hydroxyapatite/poly(l-lactide acid) composite scaffold for bone tissue engineering application," *Materials Science and Engineering C*, Vol. 29, no. 3, pp. 942–949, 2009.

219. Schaap-Oziemlak, A. M., P. T. KÂhn, T. G. van Kooten, and P. van Rijn, "Biomaterial-stem cell interactions and their impact on stem cell response," *RSC Adv.*, Vol. 4, no. 95, pp. 53307–53320, 2014.

220. Schaub, N. J., C. L. Beux, J. Miao, R. J. Linhardt, J. G. Alauzun, D. Laurencin, and R. J. Gilbert, "The effect of surface modification of aligned poly-l-lactic acid electrospun fibers on fiber degradation and neurite extension," *PLoS ONE*, Vol. 10, no. 9, 2015.

221. Ma, Z., C. Gao, Y. Gong, J. Ji, and J. Shen, "Immobilization of natural macromolecules on polyâlâlactic acid membrane surface in order to improve its cytocompatibility," *Journal of Biomedical Materials Research: An Official Journal of The Society for Biomaterials, The Japanese Society for Biomaterials, and The Australian Society for Biomaterials and the Korean Society for Biomaterials*, Vol. 63, no. 6, pp. 838–847, 2002.

222. Ge, M., K. Ge, F. Gao, W. Yan, H. Liu, L. Xue, Y. Jin, H. Ma, and J. Zhang, "Biomimetic mineralized strontium-doped hydroxyapatite on porous poly(l-lactic acid) scaffolds for bone defect repair," *International Journal of Nanomedicine*, 2018.

223. Wenzel, R. N., "Surface roughness and contact angle," *Journal of Psychosomatic Research*, Vol. 30, no. 3, p. 387, 1986.

224. Xiao, H., G. Cai, and M. Liu, "Hydroxyl radical induced structural changes of collagen," *Spectroscopy*, Vol. 21, no. 2, pp. 91–103, 2007.

225. Kloprogge, J. T., D. Wharton, L. Hickey, and R. L. Frost, "Infrared and raman study of interlayer anions co32-, no3-, so42- and clo4- in mg/al-hydrotalcite," *American Mineralogist*, Vol. 87, no. 5-6, pp. 623–629, 2002.

226. Aubry, C., S. Camy, C. Combes, O. Marsan, T. Canceill, and S. Cazalbou, "Bioceramic powders for bone regeneration modified by high-pressure co2 process," *Journal of Materials Science*, Vol. 56, no. 4, pp. 3387–3403, 2021.

227. Beamson, G., and D. Briggs, "High resolution monochromated x-ray photoelectron spectroscopy of organic polymers: A comparison between solid state data for organic polymers and gas phase data for small molecules," *Molecular Physics*, Vol. 76, no. 4, pp. 919–936, 1992.

228. Paragkumar, N. T., D. Edith, and J. L. Six, "Surface characteristics of pla and plga films," *Applied Surface Science*, Vol. 253, no. 5, pp. 2758–2764, 2006.

229. Mas, B. A., S. M. de Mello Cattani, R. de Cassia Cipriano Rangel, G. D. A. Ribeiro, N. C. Cruz, F. D. L. Leite, P. A. D. P. Nascente, and E. A. D. R. Duek, "Surface characterization and osteoblast-like cells culture on collagen modified pldla scaffolds," *Materials Research*, Vol. 17, no. 6, pp. 1523–1534, 2014.

230. Cui, M., L. Liu, N. Guo, R. Su, and F. Ma, "Preparation, cell compatibility and degradability of collagen-modified poly (lactic acid)," *Molecules*, Vol. 20, no. 1, pp. 595–607, 2015.

231. Liu, G., C. Xue, and P. Zhu, "Removal of carmine from aqueous solution by carbonated hydroxyapatite nanorods," *Nanomaterials (Basel, Switzerland)*, Vol. 7, pp. 27–36, 2017.

232. Bottino, M. C., V. Thomas, and G. M. Janowski, "A novel spatially designed and functionally graded electrospun membrane for periodontal regeneration," *Acta Biomaterialia*, Vol. 7, no. 1, pp. 216–224, 2011.

233. Hoffman, B. N., A. D. V. Tran, O. Ojugbele, S. C. Pryor, J. A. Bonventre, K. Flynn, and B. S. Weeks, "Bifenthrin activates homotypic aggregation in human t-cell lines," *Med Sci Monit*, Vol. 12, no. 3, p. 94, 2006.

234. Alipour, F., D. V. M., D. V. M. A. Parham, D. V. M. H. K. Mehrjerdi, and D. V. M. H. Dehghani, "Equine adipose-derived mesenchymal stem cells: Phenotype and growth characteristics, gene expression profile and differentiation potentials," *Cell Journal*, Vol. 16, no. 4, pp. 456–465, 2015.

235. Guilak, F., K. E. Lott, H. A. Awad, Q. Cao, K. C. Hicok, B. Fermor, and J. M. Gimble, "Clonal analysis of the differentiation potential of human adipose-derived adult stem cells," *Journal of Cellular Physiology*, Vol. 206, no. 1, pp. 229–237, 2006.

236. Byth, H., B. I. Mchunu, I. A. Dubery, and L. Bornman, "Assessment of a simple, non-toxic alamar blue cell survival assay to monitor tomato cell viability," *Phytochemical Analysis: An International Journal of Plant Chemical and Biochemical Techniques*, Vol. 12, no. 5, pp. 340–346, 2001.

237. Rampersad, S. N., "Multiple applications of alamar blue as an indicator of metabolic function and cellular health in cell viability bioassays," *Sensors*, Vol. 12, no. 9, pp. 12347–12360, 2012.

238. Dinh, M. N., M. Hitomi, Z. A. Al-Turaihi, and J. G. Scott, "Alamar blue assay optimization to minimize drug interference and inter-assay viability," *Biorxiv*, 2023.

239. Zhou, S., J. S. Greenberger, M. W. Epperly, J. P. Goff, C. Adler, M. S. LeBoff, and J. Glowacki, "Age-related intrinsic changes in human bone-marrow-derived mesenchymal stem cells and their differentiation to osteoblasts," *Aging Cell*, Vol. 7, no. 3, pp. 335–343, 2008.

240. Ahn, H. H., I. W. Lee, H. B. Lee, and M. S. Kim, "Cellular behavior of human adipose-derived stem cells on wettable gradient polyethylene surfaces," *International Journal of Molecular Sciences*, Vol. 15, no. 2, pp. 2075–2086, 2014.

241. Barry, F., R. E. Boynton, B. Liu, and J. M. Murphy, "Chondrogenic differentiation of mesenchymal stem cells from bone marrow: differentiation-dependent gene expression of matrix components," *Experimental Cell Research*, Vol. 268, no. 2, pp. 189–200, 2001.

242. Stolzing, A., E. Jones, D. Mcgonagle, and A. Scutt, "Age-related changes in human bone marrow-derived mesenchymal stem cells: consequences for cell therapies," *Mechanisms of Ageing and Development*, Vol. 129, no. 3, pp. 163–173, 2008.

243. Lee, I., Y. Lee, B. Yu, J. Lai, and T. Young, "The behavior of mesenchymal stem cells on micropatterned plla membranes," *Journal of Biomedical Materials Research Part A: An Official Journal of The Society for Biomaterials, The Japanese Society for Biomaterials, and The Australian Society for Biomaterials and the Korean Society for Biomaterials*, Vol. 91, no. 3, pp. 929–938, 2009.

244. Wan, Y., Y. Wang, Z. Liu, X. Qu, B. Han, J. Bei, and S. Wang, "Adhesion and proliferation of oct-1 osteoblast-like cells on micro-and nano-scale topography structured poly (l-lactide)," *Biomaterials*, Vol. 26, no. 21, pp. 4453–4459, 2005.

245. Bernardo, M. P., B. C. R. da Silva, A. E. I. Hamouda, M. A. S. de Toledo, C. Schalla, S. RÂtten, R. Goetzke, L. H. C. Mattoso, M. Zenke, and A. Sechi, "Pla/hydroxyapatite scaffolds exhibit in vitro immunological inertness and promote robust osteogenic differentiation of human mesenchymal stem cells without osteogenic stimuli," *Scientific Reports*, Vol. 12, no. 1, p. 2333, 2022.

246. Popov, T., *Characterization of human mesenchymal stem cells by the appearance of integrins and functional analysis of collagen I-binding integrins.* Phd dissertation, Ludwig Maximilian University of Munich (LMU), 2011.

247. Wojak, I., D. Scharnweber, and E. Pamu?a, "Resorbable scaffolds modified with collagen type i or hydroxyapatite: in vitro studies on human mesenchymal stem cells," *Acta of Bioengineering and Biomechanics*, Vol. 15, no. 1, pp. 61–67, 2013.

248. Zhou, G., S. Liu, Y. Ma, W. Xu, W. Meng, X. Lin, W. Wang, S. Wang, and J. Zhang, "Innovative biodegradable poly (l-lactic)/collagen/hydroxyapatite composite fibrous scaffolds promote osteoblastic proliferation and differentiation," *International Journal of Nanomedicine*, pp. 7577–7588, 2017.

249. Schofer, M. D., A. Veltum, C. Theisen, F. Chen, S. Agarwal, S. Fuchs-Winkelmann, and J. R. J. Paletta, "Functionalisation of plla nanofiber scaffolds using a possible cooperative effect between collagen type i and bmp-2: impact on growth and osteogenic differentiation of human mesenchymal stem cells," *Journal of Materials Science: Materials in Medicine*, Vol. 22, pp. 1753–1762, 2011.

250. Peng, H., Z. Yin, H. Liu, X. Chen, B. Feng, H. Yuan, B. Su, H. Ouyang, and Y. Zhang, "Electrospun biomimetic scaffold of hydroxyapatite/chitosan supports enhanced osteogenic differentiation of mmscs," *Nanotechnology*, Vol. 23, no. 48, p. 485102, 2012.

251. Mansourizadeh, F., *et al.*, "Plla/ha nano composite scaffolds for stem cell proliferation and differentiation in tissue engineering," *Molecular Biology Research Communications*, pp. 1–10, 2013. Unpublished manuscript.

252. Ebrahimi, Z., S. Irani, A. Ardeshirylajimi, and E. Seyedjafari, "Enhanced osteogenic differentiation of stem cells by 3d printed pcl scaffolds coated with collagen and hydroxyapatite," *Scientific Reports*, Vol. 12, no. 1, p. 12359, 2022.

253. Cheng, Y., D. Ramos, P. Lee, D. Liang, X. Yu, and S. G. Kumbar, "Collagen functionalized bioactive nanofiber matrices for osteogenic differentiation of mesenchymal stem cells: bone tissue engineering," *Journal of Biomedical Nanotechnology*, Vol. 10, no. 2, pp. 287–298, 2014.

254. Yang, X., Y. Li, W. He, Q. Huang, R. Zhang, and Q. Feng, "Hydroxyapatite/collagen coating on plga electrospun fibers for osteogenic differentiation of bone marrow mesenchymal stem cells," *Journal of Biomedical Materials Research Part A*, Vol. 106, no. 11, pp. 2863–2870, 2018.

255. Hu, Y., K. Cai, Z. Luo, D. Xu, D. Xie, Y. Huang, and P. Liu, "Effect of nanostructured titanium coatings on osteogenic differentiation of bone marrow mesenchymal stem cells," *Materials Science and Engineering: C*, Vol. 73, pp. 343–352, 2017.

256. Wu, X., M. Zhou, X. Lin, W. Jing, J. Wu, S. Wang, and L. Chen, "Osteogenic differentiation of human amnion mesenchymal stem cells on hydroxyapatite/collagen/pla scaffolds: In vitro and in vivo," *Biomedical Materials*, Vol. 13, no. 5, p. 55001, 2018.

257. Martinez, E. F., E. A. Elizondo, G. M. Banuelos, and J. G. Salinas, "Hydroxyapatite structures enhance osteogenesis of human mscs," *Journal of Biomedical Materials Research Part A*, Vol. 110, no. 4, pp. 770–781, 2022.

258. Calabrese, G., R. Giuffrida, C. Fabbi, E. Figallo, L. Salvatorelli, I. Pucci-Minafra, and R. Parenti, "Collagen-hydroxyapatite scaffolds induce human adipose derived stem cells osteogenic differentiation in vitro," *PloS One*, Vol. 11, no. 3, p. e0151181, 2016.

259. Rabadan-Ros, R., M. Vallet-Regi, A. J. Salinas, and J. Roman, "Nurse's aphase-silicocarnotite ceramic-bone tissue interaction in a rabbit tibia defect model," *Journal of Biomedical Materials Research Part B: Applied Biomaterials*, Vol. 105, no. 3, pp. 528–536, 2017.

260. Assaf, R. B., R. Sader, and N. Naaman, "Evaluation of gelatin scaffold-embedded mscs for bone regeneration," *Journal of Biomedical Materials Research Part B: Applied Biomaterials*, Vol. 107, no. 6, pp. 1921–1928, 2019.

261. Hild, N., O. D. Schneider, D. Mohn, N. A. Luechinger, F. M. Koehler, S. Hofmann, and W. J. Stark, "Two-layer membranes with calcium phosphate/collagen/plga nanofibers as osteogenic scaffolds for human mesenchymal stem cells," *Biomaterials*, Vol. 32, no. 28, pp. 7021–7030, 2011.

262. Thein-Han, W. W., and H. H. Xu, "Collagen-calcium phosphate cement scaffolds seeded with umbilical cord stem cells for bone tissue engineering," *Tissue Engineering Part A*, Vol. 17, no. 23-24, pp. 2943–2954, 2011.

263. Favi, P. M., R. S. Benson, N. R. Neilsen, R. L. Hammonds, M. L. Bates, C. M. Stewart, and J. Sankar, "Cell proliferation, viability, and in vitro differentiation of equine mesenchymal stem cells seeded on bacterial cellulose hydroxyapatite composite scaffolds," *Materials Science and Engineering: C*, Vol. 46, pp. 141–150, 2014.

264. Song, K., Z. Yang, T. Liu, W. Zhi, X. Li, L. Deng, Z. Cui, and X. Ma, "Fabrication and detection of tissue-engineered bones with bio-derived scaffolds in a rotating bioreactor," *Biotechnology and Applied Biochemistry*, Vol. 45, no. Pt 2, pp. 65–74, 2006.

265. Song, K., T. Liu, Z. Cui, X. Li, and X. Ma, "Three-dimensional fabrication of engineered bone with human bio-derived bone scaffolds in a rotating wall vessel bioreactor," *Journal of Biomedical Materials Research - Part A*, Vol. 86, no. 2, pp. 323–332, 2008.

266. Sandhiutami, N. M. D., M. Moordiani, D. R. Laksmitawati, N. Fauziah, M. Maesaroh, and W. Widowati, "In vitro assesment of anti-inflammatory activities of coumarin and indonesian cassia extract in raw264.7 murine macrophage cell line," *Iranian Journal of Basic Medical Sciences*, 2017.

267. Muniandy, K., S. Gothai, K. M. Badran, S. S. Kumar, N. M. Esa, and P. Arulselvan, "Suppression of proinflammatory cytokines and mediators in lps-induced raw 264.7 macrophages by stem extract of alternanthera sessilis via the inhibition of the nf-?b pathway," *Journal of Immunology Research*, 2018.

268. Boraschi-Diaz, I., J. Wang, J. S. Mort, and S. V. Komarova, "Collagen type i as a ligand for receptor-mediated signaling," *Frontiers in Physics*, Vol. 5, p. 12, 2017.

269. Karimi, F., A. J. OÃConnor, G. G. Qiao, and D. E. Heath, "Integrin clustering matters: a review of biomaterials functionalized with multivalent integrin-binding ligands to improve cell adhesion, migration, differentiation, angiogenesis, and biomedical device integration," *Advanced Healthcare Materials*, Vol. 7, no. 12, p. 1701324, 2018.

270. Jha, A., and E. Moore, "Collagen-derived peptide, dgea, inhibits pro-inflammatory macrophages in biofunctional hydrogels," *Journal of Materials Research*, Vol. 37, no. 1, pp. 77–87, 2022.

271. Chandran, S. V., T. S. Amritha, G. Rajalekshmi, and M. Pandimadevi, "A preliminary in vitro study on the bovine collagen film incorporated with azadirachta indica plant extract as a potential wound dressing material," *International Journal of PharmTech Research*, Vol. 8, no. 6, pp. 248–257, 2015.

272. Schaub, N. J., T. Britton, R. Rajachar, and R. J. Gilbert, "Engineered nanotopography on electrospun plla microfibers modifies raw 264.7 cell response," *ACS Applied Materials and Interfaces*, Vol. 5, no. 20, pp. 10173–10184, 2013.

273. Wang, Y., Y. Zhang, J. Wang, J. Du, P. K. Chu, and X. Ge, "Modulation of macrophage behavior by modified tio2 nanotubes," *Acta Biomaterialia*, Vol. 77, pp. 397–409, 2018.

274. Majidi, M., S. Pakzad, M. Salimi, A. Azadbakht, S. Hajighasemlou, M. Amoupour, Z. Nokhbedehghan, S. Bonakdar, K. S. Sepehr, N. P. S. Chauhan, and M. Gholipourmalekabadi, "Macrophage cell morphology-imprinted substrates can modulate mesenchymal stem cell behaviors and macrophage m1/m2 polarization for wound healing applications," *Biotechnology and Bioengineering*, Vol. 120, no. 12, pp. 3638–3654, 2023.

275. Kim, M., S. Lee, and C. S. Ki, "Cellular behavior of raw264.7 cells in 3d poly(ethylene glycol) hydrogel niches," *ACS Biomaterials Science and Engineering*, Vol. 5, no. 2, pp. 922–932, 2019.

276. Neacsu, P., A. Mazare, A. Cimpean, J. Park, M. Costache, P. Schmuki, and I. Demetrescu, "Reduced inflammatory activity of raw 264.7 macrophages on titania nanotube modified ti surface," *International Journal of Biochemistry and Cell Biology*, Vol. 55, pp. 187–195, 2014.

277. Heinrich, F., A. Lehmbecker, B. B. Raddatz, K. Kegler, A. Tipold, V. M. Stein, A. Kalkuhl, U. Deschl, W. BaumgÂrtner, R. Ulrich, and I. Spitzbarth, "Morphologic, phenotypic, and transcriptomic characterization of classically and alternatively activated canine blood-derived macrophages in vitro," *Frontiers in Immunology*, Vol. 12, 2017.

278. Schmitz, T., M. Jannasch, T. Weigel, C. Moseke, U. Gbureck, J. Groll, H. Walles, and J. Hansmann, "Nanotopographical coatings induce an early phenotype-specific response of primary material-resident m1 and m2 macrophages," *Materials*, Vol. 13, no. 5, pp. 1–20, 2020.